

SYNTHESIS REPORT

FOR PUBLICATION

Contract #: BREU -390
Project #: BE -4484-89

title: "IN - SITU CONTROL OF PLASMA CHEMICAL
VAPOR DEPOSITED CUBIC BORON NITRIDE
FILMS."

**Project
Coordinator:** Professor R. WINAND
Université Libre de Bruxelles

Partners: University of Kassel, Germany
Institute of Technical Physics

Université Libre de Bruxelles, Belgium
Faculty of Applied Sciences
Department of Metallurgy - Electrochemistry

Reference period from 01/09/91 to 31/08/95

Starting date: September 1st 1991

Duration: 48 months

* * *
* * *
* * *
* * *

PROJECT FUNDED BY THE EUROPEAN
COMMUNITY UNDER THE BRITE/EURAM
PROGRAMME

DATE: September 95

In-situ control of plasma chemical vapor deposited cubic boron nitride films.

R. Kassing, W. Kulisch, S. Reinke, M. Kuhr
Institute of Technical Physics
Microsystems Technology
University of Kassel - Germany

R. Winand, M. I. Delplancke, F. Kiel, M. Cotarelo
Department of Metallurgy and Electrochemistry
Faculty of Applied Sciences
University Libre de Bruxelles - Belgium

Abstract

This paper summarizes the work done in the framework of the BRITE-EURAM Contract BREU-390, devoted to the preparation and characterization (in-situ and ex-situ) of cubic boron nitride containing films by plasma enhanced chemical vapor deposition techniques.

Deposition equipments were built and modified and in-situ diagnostic techniques were implemented on the deposition chambers. Two of the deposition methods were successful in the preparation of cubic phase containing films: the inductively coupled r.f. plasma one (ICP) and the electron cyclotron resonance microwave plasma (ECR). Other methods like remote plasma and hot filament were tried and abandoned.

The in-situ diagnostic techniques giving the most interesting information were the Langmuir probe and the retarding energy analyzer that both provided insight in the ion energy and density.

A theoretical model of steady-state growth of cubic boron nitride assisted by energetic particles was developed and correlated with the present experimental data as well as with literature one.

1. Introduction

Boron nitride exists similar to carbon in two main crystalline modifications, hexagonal BN (h-BN) and cubic BN (c-BN) which are similar to graphite and diamond, respectively. C-BN was first synthesized by Wentorf under high-pressure high-temperature (HP-HT) conditions [1]. It raised a wide interest because of its excellent properties [2]. C-BN is the second hardest material just after diamond, exhibits high thermal conductivity and chemical inertness and is optically transparent in a wide range of wavelengths. Its specific advantages in comparison with diamond are its inertness with respect to iron based materials even at high temperature and the possibility to dope it n- or p-type. Therefore many applications **such as protective coatings, cutting tools, optical windows, heat sinks, and high temperature electronic devices** are in principle imaginable. However, nowadays only grinding powder and tools made of sintered HP-HT c-BN are commercially available because most of the above mentioned

applications require high quality c-BN films which are not reached by the current technology.

Despite the close similarities of both materials, the c-BN deposition processes as well as the resulting film properties are very different from the diamond ones and are less well investigated. In the early 80's first attempts of c-BN thin film deposition were published [3]. Since then, a large number of different CVD and PVD methods were used to prepare hard BN films [4]. Nevertheless deposition rates and surface areas that can be coated are rather small so that great scale applications are not yet available. A better understanding and control of the deposition could change this situation. This is requiring an investigation of the influence of the working parameters on the film growth rate, composition, and morphology simultaneous to a study of the gas phase composition and nature as well as modelization efforts.

This paper is summarizing the results obtained in the framework of the BRITE-EURAM contract BREU-390 devoted to the preparation and characterization (in-situ and ex-situ) of cubic boron nitride containing films by plasma enhanced chemical vapor deposition techniques.

2. The sputter model

At the beginning of the project, a great uncertainty about the requirements of c-BN deposition existed in literature. Therefore, criteria to prove the existence of c-BN in thin films had to be derived yielding to a combination of IR spectroscopy, diffraction and compositional analysis. Based on this criteria, a literature survey showed that only ion assisted deposition methods were suited for c-BN deposition.

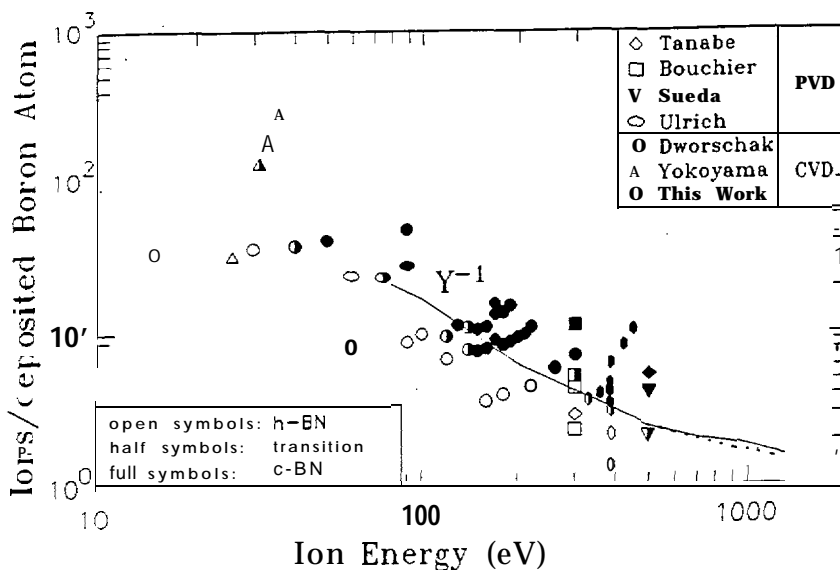


Figure 1 : F^* / E_{ion} diagram for all evaluable c-BN deposition experiments. For details of the data evolution see [K5]. From data published at the recent DIAMOND FILMS'95 conference, 6 more data points from three independent experiments could be added to this diagram, laying directly on the established boundary.

The data were quantified in terms of the microscopic deposition parameters: ion energy, ion to boron-atoms flux ratio, ion angle of incidence, ion mass and substrate temperature. This for the *first time* led to the evaluation of reliable, universal parameter ranges for c-BN deposition. It was shown that with increasing ion bombardment (ion energy as well as ion to boron flux) regions of h-BN, c-BN and no deposition at all appear in the parameter space. Figure 1 shows ion assisted CVD and PVD processes to rely on a common parameter range and therefore common growth mechanisms, and that low ion energies can be compensated by high ion to boron flux ratios. A model based on selective sputtering was proposed (sputter model). The different of sputter yield between h-BN and c-BN influences the growth velocities of the respective materials, an effect becoming more pronounced close to the relevant no growth condition. Assuming the modification with the highest growth velocity to be favoured, the model is able to explain all experimental data within the limits of experimental uncertainty. The dependencies of c-BN deposition on ion energy, ion flux, ion mass and angle of incidence reflect typical sputter behaviors; the temperature influence shows an additional thermal resorption mechanism. It should be noted that the angle dependency was predicted correctly before it was measured. Other models based on stress and subplantation show less agreement or give no quantitative predictions for the deposition parameters.

Experimental

Parallel to the theoretical investigations, several experimental set-ups were tested, in Germany, for their suitability for c-BN deposition. As expected from the sputter model, non-ion assisted methods like hot filament and (remote) plasma CVD led only to h-BN films. Therefore, the hot filament set-up was modified allowing plasma assisted deposition. This finally led to the ICP (inductively coupled plasma) method which will be described briefly below. The plasma is generated by coupling a 13.56 MHz signal inductively via a copper coil into a quartz tube. The plasma expands into the stainless steel reactor (diameter 14 cm) in which the up to 800 C heatable substrate holder is mounted. An additional 13.56 MHz signal is coupled capacitively to the substrate holder generating a bias voltage, by which ions from the plasma are accelerated towards the substrate. The chamber is pumped by a turbomolecular pump, its base pressure is $1 \cdot 10^{-6}$ mbar. During deposition, a gas mixture of trimethyl borazine (TMB), nitrogen and argon was used. The liquid TMB was slightly heated and introduced by its own vapour pressure, the other gases were injected by mass flow controllers. With typical gas flows from table 2, the working pressure was 210-2 mbar. As substrates, mainly (100) silicon wafers were used which were cleaned in situ by a plasma process. The area which can be coated homogeneously is quite small, about 1 cm^2 . Plasma characterization with the Langmuir double probe technique showed high plasma densities up to $5 \cdot 10^{11} \text{ cm}^{-3}$ which are suited to achieve a sufficient growth rate even at bias voltages below 100 V. A very important advantage of the ICP set-up is the independence of plasma density which controls the ion current from the bias voltage which determines the ion energy. Both quantities can be determined quantitatively making the ICP method well suited for basic investigations of the deposition mechanisms. Furthermore, our experiments cover the widest range of ion energies investigated with a single experimental set-up up to now.

In Belgium, one of the reactor consists of a commercial ECR-microwave reactor built by Leybolt [5] and modified in view of the present experiments. The magnetic flux density of 87.5 mT is generated by two rings of permanent magnets. The 2.45 GHz excitation is coupled into the plasma via an antenna. The plasma is generated inside a quartz dome (40 mm in diameter). The nitrogen precursors were fed into the reactor from the level of the magnet rings. The boron precursors were introduced into the plasma via a dispersal ring placed below the magnet rings. The substrates were held on a substrate holder that could be heated up to 900K. The temperature of the substrate holder was measured by a Ni-NiCr thermocouple and regulated by a thermostat. The substrate holder was powered by a radio frequency supply via coupling capacitor in order to create a bias controlling the ion energy. Two boron precursors and two nitrogen ones were used in this chamber: diborane (B_2H_6) diluted at 10 vol. % in argon, 1,3,5-N-trimethyl borazol (TMB), nitrogen and ammonia. The deposition was taking place in a dynamic mode: the reactants being pumped continuously. The fluxes of the incoming gases and the pressure could be controlled independently in the chamber. Prior to deposition, the various substrates were treated ex-situ or in-situ: HF etching for silicon (100) wafers, polishing for steel sheets, argon etching, nitriding. All gases were of high purity and their fluxes were controlled by mass flow controllers. The working pressure was monitored by a baratron and a ionization gauges. After deposition, films were cooled down under vacuum. Another set-up was an inductively coupled radio frequency plasma (ICP) reactor. The 13.56 MHz r.f. excitation was coupled into the plasma with a five turn coil that was water cooled. The plasma was generated inside a 50 mm in diameter quartz tube. The precursors were fed into the reactor with a multilevel injection head that allowed the mixing of the precursor gases just at the entrance of the excitation coil. The substrates were mechanically fixed to the holder that could be heated up to 1073K with a doped SiC heating element. Direct current (d.c.) bias could be applied to the substrate during deposition. The shallow angle of the substrate holder was designed in order to reduce the effect of the turbulences and to allow the examination of the effect of the distance from the coil on the composition, thickness and structure of the films. Depositions were carried on in the dynamic mode. Diborane and ammonia were used as precursors. Table 1 compares the two set-ups in terms of working pressure, residence time, flow rates, and excitation power.

Table 1:

	ECR-MW	ICP-RF
working pressure (Pa)	$7 - 8 \times 10^{-1}$	20
total flow rate (seem)	35-50	14
residence time (s)	$\tau \leq 1$	$\tau \geq 0.5$
excitation power (W)	720-960	200
bias	r.f.	d.c.
(v)	0->-150	0->-150
temperature (K)	673-873	473-773

Films were characterized by Fourier Transform Infrared Spectroscopy (FTIR) in transmittance mode (Perkin Helmer 1725X) using a bare silicon wafer as

reference. Film thickness and index of refraction were obtained by ellipsometry (Sentech SE400). The morphology and crystallinity were examined by scanning electron microscopy (SEM) (Jeol 820 and Hitachi S-4000) and transmission electron microscopy (Philips EM300) operating at 100 kV. The surface and compositional depth profile were obtained by Auger electron spectroscopy (AES) with a PHI 590A system.

4. Results and discussion

In Germany, with the ICP method, films containing up to 75% c-BN could be deposited. The existence of c-BN was proved independently by infrared spectroscopy (FTIR) and transmission electron diffraction (TED). With Auger electron spectroscopy (AES), c-BN films were found to be very close to stoichiometry tolerating carbon and oxygen impurities as high as 15 % and 5 %, respectively. Typical growth rates achieved with the ICP method lay between 300 and 900 nm/hr and are within the range of other CVD as well as PVD deposition methods. The first aim was to evaluate the influences of the primary deposition parameters ion flux (plasma density), ion energy (bias voltage) and substrate temperature which actively contribute to the formation of c-BN. Further secondary mechanisms which may hinder or even prevent c-BN formation will be discussed in a special section. Several bias voltage sequences with different plasma densities are shown in figure 2.

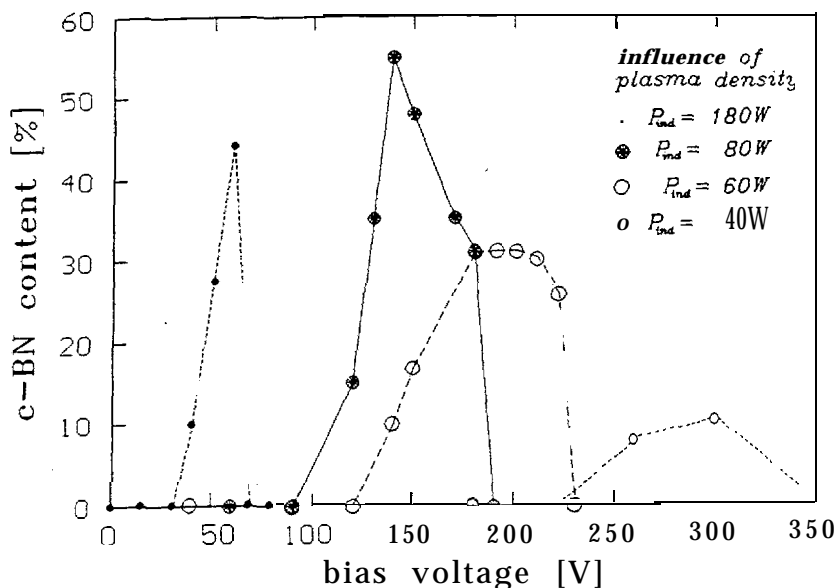


Figure 2 :: Dependence of the bias voltage sequence on the inductively plasma power which determines the plasma density and therefore finally the ion current).

All show the same general behaviour: at low bias voltages only h-BN is obtained, at a certain transition voltage which depends on the plasma density, c-BN is also deposited and the c-BN content increases up to a maximum. With a further increase of the bias voltage, the c-BN content decreases again and finally drops down to zero. Under this conditions, again sp^2 bonded BN is deposited which was named x-BN because its detailed structure is unclear so far. In this case, nonstoichiometry prevents c-BN deposition (see discussion below about secondary mechanisms). The onset of the c-BN deposition is shifted to higher ion energies with lower ion currents (lower inductive power). A similar behaviour is found with decreasing substrate temperature. These effects can be well explained by the sputter model because in both cases, increasing material loss processes (sputtering and thermal resorption, respectively) lead to a reduction of incorporated material. Therefore, a lower ion current is sufficient to reach the same number of ions per deposited boron atoms which figure 1 shows to be the relevant parameter. Furthermore, a reduction of the growth rates found with increasing ion energy and substrate temperature directly reflects the above effect. Therefore, it can be concluded that the behaviour of the primary deposition parameters found with our ICP experiments is in good agreement with the sputter model, which originally was derived from PVD data. With figure 1, it could be shown that even quantitatively, CVD and PVD use the same primary deposition parameters, a central result of our work which was achieved due to a close interaction of experimental (ICP deposition) and theoretical work (sputter model). Up to now, only the growth process of c-BN has been addressed (i.e. the addition of c-BN on a c-BN film). Nevertheless the initial formation of c-BN is of great importance and up to now only transmission electron microscopy (TEM) investigations of PVD films exist. All of them find a sequence of a thin amorphous layer, followed by a h-BN layer and finally the nanocrystalline c-BN. The h-BN is textured with its c-axis parallel to the substrate surface. An investigation of PVD films performed in cooperation with the University of Konstanz revealed an orientational relationship between the (0002) plane of the textured h-BN and the (111) plane of the c-BN on top of it. A very similar relationship was found to strongly enhance the nucleation effectivity in case of diamond deposition on HOPG. Although the poor mechanical properties of the c-BN films deposited with the ICP method prevented a TEM investigation, the nucleation sequence was investigated indirectly by a combination of infrared spectroscopy, ellipsometry, TED and elastic recoil detection (ERD). In principle, the same nucleation sequence as with PVD was found but in contrast to PVD, the textured h-BN layer was less dense and only partly textured. This may decrease the nucleation effectivity and lead to thicker nucleation layers as well as a lower c-BN contents which both are characteristic for CVD c-BN films. Although the nucleation process can not be described by the sputter model, the experimental findings are not contradiction with it. On the contrary, the great differences between nucleation and growth processes point out that different mechanisms occur. Above, it has been shown that nucleation as well as growth of ion assisted CVD and PVD rely on the same basic mechanisms. Slight differences were found in the nucleation step and further experimental investigations showed that besides the primary physical mechanisms additional secondary mechanisms influence c-BN growth. The most important ones are stoichiometry and the effect of hydrogen which will be discussed in the following section.

C-BN films were found to exhibit a nearly stoichiometric B/N ratio. From our own as well as literature data, a narrow range between 0.9 and 1.1 was estimated

to be suited for c-BN deposition. Although the mechanism by which nonstoichiometry prevents c-BN formation is not clear so far, at least the reasons for its occurrence can be investigated. Therefore, a detailed analysis of several bias voltage sequences was performed which revealed an interesting general behaviour: At zero bias, the films are stoichiometric h-BN and the hexagonal layers are oriented in plane of the substrate. With increasing bias voltage, the B/N ratio increases and the hexagonal layers tend to orientate perpendicular to the substrate surface. With the onset of c-BN deposition, the B/N ratio drops down to a nearly stoichiometric value and increases again. Finally, x-BN is reached which is markedly different from h-BN achieved with low ion bombardment. It is boron rich, contains a high carbon content and exhibits a strange surface morphology. Furthermore, it shows additional features in infrared absorption. The B/N ratios found lay always above the upper stoichiometry limit of 1.1 preventing the growth of c-BN. On the other hand, high boron and carbon contents are known to reduce the sputter yields of BN films so that x-BN is even more stable under ion bombardment than c-BN and can therefore exist at higher ion energies. The B/N ratio of a deposited film is not only governed by the relevant boron and nitrogen fluxes to the surface but also by sputter processes. From investigations of similar systems, nitrogen is expected to be sputtered preferentially. The influence of this effect on the B/N ratio is most pronounced close to the 'no growth' condition. Assuming a stronger preferential sputtering for h-BN than in case of c-BN, the experimental data can be well explained. Therefore, the drastic changes of the B/N ratio at the phase transitions indicate changes in the sputter conditions and again point out the relevance of sputter processes in c-BN deposition. Systematic changes in the B/N ratio were also observed in the nucleation layer, but their implications for the nucleation process are not clear up to now. The main difference between CVD and PVD deposition is the existence of hydrogen in the gas phase of the first method. Therefore, the influence of hydrogen was investigated by deposition experiments as well as by film characterization with ERD. Addition of small amounts of hydrogen in ICI² deposition prevented c-BN formation although the physical deposition parameters remained nearly unchanged. Hydrogen is regarded to be detrimental for c-BN deposition which is in agreement with the fact that in CVD an upper boundary of about 75 % c-BN exists whereas with PVD nearly 100 % c-BN can be achieved. Interestingly, the addition of hydrogen did not affect c-BN nucleation; if after the nucleation process hydrogen addition was stopped, c-BN grew immediately. This again is a hint of fundamental differences between c-BN nucleation and growth. ERD measurements which were performed at the Technical University of Munich showed hydrogen to be mostly located in the sp² fractions of the films, especially the nucleation layer. Infrared spectroscopy showed only small amounts of the hydrogen to be bonded in the BN lattice. In light of this, the destruction of the crystalline lattice due to hydrogen can not be the main reason for c-BN suppression, and the fundamental mechanisms are not clear so far.

C-BN films deposited with ion assisted methods do not fulfill the requirements of industrial processes. The most important problem is the poor adhesion which is a consequence of a large stress within the coatings and a low adhesion strength between the film and the substrate. Some measures of stress reduction and adhesion improvement have been reported in literature so far but these up to now are more or less isolated empirical results. In light of this, a model based on the sputter model and experimental findings was developed to describe the build-

up of compressive stress. Very briefly, the stress is regarded to be proportional to the fraction of interstitial atoms which itself is modelled by a balance of ion induced interstitial production and thermal as well as ion induced interstitial relaxation. Despite the simplicity of the model it is able to describe the experimental tendencies correctly. It predicts the stress to be reducible by using high ion energies, high angles of ion incidence and high substrate temperatures. Furthermore, conventional measures of stress reduction like post-deposition annealing and interlayers between substrate and c-BN film fit well into the context of the model. Further, the question of improvement of the adhesion strength between film and substrate has to be addressed. The underlying physical mechanisms are quite complex, especially if one takes the nucleation sequence into account. One strategy may be to try to avoid the textured h-BN layer. This is probably the weakest link limiting adhesion either by its mechanical properties or by a chemical instability with respect to water.

For films prepared by ECR-microwave in Belgium, the chemical composition obtained by AES was compared for four different types of gas mixtures: $N_2 + B_2H_6/Ar$, $NH_3 + B_2H_6/Ar$, $NH_3 + MB$, $N_2 + TMB$. If B_2H_6 was used as the boron precursor, there was no clear difference between the films prepared with N_2 and NH_3 . The films were contaminated with C and O at the surface due to atmosphere exposure but the contamination level was very low in the bulk. If TMB was used as the boron precursor, the films were carbon contaminated in the bulk. For identical deposition conditions (including the B/N ratio in the gas phase), the use of NH_3 in place of N_2 reduced the C/N ratio in the film. The H α created by the decomposition of NH_3 in the plasma and detected by optical emission spectroscopy, was probably etching the carbonaceous component. This effect was not present if N_2 was used. Another effect of NH_3 as nitrogen precursor was to reduce drastically the ion density and to increase the electron temperature in the plasma, thus modifying the growth conditions for all other parameters kept identical. This was most probably related to the presence of hydrogen in the plasma, it could affect the quality of the deposited films as mentioned in reference [6]. In the case of a TMB + N_2 mixture, increasing the temperature from 523 to 673 K reduced the carbon and oxygen content of the films. Most of the C and O containing species were probably desorbing in between these two temperatures. After an initial rise of the B/N ratio perhaps due to preferential sputtering, the composition was homogeneous in the bulk of the films, as shown by sputter depth profiling (figure 3). This type of profile was also observed by other groups [7]. We did not detect any influence of the distance from the coil on the composition of the ICP films.

The treatments of substrates (ex-situ or in-situ) had basically no major influence on the adhesion of the films. The most important factor affecting this property was the B/N ratio in the gas phase and so in the films. Increasing the B/N ratio resulted in flaking of the films and in a high sensitivity to moisture at the substrate-deposit interface independent of the preparation method. The sensitivity to moisture was very well localized at the substrate-film interface and could probably indicate a higher boron concentration at that level. The surface structure was not affected by moisture. Layer deposited on silicon and steel were stable in air (B/N ratio close to 1) and withstood the tape adhesion test and scratch test with a steel needle. The films prepared by both methods were made of micro- or nanocrystallites 10 to 50 nm large, uniformly spread on the whole surface. The microstructure did not change with the substrate. The films prepared by ICP and ECR-microwave could not be distinguished by their

microstructure. No major influence of other parameters like temperature or substrate bias could be detected.

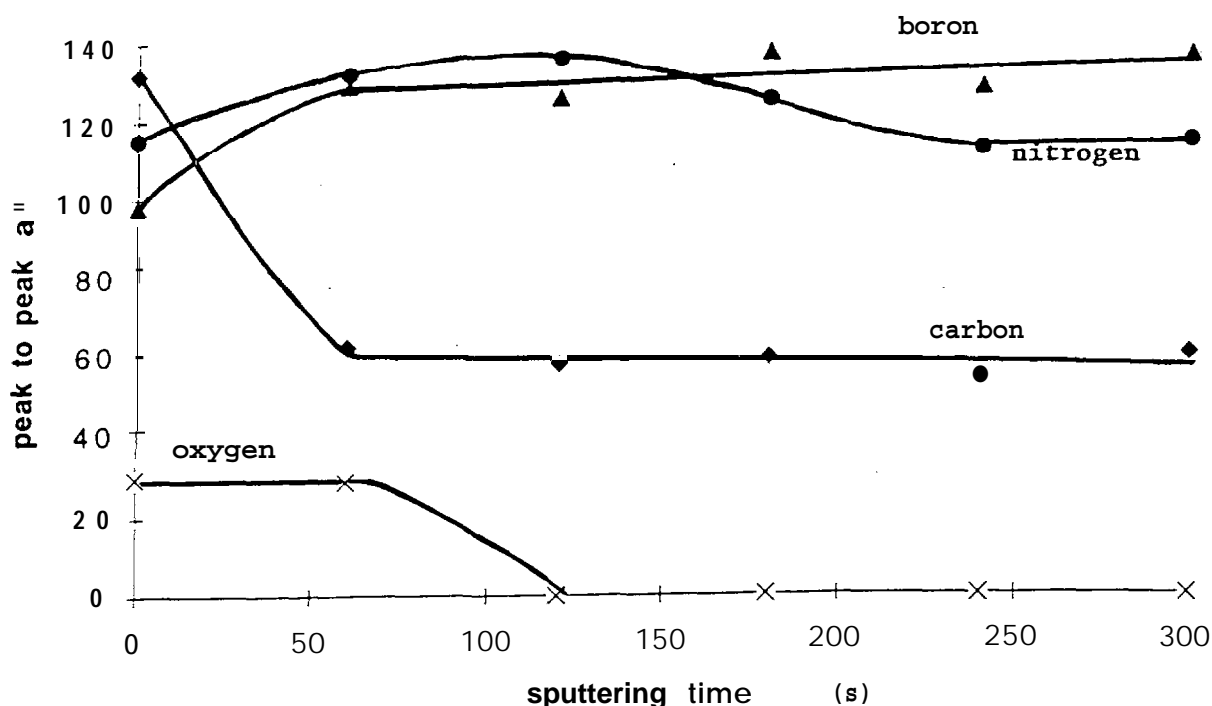


figure 3: AES depth profile of a BN film prepared by ECR-microwave with TMB as boron precursor

As the deposition of passivating and insulating films onto III/V semiconductor surfaces is still a major problem to be overcome in the developing III/V technology, we tried to deposit boron nitride on n type InP by ECR-microwave in absence of bias. The ion bombardment induced a segregation of the iridium at the surface of the InP substrate. The process was too energetic for the sensitive nature of these surfaces.

In the range between 400 and 4000 wavenumbers, IR spectra of c-BN containing films exhibited only three distinct peaks at more or less 1080, 1380, and 800 cm^{-1} . These peaks were representative respectively of the c-BN reststrahlen band, the h-BN in plane stretching and out of plane bending vibrations. The 1380 and 800 cm^{-1} peaks are also present for other sp^2 phases of BN, so IR spectra did not tell us which form we were producing with precision. The characteristic c-BN peak at 1080 cm^{-1} was only detected for films prepared by ECR-microwave plasma at high bias voltage (-150 V) with substrates close to the ionization region. Similar IR spectra were obtained with $\text{B}_2\text{H}_6/\text{Ar} + \text{N}_2$, and TMB + NH_3 mixtures. The width at half height of the c-BN peak was very narrow in comparison with the published results of other groups. This feature was related to the film itself and not to the substrate as proven by cross checking the IR spectrum of the substrate. By ICI, we never obtained the characteristic peak of c-BN, but spectra of h-BN very similar to those published by other authors for films deposited by ICP in the

absence of or with a low substrate bias -20, -50 V). The peak shapes were not influenced by the applied d.c. bias and by the substrate temperature (200-500°C). Since all forms of BN are electrical insulators, it was very probable that after several nanometers of deposit, the resulting layer prevented the development of a high enough negative potential at the surface of the growing film in such a way that ion bombardment was not energetic or intense enough to favor the growth of the c-BN phase.

The effect of deposition parameters on the deposition rate was also investigated. In ICP, increasing the bias induced a decrease of the deposition rate. This seemed to indicate that despite the insulating character of the depositing layer, ion bombardment was still present and was affecting adsorbed species. In the absence of bias or with a bias of -50V, increasing the temperature from 220°C to 475°C increased the deposition rate from 126 nm/hr to 168 nm/hr. The distance separating the substrate from the coil influenced greatly the deposition rate it dropped by a factor 1.8 at a distance of 25mm. This decrease in the deposition rate with distance was not accompanied with a change in the composition.

For films deposited by ECR-microwave plasma, the deposition rate was dropping from 540 nm/hr to 120 nm/hr when the substrate bias was varied from -10 to -150 V. This variation of the deposition rate was accompanied by a substantial variation of the composition: the B/N ratio in the film decreased from 2 at -70 V bias to 1 at -150 V bias. This indicated a major contribution of the sputtering phenomenon in agreement with the sputter model. Depositions carried on onto silicon wafers, 100 mm in diameter, showed a maximum thickness variation of 20 % (measured between the center and the far edge of the wafer). This is a major advantage of the ECR-microwave method.

Samples prepared in the ICP machine were examined by atomic force microscopy (AFM) to evaluate their roughness and grain size. All images were taken in air with force ranging between 10^{-8} and 10^{-9} N. The roughness was determined on lengths of 2 μm and averaged on segments in different areas of the same films.

The smoothest film were prepared at low temperature and without any bias. This very low roughness (RMS roughness = 2-3 nm, T=230°C) of films deposited on silicon wafers was associated with the absence of crystallinity. A d.c. bias of -150 V was associated to an increase by a factor of three of the roughness (RMS roughness = 10-11 nm, T=250°C), but a bias of -50V did not modify significantly the roughness. The threshold for ion erosion was probably not reached for this bias value. Increasing the temperature from 200°C to 500°C increased the roughness by a factor of two (from 2-3 nm to 6-7 nm). This increase was probably associated to the increase in the crystallinity of the films. By electron microscopy, crystallites of few nanometers were observed for the high temperature films. Nevertheless, no significant signal could be obtained by X-ray diffraction.

5. Conclusions

Great progress has been achieved compared to the state of the art of c-BN deposition at the beginning of the project. An extensive data collection reduced the uncertainties concerning c-BN deposition existing so far. Due to the knowledge of the required deposition parameters, the ICP deposition method could be adapted successfully to c-BN deposition.

A model was developed which showed selective sputtering of h-BN to be the dominating mechanism for c-BN deposition. This model is in good quantitative

agreement with ion assisted CVD as well PVD experiments and shows both to rely on the same parameter ranges. C-BN nucleation was investigated experimentally revealing also in this point the same principle mechanisms in CVD and PVD. With PVD, lattice matching between the nucleation layer and the c-BN on top of it was found which is expected to strongly influence the nucleation step. Further experimental work showed hydrogen to be detrimental for c-BN growth which can explain some slight differences between CVD and PVD deposition. Furthermore, the effect of stoichiometry was investigated which led to the discovery of a preferential nitrogen sputtering mechanism.

The comparison of two boron precursor showed that the contamination level is highly reduced by the use of B₂H₆. Films containing a fraction of c-BN were also prepared by ECR-microwave method for high ion density and ion energy in agreement with the proposed model. In addition this method is very promising in terms of up-scaling as homogeneous deposits can be obtained for substrates larger than 50 mm in diameter.

Due to adhesion failure, c-BN films are not suited for industrial applications so far. Concerning this, the situation is comparable to the knowledge about the basic deposition process at the beginning of this project: isolated studies exist but a general concept and systematic investigations are missing so far. First approaches, which include a simple model of stress build-up were undertaken to solve this problem. However, a large quantity of experimental as well as theoretical work is necessary to get more insight into this complex phenomenon. It is expected that the quality of c-BN films strongly benefits from a more detailed understanding of the deposition process.

References

- [1] R.H. Wentorf, J. Chem. Phys. 26 (1957) 956
- [2] L. Vel, G. Demazeau, J. Etourneau, Mat. Sci. Eng. B 10 (1991) 149
- [3] C. Weissmantel, K. Bewiloga, D. Dietrich, H.J. Erler, H.J. Hinneberg, S. Klose, W. Nowick, G. Reisse, Thin Solid Films 153 (1987) 1
- [4] S. Reinke, M. Kuhr, W. Kulisch and R. Kassing, Invited Paper presented at the Diamond Films 94 Conference, 11 Ciocco, Italy, September, 1994.
- [5] K.-H. Kretschmer, K. Matl, G. Lorenz, I. Kessler, B. Dumbacher, Solid State Technology 33(2) (1990) 53
- [6] T. Ichiki, M. Takamura, T. Yoshida, Proc. Jpn. Symp. Plasma Chem. 4 (1991) 227
- [7] T. Ichiki, T. Yoshida, Appl. Phys. Lett. 64 (7) (1994) 851

Acknowledgements

The work presented in this paper was supported by the European Community under the BRITE-EURAM contract BREU-390 [BE-4484-89].

The authors would like to acknowledge the help of the following persons: Prof. J.C. Bauwens and Dr. N. Heymans for FTIR analysis, Dr. W. Scholtz for micrographs, Dr. Segers for fruitful discussions, J.M. Vanseveren for the AES analysis, and C. Maboge for technical assistance and devices realization.



EUROPEAN COMMISSION

DIRECTORATE GENERAL XII

SCIENCE, RESEARCH AND DEVELOPMENT

DIRECTORATE C INDUSTRIAL AND MATERIALS TECHNOLOGIES

Unit C-4 : Research & Horizontal Issues.

Head of Unit, a.i

Brussels, May2, 1996
NH/abd

Note to the File

Subject: BRITE-EuRAM Project No. 4484
"Cubic Boron Nitride Films"

This basic research project has tackled the tough problem of generating, and understanding the mechanisms of deposition of, high-performance thin surface films. Cubic Boron Nitride has attractive properties for the production of extremely hard films and also films which have certain electrical and optical properties. These relatively "high tech" surface films, usually of a few microns thickness, are of particular interest where either highly durable critical surfaces are required (i.e. wear resistance, corrosion resistance, etc.) or where certain electrical insulating properties are required. Examples for the latter include parts for electro-mechanical devices, micro-electronic circuits, capacitors, etc.

The attraction of Cubic Boron Nitride is firstly that the source elements, carbon, boron and nitrogen are extremely abundant, and secondly that the mechanical properties of these films are second only to diamond. Cubic Boron Nitride has the potential of a cheap and versatile alternative to diamond layers.

The principal disadvantage of working with Cubic Boron Nitride is that the precise deposition parameters must be absolutely correct in order to generate good quality films. The most favorable technique of achieving deposition is to "grow" the films under plasma activated chemical vapour deposition (PACVD). This process involves the electrical discharge at relatively low pressure of different chemical species in order to produce a solid, adherent, deposit on the item to be coated.

Cubic Boron Nitride can exist in many stable forms, but only a very precise formulation is the correct one for surface durability and/or electronic and optical properties. The project team have not only managed to establish the optimum conditions for producing high quality films, but they have also managed to produce surface films of acceptable performance.

The need now is to demonstrate the technology on industrial size parts, and to carry out an effective market survey in this highly competitive field. No patents have been filed.

cc: Mr. P. Trousson


N. Hartley

NH

Project #: 4484

End date: ,31108195

Cost (MECU): ?

Title: In-Situ Control of Plasma Chemical Vapour Deposited Cubic Boron Nitride Films

Achievements: Production and characterisation of high performance thin surface coatings.

Needs:

Project Partners: Univ. Libre de Bruxelles (B), Gesamthochschule Kassel Univ. (D)

Contact Person: R. Winand, tél. +32.2.650.30.10 (Head of Department)

Responsible Scientist: Dr. Marie-Paul Delplancke-Oglethorpe, ULB

If available:

Forseen Economic Gain (MECU): 10 x Costs Time to market

(from end date, in months) : 36

Estimated costs to exploit (MECU): ?

Patrick -

Rather more than 10 lines, but at least you have a text now!

me

In order to prepare a meeting with Venture Capitalist, the following finished projects have been selected because they mentioned (in the PQI) the fact that **they** would need access to venture capital.

a 10-lines text answering the following :

a) achievements :

- what is it ?
- useful to
- potential customers are . . .
- patent situation (ownership is . . .)
- planed exploitation

b) needs :

- general needs
- need of venture capital in order to . . .

Thank you in advance

Mechanisms in ion induced c-BN growth

S. Reinke, M. Kuhr and W. Kulisch

University of Kassel, Institute of Technical Physics, Heinrich Plett Strasse 40, 34109 Kassel (Germany)

Abstract

A literature survey on ion beam assisted deposition of boron nitride shows well defined ranges (domains) of microscopic parameters in which different phases of boron nitride occur. These are interpreted in terms of a growth model in which temperature dependent resorption of incoming material and selective sputtering of h-BN play dominating roles. This concept is transferred to chemical vapour deposition in which microscopic parameters cannot be quantified well. For this case a simple rule is developed which also shows the influence of sputtering during deposition. c-BN is compared with diamond-like carbon with respect to dominating deposition mechanisms.

1. Introduction

In recent years, much work on c-BN film formation has been performed with physical vapour deposition techniques such as ion beam assisted deposition (IBAD) [1-5], ion plating [6-8] and r.f. sputtering [9, 10]. Also chemical vapour deposition (CVD) techniques such as electron cyclotron resonance CVD [11, 12] and r.f. CVD [13, 14] have been used successfully. In all these techniques impact of "energetic ions" onto the growing BN film occurs. Our aim was to investigate the role of ion "bombardment during deposition and to identify basic mechanisms. Collected experimental data are interpreted in terms of a growth model which is also applicable to CVD.

2. Data collection

The following is a list of relevant microscopic deposition parameters: boron striking rate F_B (the number of boron atoms striking the substrate per unit time and area); ion flux F_{ion} ; ion energy E_{ion} ; ion angle of incidence Θ ; ion mass (distribution); substrate temperature T_s .

In IBAD these parameters can be measured and controlled independently. Thus from a collection of IBAD data, information about the basic mechanisms in c-BN growth can be gathered. Details of our data evaluation are given elsewhere [15]. For a flux independent description of the deposition process, the ion to atom arrival ratio $F = F_{ion}/F_B$ is introduced. In Fig. 1, all available data points for 1:1 mixtures of argon and nitrogen at temperatures between 350 and 400 °C are given in an E_{ion} - F plot. The data of Djouadi *et al.* [4] seem to be shifted about 150 eV on the energy scale which can be attributed at least in part to different

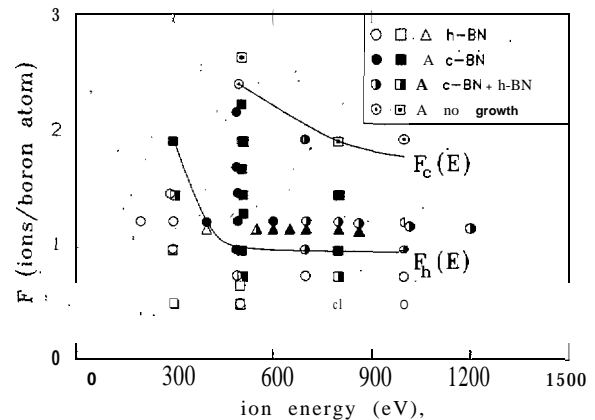


Fig. 1. Dependence of the structure of ion beam assisted deposition BN films on ion energy E_{ion} and the ion to boron atom arrival ratio "F": circles, data from Tanabe *et al.* [2]; squares, data from Kester and Messier [1]; triangles, data from Djouadi *et al.* [4].

reference potentials, (anode or cathode) in the evaluation of the acceleration voltage [16].

In Fig. 2 all available data with a fixed ion energy, 500 eV (600 eV for Djouadi *et al.*) are shown. Figures 1 and 2 both show h-B-N for low F values, and with increasing ion bombardment a sharp transition to c-BN. If the ion flux is increased further, no net film growth can be detected. At high energies a transition from pure c-BN to a mixture of h-BN and c-BN is observed [2, 17] which is commonly attributed to radiation damage processes and is not treated further here.

3. Basic mechanisms

For all points, lying on, the boundaries F_c (see Figs. 1 and 2), the yield of removed material equals the growth

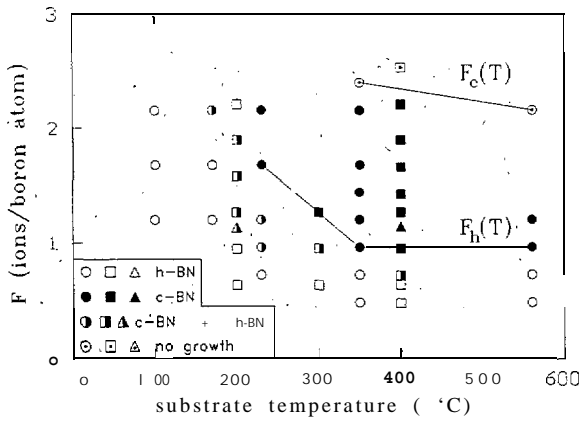


Fig. 2. Dependence of the structure of ion beam assisted deposition BN films on substrate temperature T_s and ion to boron atom arrival ratio F : circles, data from Tanabe *et al.* [3]; squares, data from Kester and Messier [1]; triangles; data from Djouadi *et al.* [4].

rate, so no net growth occurs. Two effects can be responsible for this 'material loss'. First, incoming boron atoms may have a temperature dependent sticking probability less than unity, thus some of them desorb. Second, the energetic ions may sputter part of the 'already deposited' material. The term resorption is used in the following for all 'material striking the surface that is removed not by collision cascades due to ion bombardment. To fulfill a no growth condition the removal rate of c-BN per incoming ion Y_c^* must be twice the rate of incoming boron atoms per ion $F_c^{-1}(E, T)$. The factor 2 occurs because with every boron atom also one nitrogen atom has to be removed. Surplus nitrogen diffuses out of the film and desorbs (see Fig. 3, right hand side):

$$\frac{2}{F_c(E, T)} = Y_c^*(E, T) = \frac{Y_c(E)}{SC(T)} \quad (1)$$

$Y_c(E)$ denotes the energy dependent sputter yield of

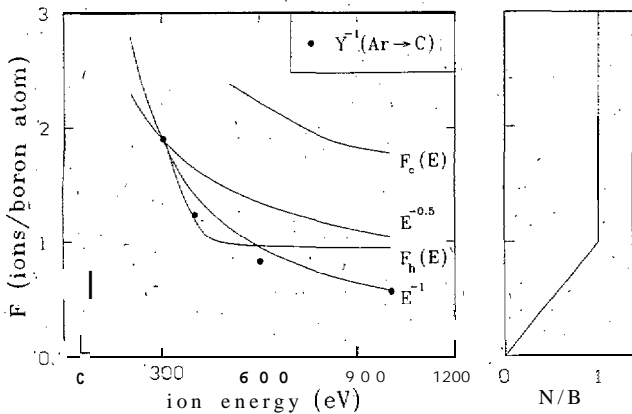


Fig. 3. Energy dependence of the boundary F_h compared with different models; \bullet , inverse proportional sputter yield Ar \rightarrow graphite [18] fitted to F_h at 300 eV. Right hand side: film comparison (N/B ratio) as a function of F (shown schematically).

c-BN and $s(T)$ the temperature dependent sticking probability of the incoming boron atoms on c-BN. It should be, 'noted that eqn. (1) reads in units of atoms per "ion. The right-hand side of eqn. (1) indicates the difference between the removal rate. and the corresponding sputter yield. If for example $s_c = 0.5$, the removal rate equals twice the sputter yield because every second atom is desorbed.

Let us, now focus on the boundary F_h between the h-BN and the c-BN domains. No pure c-BN is observed with F values lower than unity representing the condition for film stoichiometry [15]. For low ion energies and substrate temperatures the boundary F_h rises to higher F values. Let us assume that F_h also represents a "no" growth condition, this time for h-BN. The corresponding removal rate of h-BN, Y_h^* , must than be similar to eqn. (1)

$$\frac{2}{F_h(E, T)} = Y_h^*(E, T) = \frac{Y_h(E)}{s_h(T)} \quad (2)$$

where $Y_h(E)$ denotes the sputter yield of h-BN and s_h the sticking probability of boron on h-BN.

3.1. Deposition parameters .

Figure 1 clearly indicates c-BN deposition to be a function of the ion energy. At fixed temperatures it follows from eqn. (2) that the energy dependency of $F_h(E)$ should be inversely proportional to $Y_h(E)$. To our knowledge $Y_h(E)$ is not known, therefore we compare the energy dependence of the similar system Ar \rightarrow graphite [18], fitted at 300 eV. As can be seen from Fig. 3, $F_h(E)$ is well reproduced for energies below 500 eV. The right side of Fig. 3 indicates that correct stoichiometry of $[N]/[B] = 1$ is a necessary condition for c-BN growth determining ' F_h at energies above 500 eV. Also shown in Fig. 3 are the energy dependence $F \propto E^{-0.5}$ and $F \propto E^{-1}$. The first does not fit the data well, showing that Kester's proposal [1] of ion momentum per boron atom being the decisive quantity in c-BN deposition is not supported. The $F \propto E^{-1}$ dependence fits reasonably well. This is no contradiction to our model because in the relevant energy range the sputter yields of light elements are often found to be nearly proportional to the ion energy [19]. From eqns. (1) and (2) it follows for the ratio of the sputter yields of h-BN and c-BN that

$$\frac{Y_h}{Y_c} = \frac{F_c s_h}{F_h s_c} \quad (3)$$

Assuming the sticking probability to be independent" of the crystal structure, a selectivity in the sputter yield like $Y_h/Y_c \approx F_c/F_h = 2.4$ is determined from Fig. 1 (at 500 eV). Preferential etching of h-BN has already been observed in the literature [11, 14]. Correcting the reported etch

rates by film densities yields $Y_h/Y_c \approx 2$, showing indeed that preferential sputtering occurs.

As can be seen from Fig. 2, the c-BN domain is also temperature dependent, Below 350 °C $F_h(E)$ rises to higher F values with decreasing T_s . Since sputter processes have been shown to be temperature independent [21], resorption processes have to be responsible for this. With a fixed sputter yield, from eqn. (2) follows $F_h(T) \propto s_h(T)$. This means that at low temperatures, where the sticking probability of incoming boron atoms is close to unity, high values of F_h are expected which decrease with temperature owing to resorption processes ($s_h < 1$). This is actually observed in Fig. 2 between 230 and 350 °C. The flat dependence at high temperatures is again attributed to film stoichiometry.

Investigations of c-BN deposition with different masses of bombarding ions (Ar, Kr, Xe) showed a sharp threshold in momentum per boron atom, $p/a = F(2myE)^{0.5}$, separating the h-BN and c-BN domains [1]. E denotes the ion energy, m and M ion and target masses respectively and $y = 4mM/(m + M)^2$. As shown above, the derived energy dependence $F_h \propto E^{-0.5}$ does not fit the experimental data. However, the mass dependence of p/a could be the reason for the observed threshold. In Table 1 (again for Ar → graphite) it is seen that the mass dependence of sputter yields, can be approximated well by $Y \propto (\gamma m)^{0.5}$, thus showing that our model is able to explain the above findings.

3.2. Material loss

Sputtering and resorption both lead to material loss during deposition. Therefore, the probability of incoming boron atoms being incorporated into the growing BN film p_B can be calculated from the measured boron flux R_B and growth rate of BN films R_{BN} . As expected, Table 2 shows that strong material loss occurs under

TABLE 1. Dependence $(\gamma m)^{0.5}$ fitted to sputter yields Y of Xe, Kr [22] and Ar [18] on graphite at 600 eV

Ion	Y	$(\gamma m)^{0.5}$ (au.)
Xe	0.21	0.21
Kr	0.17	0.189
Ar	0.15	0.146

TABLE 2. Deposition conditions and growth rates of different experiments

Reference	E_{ion} (eV.)	F	T_s (°C)	R_B (nm rein ⁻² *)	R_{BN} (nm rein ⁻¹ .)	Modification	p_B
2	300	1.23	350	3.3	2.5	h-BN	0.3
2	1200	1.23	350	3.3	0.42	Mixed	≈ 0.06
2,3	500	1.23	350	3.3	0.83	c-BN	0.16
5	500	1.08-2.2	Water cooled	18	8.4-13.8	c-BN	0.29-0.47

The abbreviations are explained in the text. p_B was calculated assuming densities $\rho_B = 2.48$, $\rho_h = 2.29$ and $\rho_c = 3.48$ g cm⁻³ for boron, h-BN and c-BN respectively.

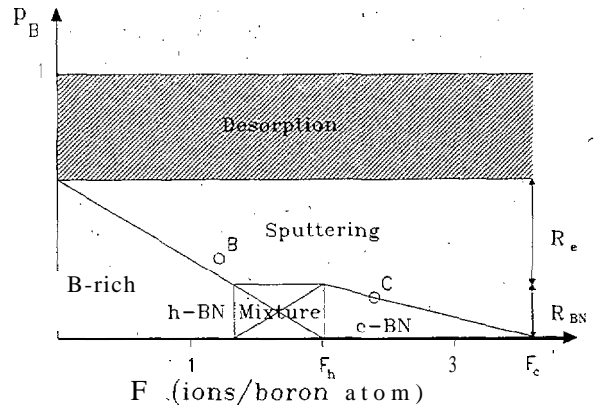


Fig. 4. Predicted dependence of the boron incorporation probability p_B on the ion to boron atom arrival ratio F .

c-BN deposition conditions. The consequences of our model with respect to the incorporation-probability are shown schematically in Fig. 4 for 300 eV and 350 °C. A certain amount of boron is removed via resorption, indicated by the hatched region. If ion bombardment is now taken into account, this results in a linear decrease in p_B down to F_h where h-BN is no longer stable. The c-BN domain will also show a linear decrease in p_B with increasing F down to F_c where the no growth boundary is reached. Points B and C represent p_B values from Table 2 at 350 °C relative to F_h (40% below and 2W0 above F_h) respectively. "Between the two domains a mixed phase occurs" for which no growth rate data are available. Although there are many uncertainties, Fig. 4 shows our model to predict the trends correctly. It seems as if c-BN only has a chance to grow if h-BN is not stable with respect to ion bombardment, Below F_h , c-BN nucleation sites are probably instantly grown over by h-BN which is the thermodynamic stable modification.

Temperature also affects p_B . Figure 5 shows schematically the behaviour at two different substrate temperatures and fixed ion energy of 500 eV. At 350 °C the situation is the same as shown in Fig. 4. Low substrate temperatures lead to an increase in F_h (and probably also F_c). Also p_B is expected to increase. Actually, from Table 2 it can be seen that for c-BN p_B is distinctly higher with a water cooled substrate holder (0.29-0.46) than at 350 °C (0.16).

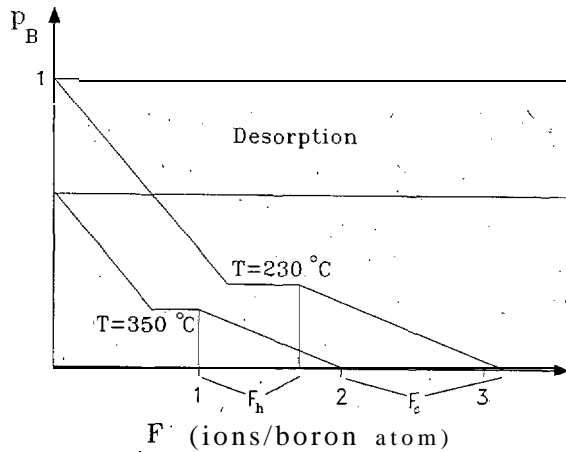


Fig. 5. Influence of the substrate temperature on the dependence of the boron incorporation rate p_B on the ion to boron atom arrival ratio F .

3.3. Chemical vapour deposition of c-BN

In CVD of c-BN with the methods cited above, massive ion bombardment of the growing film can also be expected but the parameter F and also the ion energy cannot be determined. Nevertheless, the integrated effect of ion bombardment can be evaluated by measuring the etch rate R_e of h-BN films under deposition-like conditions without boron source gas. Also, the net growth rate of BN films R_{BN} can be easily determined. In Table 3 we compare typical data for the ratio $R = R_e/R_{BN}$ for different CVD experiments showing that $R > 2$ can be regarded as a necessary condition for c-BN growth. This is in accordance with Fig. 4 where R_e and R_{BN} are indicated schematically. The condition $R > 2$ again shows that most of the incoming material must be removed via sputter processes.

Yokoyama *et al.* [12] used very low ion energies close to the sputter threshold and measured typical ion current densities of $5 \mu\text{A cm}^{-2}$. For similar plasma conditions without substrate-bias they observed a growth rate of 13 nm min^{-1} . From this, $F = 28$ can be calculated. It seems that it is possible to compensate low ion energies with high F values if only the condition $R > 2$ is fulfilled. Other successful CVD experiments probably lie in between the parameter range of Yokoyama *et al.* and the IBAD range.

TABLE 3. Growth parameters for CVD c-BN deposition

Reference	Bias voltage (eV)	R_e (rim min ⁻¹)	R_{BN} (nm min ⁻¹)	$R = R_e/R_{BN}$
20	200	28	14	2.0
24	600	8	3.6	2.2
12	15+15 PP	12	2.4	5.0

R_e etch rate of h-BN under deposition-like conditions; R_{BN} growth rates of deposited c-BN films. PP stands for plasma potential.

4. Discussion

c-BN is often, compared with sp^3 bonded carbon modifications such as diamond and diamond-like carbon (DLC). In Table 4 typical deposition conditions of DLC and c-BN are compared showing distinct differences, for example in the ion energy. Therefore, theoretical approaches to DLC [25] cannot be transferred to c-BN because the energy at which the maximum sp^3 content is predicted for DLC is closely related to the displacement energy. This quantity surely is not that different for BN. McKenzie *et al.* proposed that film stress creates high pressure like conditions in thin film DLC growth [26] and extended this concept to c-BN [27]. Nevertheless, it remains unclear how the transition of deposited h-BN (no stress at the surface) to c-BN in deeper layers can occur at low substrate temperatures. In our opinion the different deposition conditions and the fact that sputter processes play no role in DLC deposition are hints that different effects dominate in DLC and c-BN deposition.

In the deposition of metastable materials (e.g. diamond, DLC or c-BN) generally two steps have to be distinguished: nucleation and growth. Recent investigations of the very first stage of c-BN deposition with transmission electron microscopy and IR spectroscopy showed that first a thin layer of amorphous material (2 nm) and then a layer of h-BN (2-5 nm) is deposited until c-BN grows [28]. The h-BN layer is textured with the c-axis parallel to the substrate surface, perhaps as a result of compressive stress. This is not in contradiction

TABLE 4. Comparison of deposition conditions and film properties of DLC and c-BN

	DLC	c-BN
T_s (°C)	< 150	up to 850
E_{ion} (eV)	<150	up to 800
F (ions per C, B-atom)	≈ 1	>1
Sputtering	Plays no role	Dominant
Transition $sp^2 \rightarrow sp^3$	Smooth	Sharp
Film crystallinity	Amorphous	Nanocrystalline (5-20 nm)
Maximum sp^3 content (%)	90	95

to our model if one assumes that under these conditions the ion range is enhanced, leading to a reduction in sputter yield (channeling effect). This seems reasonable if one keeps in mind the bond lengths in h-BN of approximately 3,33 Å in the c-direction and 1.45 Å perpendicular to this direction.

5. Summary

It must be stated that the nucleation process in c-BN deposition" is not yet understood at all. For the growth phase it was shown that processes leading to the removal of material play a decisive role. This can be seen directly in the low boron incorporation probabilities (below 0.5). The dependence of the c-BN domain on ion energy, substrate temperature and ion mass have been interpreted in terms of sputtering and resorption" processes. c-BN deposition takes place just beneath the resputter region, and the sputter yield of c-BN was found to be lower than that of h-BN. From these facts the experimentally observed c-BN domain is a logical consequence. Additionally, film stoichiometry has been found to be a necessary condition for c-BN growth. Measurements of the dependence on the angle of incidence of the c-BN domain and of the energy and ion mass dependence of the h-BN and c-BN sputter yields may be suitable" tests for our model.

References

- 1 D. J. Kester and R. Messier, *J. Appl. Phys.*, 72 (1992) 504.
- 2 N. Tanabe, T. Hayashi and M. Iwaki, *Diamond Relat. Mater.*, 1 (1992) 883.
- 3 N. Tanabe, T. Hayashi and M. Iwaki, *Diamond Relat. Mater.*, 1 (1992) 151.
- 4 M. A. Djouadi, D. Bouchier, P. Möller and G. Sene, paper presented at 9th Int. Colloq. on Plasma Processes (CIP93), Antibes, June 1993, Société Française du Vide.
- 5 M. Sueda, T. Kobayashi, H. Tsukamoto, T. Rokkaku, S. Morimoto, Y. Fukaya, N. Yamashita and T. Wada, *Thin Solid Films*, 228 (1993) 97.
- 6 T. Ikeda, T. Satou and H. Satoh, *Surf. Coat. Technol.*, 50(1991).
- 7 K. Inagawa, K. Watanabe, K. Saitoh, Y. Yuchi and A. Itoh, *Surf. Coat. Technol.*, 39-40(1989) 253.
- 8 M. Murakawa and S. Watanabe, *Surf. Coat. Technol.*, 43-44 (1990) 128.
- 9 M. Mieno and T. Yoshida, *Surf. Coat. Technol.*, 52(1992) 87.
- 10 K. Bewilogua, J. Buth, H. Hübsch and M. Grischke, *Diamond Relat. Mater.*, 2 (1993) 1206.
- 11 A. Weber, U. Bringmann, R. Nikulski and C. P. Klages, *Diamond Relat. Mater.*, 2 (1993) 201.
- 12 H. Yokoyama, M. Okamoto and Y. Osaka, *Jpn. J. Appl. Phys.*, 30 (1991) 344.
- 13 W. Dworschak, K. Jung and H. Ehrhardt, *Diamond Relat. Mater.* 3 (1994) 337.
- 14 Y. Osaka, A. Chayahara, H. Yokoyama, T. Hamada, T. Imura and M. Fujisawa, *Mater. Sci. Forum*, 54-55 (1990) 277.
- 15 S. Reinke, M. Kuhr, R. Beckmann, W. Kulisch and R. Kassing, *Proc. 3rd Int. Symp. on Diamond Materials, Honolulu, HI, May 1993*, The Electrochemical Society, Pennington, NJ.
- 16 D. Bouchier, personal communication, 1993.
- 17 T. Wada and N. Yamashita, *J. Vac. Sci. Technol. A*, 10(1992) 515.
- 18 G. K. Wehner, in R. Behrisch (ed.), *Sputtering by particle Bombardment*, Vol. 1, Springer, Berlin, 1981, Chapter 4, p. 1660.
- 19 N. Matsunami, Y. Yamamura, Y. Itikawa, N. Itoh, Y. Kazumata, S. Miyagawa, K. Morita, R. Shimizu and H. Tawara, *Atomic Data Nucl. Data Tables*, 31(1984) 1.
- 20 A. Weber, U. Bringmann, R. Nikulski and C. P. Klages, in J. Harry (ed.), *Proc. 11th Int. Symp. on Plasma Chemistry, Loughborough, August 1993*, Vol. 3, p. 1041.
- 21 P. Sigmund, in R. Behrisch (ed.), *Sputtering by Particle Bombardment*, Vol. 1, Springer, Berlin, 1981, Chapter 2, p. 90.
- 22 D. Rosenberg and G. K. Wehner, *J. Appl. Phys.*, 33 (1962)
- 23 N. Tanabe and M. Iwaki, *Nucl. Instrum. Methods*, B80/81 (1993) 1349.
- 24 W. Dworschak, personal communication, 1993.
- 25 J. Robertson, *Diamond Relat. Mater.*, 2 (1993) 984.
- 26 D. R. McKenzie, D. Müller, B. A. Pailthorpe, Z. H. War E. Kravtchinskaja, D. Segal, P. B. Lukins, P. D. Swift, P. J. Martin, G. Amaratunga, P. H. Gaskell and A. Saeed, *Diamond Relat. Mater.*, 1 (1991) 51.
- 27 D. R. McKenzie, W. D. McFall, W. G. Sainty, C. A. Davis and R. E. Collins, *Diamond Relat. Mater.*, 2 (1993) 970.
- 28 D. J. Kester, K. S. Ailey and R. F. Davis, *J. Mater. Res.*, 8 (1993)

(paper presented at Diamond'94, Castelvecchio, Italy (26.9. - 30.9.94))

Recent Results" in Cubic Boron Nitride Deposition in Light the Sputter Model

*"S. Reinke, M. Kuhr, W. Kulisch, and R. Kassing
Institute of Technical Physics, University of Kassel
Heinrich Plett Str. 40, 34109 Kassel, FRG*

Abstract

In the field of c-BN deposition, ion assisted processes are most common and best investigated. Understanding of the deposition mechanisms is the basic key to improve film quality, and therefore, to realize potential applications. Recently, Reinke et al. developed a sputter model for ion assisted c-BN deposition in which material removal processes (sputtering and resorption) play mayor roles [1]. This model is used as guideline in order to give an overview on c-BN deposition. The first part investigates the growth mechanisms of ion assisted c-BN deposition. Therefore, a data collection which includes CVD and PVD deposition methods was" performed. The resulting dependencies are discussed in Light of the sputter model. By comparison with other models, it is found that most of the experimental facts can best be described in terms of the sputter model whereas in the nucleation step compressive stress plays an additional role. In the second part, c-BN deposition is considered in a wider cent ext. Current problems and some first approaches to overcome these problems are discussed. Furthermore boron "nitride is compared to the sp^3 carbon modifications tetrahedral amorphous carbon (ta-C) and diamond. It is concluded that c-BN and t a- C rely on different growth mechanisms; the investigation of extended parameter ranges.in search for new ion assisted, carbon and BN modifications is proposed. Some approaches in c-BN deposition without ion assistance are discussed in accordance to diamond deposition. Nevertheless the advances are small and no process yielding similar high quality material a CVD diamond exists.

1 Introduction

Boron nitride exists similar "to carbon in two main crystalline modifications, hexagonal' BN (h-BN) and cubic BN (c-BN) which are similar to graphite and diamond, respectively. C-BN was first synthesized by Wentorf under high-pressure high-temperature (HP-HT) conditions [2]. It raised much interest because of its excellent properties [3]. C-BN is the second hardest material next to diamond, exhibits high thermal conductivity and chemical inertness and is optical transparent in a wide range. Its special advantages with respect to diamond are its inertness with respect to, iron. even at high temperatures and the possibility, of p- and n-type doping. Therefore many applications such as protective coatings, cutting tools, optical windows, heat sinks, and high temperature electronic devices are principally imaginable. However, nowadays only grinding' powder and cutting tools from sintered HP-HT c-BN are commercially relevant because most of the. above. applications require high quality c-BN films which are not reached by the current technology.

Despite the close similarities of 'both materials, the c-BN deposition processes as well as the resulting film properties are very different to diamond thin films., and c-BN is less well investigated. In the early 80'ies first attemp's of c-BN thin "film deposition were undertaken [4]. Since then a large number of, at a first view, very different CVD and PVD methods were report ed leading to hard BN films. Many authors claimed to have deposited c-BN films but did not sufficiently characterize their films or misinterpreted the results. Therefore it seems to be adequate to define some criteria' for c-BN characterization" similar to the 'working definition of diamond films' by Messier et al. [5]. In our view, at least three independent methods are required' in order to prove the existence of c-BN within a BN film: , ,.

Infrared Spectroscopy Infrared (absorption) spectroscopy (IRAS) is the most common characterization technique. In the range between 400 to 4000 wavenumbers, absorption spectra of c-BN (containing) films exhibit only three distinct peaks at approx. 1080, 1380 and 800 cm⁻¹. These are representative for the c-BN reststrahlen band, and the h-BN in plane stretching and out of plane bending vibrations, respectively. The first requires long range order (at least nanocrystallinity) and is therefore only present for crystalline c-BN; the h-BN peaks are also present for every other sp² phase (amorphous, turbostratic and rhombohedral BN). Because little is known about the detailed structure of the sp² content in mixed films, in the following the term h-BN will be used in general for all sp² modifications. The absolute values of the absorption coefficients for the 1380 cm⁻¹ h-BN (A_h) and 1080 cm⁻¹ c-BN peaks (A_c) have been determined to be 3 and 2.3 pm⁻¹ for h-BN respective c-BN films [6]. There are some uncertainties about the ratio of A_h/A_c between several investigations but all of them find values close to unity. Therefore the c-BN content q_c is commonly derived from the absorption peak heights a_c and a_h ,

$$q_c = \frac{a_c}{a_c + a_h} \quad (1)$$

neglecting the influence of peak widths and differences in the absorption coefficients.

Diffraction C-BN containing films have been shown by TED and XRD to consist of randomly oriented nanocrystals. With the more sensitive TED, at least the (111), (220) and (311) reflections should be identified. Furthermore, HRTEM is a powerful tool to investigate the distribution of the different phases in c-BN films. Owing to the low scattering cross sections of boron and nitrogen, XRD requires some hundred nm of film thickness even at grazing incidence. Under these conditions at least the (111) reflection of c-BN at $2\theta = 43.3^\circ$ (with Cu K α) should be visible. Nevertheless, it should be kept in mind that h-BN has also two peaks in this range at 41.6° and 43.9° [7]. Because of the large peakwidth in nanocrystalline films, great care should be taken with the interpretation of XRD spectra.

Compositional analysis Films with high contents of c-BN have been shown to be nearly stoichiometric with B/N ratios between 0.9 and 1.1 [8, 9, 10, 11]. The reasons why c-BN tolerates only a nearly stoichiometric composition (e.g. a phase mixture of c-BN and elemental boron would be imaginable also) are not known yet. Compositional analysis methods determining either the surface composition (i.e. AES and XPS) or the bulk composition (i.e. EDX, RBS, Nuclear Reactions) are suitable. In order to exclude other phases and misinterpretations of IR spectra the level of contaminations must be in the percent range or below.

Additionally, the presence of c-BN may be confirmed by measurements of properties such as stress, density, hardness and friction, and by characterization of electronic states by EELS, XPS, AES and UV/VIS spectroscopy. According to the above criteria, several plasma CVD techniques such as electron cyclotron resonance (ECR)-CVD [12, 13], inductively coupled plasma (ICP)-CVD [6, 10], and radio frequency (RF)-CVD [14, 15] have been found suitable for c-BN deposition. Successful PVD methods can be classified into RF sputtering [16, 17], magnetron sputtering [18], ion plating [19]- [22] and ion beam assisted deposition (IBAD). In IBAD boron can be offered via electron beam evaporation [23]-[25], sputtering [26, 27] or laser ablation [28]. A detailed examination of the above techniques shows close similarities: All exhibit massive ion bombardment of the growing film. In plasma methods this is achieved by using RF substrate bias, high plasma densities and low working pressures (≤ 2 Pa). In most cases gas mixtures of nitrogen and an inert gas (commonly Ar), and elevated substrate temperatures (above 300°C) are used. Independent of the deposition technique, with increasing level of ion bombardment, the sequence h-BN, c-BN and finally no growth at all is found.

2 Data collection

The first aim of our contribution is to quantify the deposition conditions leading to c-BN growth. The following microscopic deposition parameters are independent of the deposition method and therefore best suited for comparison: boron flux F_B ; ion flux F_{ion} ; ion energy E_{ion} ; ion angle of incidence Θ ; ion mass (distribution), and substrate temperature T_s [1].

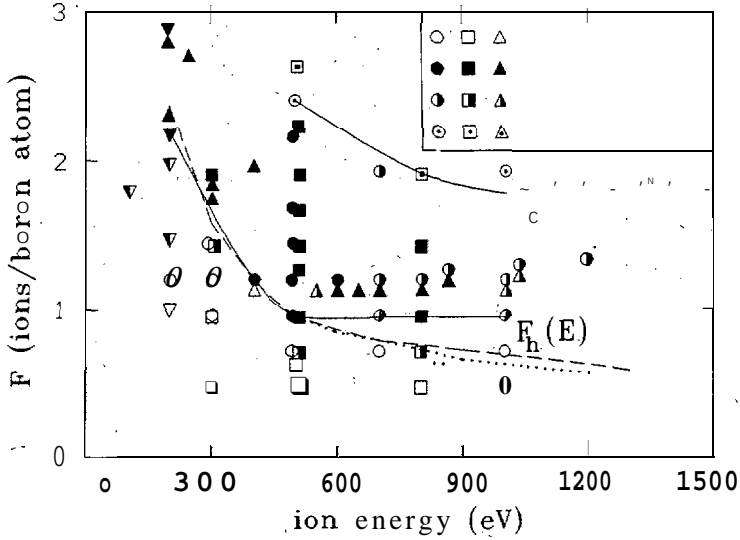


Figure 1: Dependence of the structure of IBAD BN films on ion energy E_{ion} and the ion to B atom arrival ratio F . Deposition conditions are given in Table 1. Circles, data from Tanabe et al. [26]; squares, data from Kester et al. [23]; triangles, data from Bouchier et al. [24]; up side down triangles: data from Ganzetti et al. [27]. The dotted line represents the transition evaluated by Mirkarimi et al. with laser ablation IBAD [30] and the dashed line the dependency of the inverse sputter yield Y^{-1} of Si under argon bombardment [33]. Both were fitted to F_h at 500 eV.

We will first consider IBAD only because here the above microscopic parameters can be measured and controlled nearly independently, Fig. 1 shows the crystal phase as a function of the ion energy and the flux ratio $F = F_{ion}/F_B$. In Fig. 2 all available data are shown in dependence of substrate temperature and F . The parameters not indicated in the figures were kept constant and are shown in Table 1. (It should be mentioned that in comparison to [1] some new sets of data are included). Details about the data evaluation process are described elsewhere [29].

Table 1:

author	B-source	T_s (°C)	Θ (deg.)	Ar:N ₂ flow ratio	E_{ion} (eV)
Kester [23]	evaporated B	400	30	1,	500
Tanabe [26]	sputtered B	350	0	1	500
Ganzetti [27]	sputtered B	350	15	0 . 5	
Bouchier [24]	evaporated B	400	15	0 . 5 - 2	6 0 0
Mirkarimi [30]	laser abl. BN	500	60	0.66	

Deposition conditions of the IBAD experiments shown in Fig. 1 and 2.

Fig. 1 and 2 both show h-BN for low F values and with increasing ion bombardment a quite sharp transition to c-BN. If the ion flux is increased further, no net film growth can be detected. At high energies (above 600 eV) some authors observe a transition from c-BN to a mixture of h-BN and c-BN which is commonly attributed to radiation damage processes [24, 26]. In

contrast, Mirkarimi et al. found 80 % c-BN even at an ion energy of 1200 eV [30].

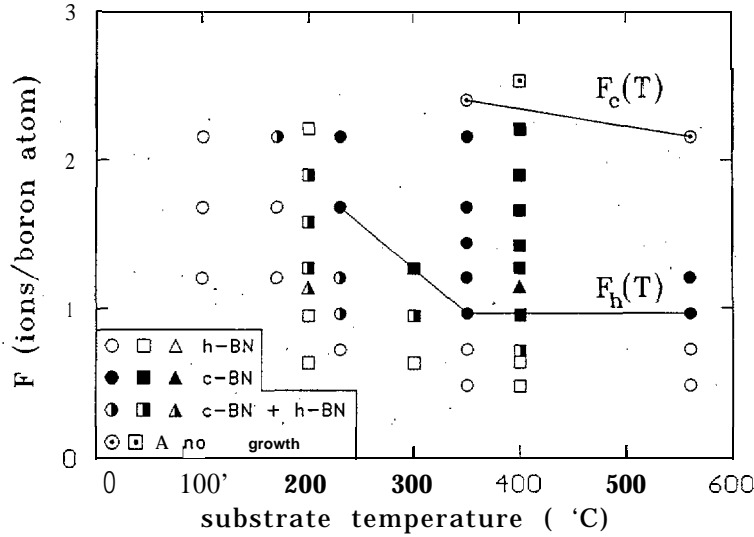


Figure 2: Dependence of the structure of ion beam assisted deposition BN films on substrate temperature T_S and ion to B atom arrival ratio F . Deposition conditions are given in Table 1. Circles, data from Tanabe, et al. [7.2]; squares, data from Kester et al. [23]; triangles, data from Bouchier et al. [53]

In a second step we compare different plasma 'deposition methods to IBAD. Data' of four experiments are shown in Table 2. With plasma methods, the determination of the microscopic deposition parameters is more difficult:

Boron flux The determination of the boron flux F_B is nearly impossible in CVD. Therefore the number of incorporated boron atoms F_B^* is considered, which can be evaluated from the grown film.

Ion energy In plasma methods using RF bias, the mean ion energy is determined by sum of bias voltage V_b and plasma potential V_p with a pressure dependent correction factor k describing collisions within the plasma sheath,

$$\bar{E}_{ion} = k \cdot e(V_b + VP) \quad (2)$$

with e , electron charge. The values of k and VP used in our data evaluation are reported in Tab. 2.

Ion flux The ion flux to the substrate which is space charge limited, was calculated according to [31]

$$J_i = 0.6 e n \sqrt{\frac{k_B T_e}{m_{ion}}} \quad (3)$$

with k_B , Boltzmann constant; m_{ion} , ion mass. The electron temperature T_e and the plasma density n were in most cases determined by double probe measurements.

In Fig. 3 all available data are shown in a $F^* - E_{ion}$ -diagram. $F^* = F_{ion} / F_B^*$ represents the number of ions per incorporated boron atom. In this parametrization the 'no growth' boundary shifts to infinity.

The different gas flow ratios (mainly Ar : N_2) and the uncertainties concerning ion flux and energy may scatter different data sets of Fig. 3 by a factor of 1.5. Nevertheless, the diagram covers wide ranges of both, F^* and E_{ion} thus allowing the following conclusions to be drawn:

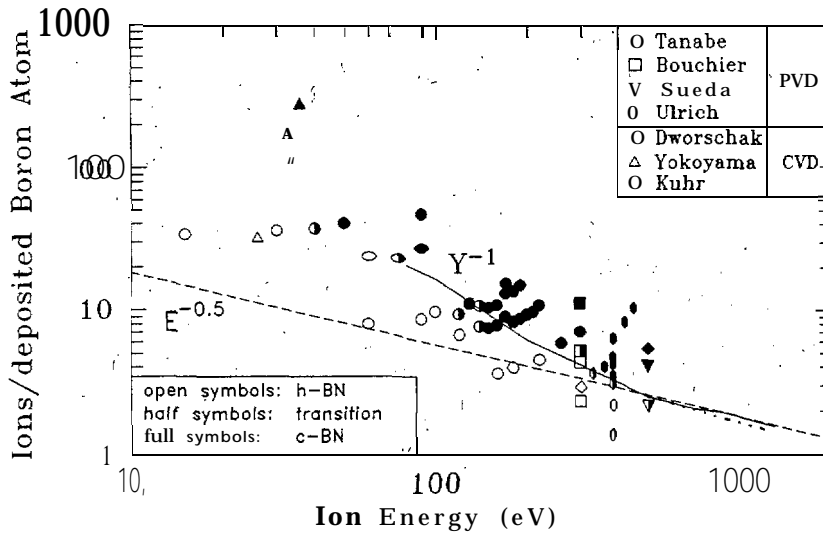


Figure 3: Dependency of the boundary between h-BN and c-BN on ion energy E_{ion} and the number of bombarding ions per incorporated B atom for CVD as well as PVD deposition methods. CVD data from Yokoyama et al. [13], Kuhr et al. [10] and Dworschak et al. [11, 73]. PVD-data from Ulrich et al. [18, 37], Bouchier et al. [24, 63], Tanabe et al. [26, 74] and Sueda et al. [35]. Full symbols: C-EN. Half symbols: Transition. Open symbols: H-EN. The dotted line represents the data of Mirkarimi et al. Also shown are: full line, dependency of the inverse sputter yield Y_1 of Si under argon bombardment [33] and dashed line, $E_{ion}^{-1/2}$ dependency according to Kester and Messier [23]. Both were fitted to the data at 500 eV.

1. C-BN can be deposited with energies well below 100 eV, (with either CVD or PVD).
2. Low energies can be compensated by high ion to boron flux ratios.
3. CVD and PVD work within the same range of parameters and therefore rely on the same deposition mechanisms. This implies that chemical effects can not be the driving force in ion assisted c-BN CVD. Nevertheless a certain influence of chemistry can also be present which may suppress the formation of c-BN under certain conditions. It is known that hydrogen is detrimental for c-BN deposition and this may explain the fact that the maximum c-BN content is nearly 100 % in PVD but only about 75 % in CVD. Nevertheless the mechanisms concerning the influence of hydrogen or other chemical effects in c-BN deposition are not well understood.

3 The sputter model , ,

In order to explain the above data collection, we will introduce the sputter model which been developed for ion induced c-BN deposition [1]:

Therein the boundaries F_h and F_c in Fig. 1 and 2 are interpreted to be due to material removal processes. Two processes are taken into account. First, resorption of incoming material which is governed by the sticking probability of boron, s_B and second sputtering of incorporated atoms by the ion bombardment. Because surplus nitrogen diffuses out, only the boron is considered, and the boundaries are characterized by the equality of incoming and removed boron:

$$F_B = F_B^{rem} = (1 - s_B(T))F_B + 0.5Y_{h,c}(E_{ion}, \Theta)F_{ion} \quad (4)$$

$Y_{h,c}$ represents the sputter, yields (B- plus N-atoms per ion) of h-BN resp. c-BN under the relevant bombardment conditions. The factor of 0.5 occurs because only sputtered boron is con-

Table 2:

author	technique	B source	gas flows	T_s ($^{\circ}C$)	p (Pa)	RF bias (V)	k	V_p (V)
Yok. [13]	ECR-CVD	B_2H_6	He: Ar: N_2 = 9:9:1	<100	0.03	5-15	1	16
Dwor. [11]	RF-CVD	B_2H_6	Ar: N_2 = 6:1	410	2	550 -750	0.6	0
Kuhr [10]	ICP-CVD	TMB*	Ar: N_2 = 2:1	450	2,	40-300	1	0
Ulr.[18, 37]	Magn. Sput.	h-BN	pure Ar	530	0.08	3 0 - 1 0 0 0	1	0

*Deposition conditions of the plasma assisted experiments shown in Fig. 3. *TMB stands for 1,3,5 tetra methyl bora.zinc ($BHN(CH_3)_3$). In the last two 'columns, the values of the correction factor k and the plasma potential V_p used to evaluate the data of Fig. 3 (according to Equ. (2)) are given. In case of [13] and [18, 37] because of the low pressures collisions within the sheath can be neglected and the plasma potentials were 'measured by the authors. In case of [11] the correction factor of 0.6 is taken from the publication and the plasma potential can be neglected with respect to the bias voltages. In ([10]) $k = 1$ and $V_p = 0$ are used because the high but unknown plasma potential and the collisional ion energy loss due to the high pressure compensate each other, at least in part.*

sidered. Desorption and sputtering are treated independently, with temperature influencing only resorption and ion energy only sputter processes. From equ. (4), it follows for the boundaries

$$F_{h,c} = \frac{2s_B(T)}{Y_{h,c}(E_{ion}, \Theta)} \quad (5)$$

In the following, some predictions "of the sputter model will be compared. to experimental findings. We'd like to 'point out that all available experiments yielding quantitative results and "proving the existence of c-BN are taken into consideration. No data known to us which are cent radictional to our model were left out;' only one point, the occasional occurrence of' a h-BN-like phase, near the resputter boundary, is' for reasons of space discussed elsewhere [32].

3.1 Selective sputtering

Following Equ. (5), selective sputtering of h-BN is the key to c-BN deposition.

Some studies of ECR [13, 12] and RF [15] plasma etching and ion beam etching [32] of BN exist. All available data are shown in Fig. 4a where a selectivity in etch rates between h-BN and c-BN of approx. 2 is found. "In order to determine the selectivity of the sputter yields, the values were corrected by the film densities (which were approximated from the c-BN 'content) resulting in a selectivity γ of the sputter yields of approx. 1.5 (compare Fig. 4b). This is not as high as expected from the width of the c-BN domain in Fig. 1 (2.4 at 500 eV). However, measurements of absolute sputter yields Support the model. For c-BN (HP-HT crystal) a value of $Y_c \approx 0.7$ under 600 eV argon bombardment at normal incidence was found [32] which is in 'good agreement with Equ. (5) using $F_c = 2.2$ (from Fig. 1) and $s_B = 0.7$. The sputter yields of h-BN under pure argon and pure nitrogen bombardment were both found to be ≈ 1 at 600 eV.

Our model may not be misunderstood in the manner that the probability of incoming material bonded as h-BN or c-BN is independent of the material already deposited. In this case a small sputter selectivity γ would never be sufficient to produce nearly pure c-BN films, and the boron incorporation probability p_B (see below) should be in the percent range in case of c-BN . A strong dependency of the bonding of an incoming atom on the surface bonding conditions must exist. In other words, an atom will be more likely sp^3 bonded on c-BN and sp^2 bonded on h-BN. Regarding the small selectivity, the boundary F_h must be interpreted as a condition where due to the ion bombardment the growth velocity of c-BN exceeds that of h-BN and the preferential bonding mechanism stabilizes the c-BN surface. Concerning this point, some more investigations are necessary.

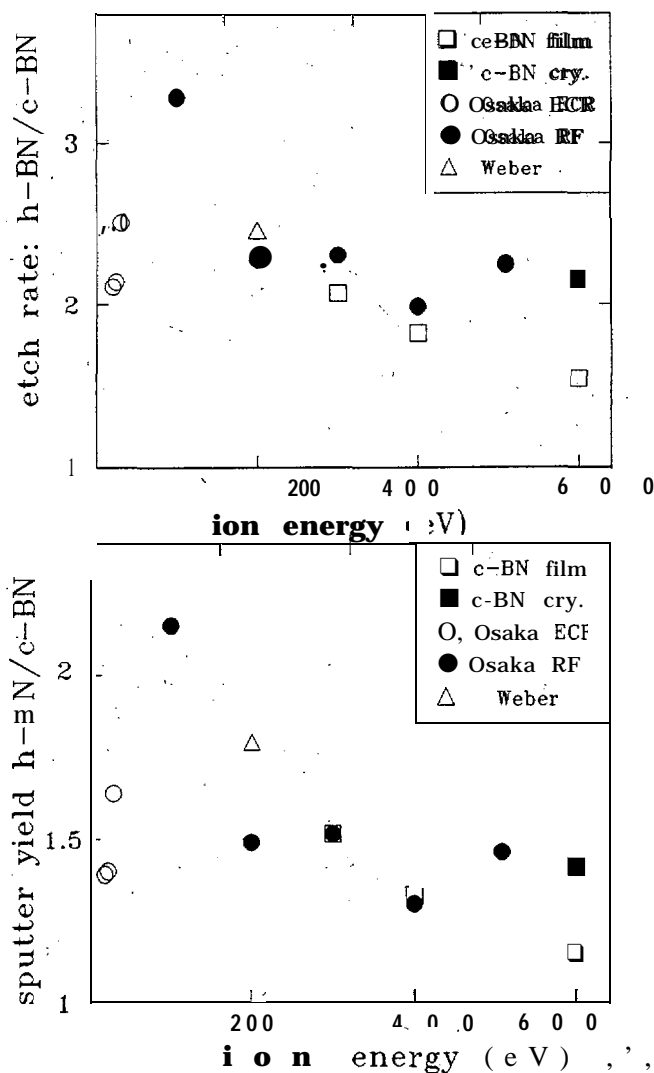


Figure 4: 4a: Measured selectivity in etch rates of h-BN and c-BN by different authors. Open squares (BN films) and full square (c-BN crystal), Reinke et al. [32]; open circles (ECR-plasma) and full circles (RF-plasma), Osaka et al. [15]; triangles, Weber et al. [12]. 4b: Selectivity in sputter yields of h-BN and c-BN. The data have been calculated from Fig. 4a by a linear density "correction". For citations, please refer to Fig. 4a.

3.2 Ion energy

Above 500 eV, F_h in Fig. 1 is governed by the stoichiometry requirement [1]. Without this influence, according to Equ. (5) for the transition from h-BN to c-BN a dependency inversely, to the sputter yield ($F_h(E) \propto Y_h^{-1}(E)$) should hold. Indeed, F_h in Fig. 1 can be simulated with an inverse sputter yield (dashed line) for all data below 500 eV, and also beyond for the from ion beam assisted laser ablation where stoichiometry is no problem (dotted line). Ar \rightarrow Si was chosen for this due to the lack of experimental sputter yields for BN. It exhibits similar features (heavy projectile on light element, high absolute yield); in addition experimental data down to 80 eV are available [33]. If p_B at the transition from h-BN to c-BN is independent of the ion energy (see below), also the boundary in Fig. 3 according to Equ. (6) should be inversely proportional to the sputter yield. Indeed, good agreement is obtained even for low energies, "in contrast to the momentum dependency proposed by Kester et al. [23] which is attributed to a build-up of compressive stress ($\sigma \propto (E_{ion})^5$) [34]. Nevertheless, we do not claim the work of Kester et al. to be wrong. But in our view, an influence of the stoichiometry condition is present

which may flatten the energy dependency (compare Fig. 1) and their threshold momentum value of $200 \text{ (eV amu)}^{0.5}$ mainly reflects the influence of the ion mass. Their energy dependency was mainly taken at high ion energies were Mirkarimi et al. also found a $(E_{ion})^{-0.5}$ -dependency of F_h (see Fig. 1), This is, consistent with the energy dependency of typical sputter yields which is approximately proportional to E between 200 and 500 eV but steeper below 200 eV and proportional to E^n (with $n < 1$) above 500 eV. This behaviour is well reflected by the data of Fig. 3.

The fact that ion assisted deposition of c-BN is only possible in a narrow region close to the no growth boundary is itself a strong argument for sputtering. If another process is the reason for the transition from h-BN to c-BN, its energy dependency between 30 eV [13] and 1200 eV [30] must be very similar to $Y_c(E)^{-1}$ which is very unlikely. ,

3.3 Substrate, temperature

According to Equ. (5), the influence of substrate temperature is attributed to changes in the sticking probability y ($F_h(T) \propto s_B(T)$). This is assumed to be near unity at low temperatures and to decrease with temperature, Therefore at high temperatures less material has to be removed by sputter processes resulting in the decrease of F_h in Fig. 2. On the other hand high values of F should compensate low temperatures. Indeed, some PVD as well as CVD deposition of c-BN at room temperature has been reported [35, 22, 13]. Furthermore, desorption is strongly supported by experimental findings: Under identical plasma parameters, with increasing substrate temperature the growth rate decreases with CVD as well as PVD [10], [36], [37], and the transit ion from h-BN to c-BN shifts to lower bias voltages [10], [14]. It should also be mentioned that some authors find a decrease of the c-BN content at substrate temperatures above 500 °C [38, 39]. A possible explanation would be an increasing thickness of the h-BN nucleation layer (compare section 4) which would lead to a decrease of the c-BN content (measured by IRAS) constant total film thickness.

Although the influence of resorption is evident, probably additional effects of the substrate temperature such as e.g. enhanced surface mobility, stress relaxation or out-diffusion of hydrogen and nitrogen have to be taken into account. More systematic investigations concerning this point are required.

3.4 Boron incorporation probability

The boron incorporation probability p_B (the probability of an incoming boron atom to be incorporated within the deposited film) may be defined and measured with IBAD and the identity

$$F^* = F / p_B \quad (6)$$

holds .

Fig. 5 shows the dependence of p_B on the flux ratio F . p_B is maximal for low values of F where h-BN is deposited and decreases with increasing amount of ion bombardment. This is a direct proof for material removal via sputtering. An upper boundary for the occurrence of c-BN of $p_B \approx 0.4$ may be derived from the data of Fig. 5. Nevertheless due to the few data points, further investigations are necessary. In our view, p_B data gain much information about the growth kinetics of c-BN deposition and therefore it is not understandable why this quantity is "so seldom, characterized.

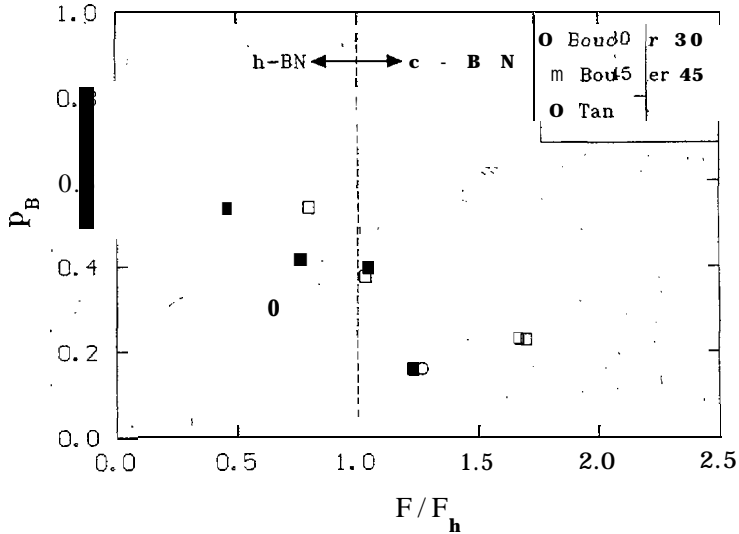


Figure 5: Boron incorporation probability P_B as a function of flux ratio. F : squares, data from Bouchier et al. [24, 63]; circles, data from Tanabe et al. [26, ?]. In order to compare different experiments, F values were normalized to F_h , representing the flux ratio at the transition from h-BN to c-BN in relevant experimental conditions.

3.5 Ion angle of incidence

Sputter yields are dependent on the angle of ion incidence. Following simple geometric considerations, the dependency $Y(\Theta) = Y(0) \cos^{-1}(\Theta)$ may be used as first approximation [40]. According to Equ. (5), the boundaries should vary like

$$F_{h,c}(\Theta) \propto Y_h^{-1}(\Theta) \propto \cos(\Theta) \quad (7)$$

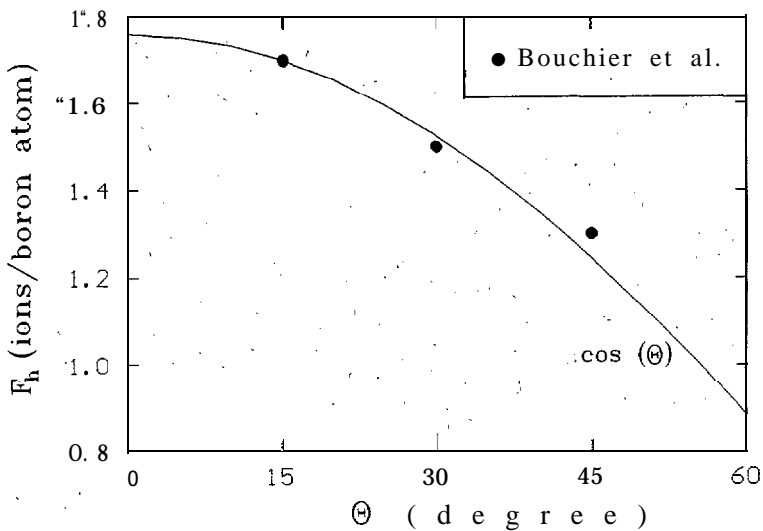


Figure 6: Dependency of F_h (see Fig. 1) on the ion angle of incidence Θ . Experimental data, Bouchier et al. [24]; full line, prediction of the sputter model.

In Fig. 6, the to our knowledge only existing systematic investigation concerning the ion angle of incidence is compared to the predicted $\cos(\Theta)$ dependency and good agreement is obtained.

This may not prove a $\cos(\Theta)$ dependency definitely but at least the tendency of decreasing transition value F_h .

The no growth boundary F_c has not been investigated systematically. Nevertheless, IBAD experiments with waving substrates showed a decrease of F_c with increasing waving angle [35]. In this investigation, the transition boundary F_h was only slightly affected because of the stoichiometry condition.

3.6 Ion mass

Two systematic IBAD investigations concerning the influence of the ion mass (Ar, Kr and Xe) exist. Both find the transition from h-BN to c-BN at lower F values, the higher the mass of the ions. Kester et al. [23] performed a study using two ion guns and therefore the ion flux ratios between nitrogen and inert gas are well known. They find a $(m\gamma)^{0.5}$ dependency of the boundary F_h between the h-BN and the c-BN domains. $\gamma = \frac{4mM}{(m+M)^2}$, and m and M are the inert gas and target mass, respectively. Contradictionally, Mirkarimi et al. [30] found a steeper $m^{0.5}$ dependency. They worked with one ion gun and assumed the ratios of inert gas ions to nitrogen ions to reflect the input gas flows. In our view, this does not hold because the different ionization potentials (Ar: 15.76 eV, Kr: 14.00 eV and Xe: 12.13 eV) lead to an overrepresentation of the heavy inert gas ions which may be the reason for the observed steeper dependency. Basing on sputter yield data of carbon [41], it has been shown that the $(m\gamma)^{0.5}$ -mass dependency can be well explained by the sputter model [1]. From the resputter boundaries of [30] it is clear that the dependency $Y_{Ar} < Y_{Kr} < Y_{Xe}$ holds also for BN. Therefore, the experimental findings of both [23, 30] that the heavier the inert gas, the lower the F_h value to reach c-BN can be explained by the sputter model. Nevertheless, the question remains why inert gas bombardment is needed at all. A markable amount of inert gas (some %) has been shown to be incorporated within the BN film [16, 12]. This may support the formation of compressive stress which is required for nucleation.

4 Nucleation

In contrast to diamond, in c-BN deposition the nucleation process is carried out under the same conditions as the growth process. Nevertheless important differences between the very first nucleation period and the growth have been observed. TEM pictures of the interface between film and substrate (commonly silicon) show a distinct sequence [28, 38]: first some nm of amorphous material, followed by a textured h-BN layer with the c-axis parallel to the substrate, and finally the actual nanocrystalline c-BN layer. The existence of the textured h-BN or turbostratic (t-BN) layer has also been confirmed by IRAS and ellipsometry [42]. The nucleation behaviour can not be understood in terms of the sputter "model which predicts statistical nucleation which in turn would imply a certain incubation time. In contrast, the experimental growth rate of the initial h-BN layer is found to be higher than that of the c-BN on top of it [36, 43]. Nevertheless, the existence of the layer structure is not contradictory to the sputter model. The amorphous layer may be a mixing layer, its thickness being comparable to the ion range. The textured h-BN layer is stable with respect to ion bombardment owing to channeling effects. It should be kept in mind that the bond lengths of h-BN are 3.33 Å in c-direction and 1.45 Å perpendicular to it. Therefore the high growth rates of the textured h-BN layer can be attributed to a lower sputter yield and additionally to its lower density compared to c-BN. The occurrence of the texture is attributed to the high compressive stress since the c-axis is the direction of highest compressibility [22]. *In situ* stress measurements indicate high stress values to occur in the beginning of c-BN deposition and a drop of the stress to a certain saturation value during the growth process [22, 39].

All the above findings show significant differences between the nucleation and the growth step so that in our view, different processes may dominate the respective step. Once c-BN is

nucleated, the growth process can be well described by the sputter model (compare also Tab. 3). on the other hand, although the basic mechanisms in nucleation are 'not well known yet, a strong influence of high compressive stress is obvious. Nevertheless, it remains unclear why the textured h-BN layer does not grow on and on. It may be speculated that the stress directly generates c-BN nuclei by a direct conversion from h-BN as was proposed by McKenzie et al. [22], or from rhombohedral BN (r-BN) [44] (see section 5.2). Alternatively, it only "creates the textured h-BN layer which may support nucleation of c-BN due to lattice matching. Comparison to diamond growth shows an interesting 'parallel. Enhanced diamond nucleation has been obtained on highly oriented graphite at the edges, of the basal planes [45] and nearly no nucleation on the basal planes themselves. Therefore, the existence of the textured layer may only be regarded as the necessary condition. for c-BN growth, the stress only being the way to reach this texture.

The question whether stress is necessary also in the growth presses or is just a consequence of the ion bombardment may be solved by the separation of nucleation and growth process with respect to deposition parameters. Maybe this could be a way to reduce the high stress values of c-BN films which nowadays hinder applications (compare section 7).

5 Other models

Contradictionally to the sputter model which predicts c-BN formation at the surface of a growing film, other models regard bulk processes to play the major role. Two main approaches exist, which both have been originally developed for tetrahedral amorphous carbon (t a- C).

5.1 Subplantation model

The term subplantation was introduced by Lifshitz et al. for low energy subsurface implantation processes" [46]. Robertson developed a quantitative model describing the density increment under ion bombardment [47] by the balance of subplantation due to ion bombardment and relaxation processes due to thermal spikes. The basic assumption that the local density determines the bonding condition of an atom has been adopted for c-BN by Dworschak et al. [11]. They performed TRIM simulations. and introduced the parameter A_n , the number of interstitials minus vacancies in a certain depth which is a measure for the local density. Maxima of A_n are found in some depth below the surface (e.g. at 2 nm for 500 eV argon plus nitrogen bombardment). In every interpretation of subplantation, the formation of sp^3 bonds takes place somewhat below the surface corresponding to the ion. range. "

5.2 Stress model

Davis developed a model for compressive stress in polycrystalline solids describing the balance of stress build-up by defect atoms and relaxation due to thermal spikes [48]. McKenzie et al. adopted, this approach and argued in terms of thermodynamics [49]. They claimed Sp^3 formation to occur if the hydrostatic pressure due to the stress 'reaches the transition boundary between sp^2 and sp^3 in the relevant phase diagram. It should be stated that the BN phase diagram is believed to be similar to that of carbon although a great uncertainty exists, especially at low temperatures [50]. Because the stress at, the surface vanishes, the formation of c-BN is expected in 'a certain depth within the bulk. Recently, Medlin et al. proposed the conversion of an initial nucleation layer of rhombohedral BN (r-BN) to c-BN by the high compressive stress [44]. This is possible without diffusion in contrast to the conversion of h-BN to c-BN.

5.3 Comparison to experiment

In Table'3, "the predictions of the above models are compared to the experimental findings of c-BN and ta-C deposition It can be seen that in case of c-BN 'some experimental findings are , in contrast to the subplantation and stress models.

The experimental angle of incidence dependency (Fig. 6) is opposite to the predictions of all bulk growth models. At high angles of incidence, the energy of a collision cascade is deposited closer to the surface. This leads to enhanced mobility and to enhanced relaxation of displacements. Therefore, the sp^3 content should decrease, as it has been experimentally observed with ta-C [51, 52]. With the subplantation model the build-up of dense amorphous films (e.g. ta-C) by local quenching processes can be well understood but c-BN is nanocrystalline. The growth of c-BN crystals in the bulk -requires not only high pressures but also sufficient mobility for the phase transition. This is believed to be sustained by thermal spikes [11, 22] but typical spike diameters are in the range of few nm, even at an ion energy of 500 eV which is by far not sufficient to explain crystal sizes of up to 50 nm. With the proposal of Medlin et al. of the direct conversion of an initial r-BN layer, such crystal sizes are imaginable. Nevertheless the resulting c-BN should be textured which was only seldom -reported. It should be noted that also the sputter model favours a certain texture for that the face with the lowest sputter yield should grow most effectively. More detailed "studies like the investigation of the influence of ion energy on the crystal size (compare last line of Tab. 3) and the search for possible textures and their dependence on deposition parameters may bring more insight into the situation.

The transition from h-BN to c-BN is extremely sharp [53, 26]. Within 10% increase of ion energy, the films turn from pure h-BN to nearly 100% c-BN. Subplantation, because of its local nature predicts a smooth transition as it is observed in case of ta-C. With the stress model, a sharp transition at the phase boundary is imaginable. Nevertheless at low temperatures the transition should be at lower stress (and therefore bombardment) levels which is in contrast to the experimental findings. The sputter model finally in its simple form (Equ. (5)) predicts a sharp transition. If one argues with the growth velocities the situation is not that clear and further theoretical investigations are under way.

Table 3:

	c-BN	sputtering	stress	subplantation	ta-C
E_{ion}	50-1200 eV	$F_h \propto Y_h^{-1}$	opt. ≈ 100 eV	opt. ≈ 100 eV	opt. ≈ 100 eV
T_s	$T_s \uparrow \Rightarrow$ c-BN \uparrow	$T_s \uparrow \Rightarrow$ c-BN \uparrow	$T_s \uparrow \Rightarrow sp^3 \downarrow$	$T_s \uparrow \Rightarrow sp^3 \downarrow$	$T_s > 150^\circ C$ $sp^3 \downarrow$
Θ	$\Theta \uparrow \Rightarrow$ c-BN \uparrow	$\Theta \uparrow \Rightarrow$ c-BN \uparrow	$\Theta \uparrow \Rightarrow sp^3 \downarrow$	$\Theta \uparrow \Rightarrow sp^3 \downarrow$	$\Theta \uparrow \Rightarrow sp^3 \downarrow$
$p_{B,C}$	$p_B < 0.4$	p_B low			$p_C = 1$
D_{CTy}	5 - 50 nm	50 nm possible	($D'' < 3$ nm)	$D < 3$ nm	amorphous
$sp^2 \rightarrow sp^3$	sharp	(sharp)	sharp	smooth	'smooth
surface	?	sp^3	sp^2	sp^2	sp^2 ?
$D_{cry}(E_{ion})$?	$E_{ion} \uparrow \Rightarrow D \downarrow$	$E_{ion} \uparrow \Rightarrow D \uparrow$	$E_{ion} \uparrow \Rightarrow D \uparrow$	-

Comparison of predictions of different models to experimental findings in c-BN and ta-C growth. The symbols if not explained in the text denote: D_{cry} , crystal size; $p_{B,C}$, incorporation probability of boron resp. carbon atoms; σ , stress.

Investigations of the surface bonding may be the best way to decide between the sputter model (sp^3 surface) and bulk models (sp^2 surface layer). For ta-C, the presence of a sp^2 surface layer of approx. 1 rim thickness is expected [54, 55]. In case of c-BN, Bouchier et al. found sp^2 -like EELS spectra with a primary electron energy of 150 eV [24]; Friedmann et al. provided evidence for sp^2 bonding by Auger electron spectroscopy (AES) [39]. It may be criticized that AES provides very indirect information only and the high energy electron bombardment may influence the surface conditions. In contrast, the existence of a sp^2 layer has not been observed with high resolution TEM, although the sensitivity was by far sufficient [56]. A possible solution may be the existence of a sp^2 reconstruction of the very first atomic layer which is well known in case of diamond [57]. We like to stress that such investigations are only sensible if the boron

and ion fluxes are stopped simultaneously (e.g. by means of a shutter) in order to exclude either additional boron deposition or ion bombardment which may convert the deposited c-BN to sp² bonded BN. A possible explanation of the above findings may also be the existence of a post deposition sp² reconstruction of the very first atomic layer which is well known in case of diamond [57]. The lack of knowledge concerning the detailed properties of c-BN surfaces is a serious problem limiting the understanding of c-BN growth. In this point much further work has to be done.

To summarize, most features of the c-BN growth process can be well explained by the sputter model whereas ta-C seems to be dominated by subplantation effects.

6 Comparison, between BN and carbon

Fig. 7 shows schematically the growth regimes of c-BN and ta-C. It can be seen that at identical ion energies, c-BN requires about 10 times more ions per incorporated atom than ta-C which supports the existence of different growth mechanisms. Consequently, the question arises whether analogous modifications to the well known, exist (i.e. ta-BN and ion assisted nanocrystalline carbon),

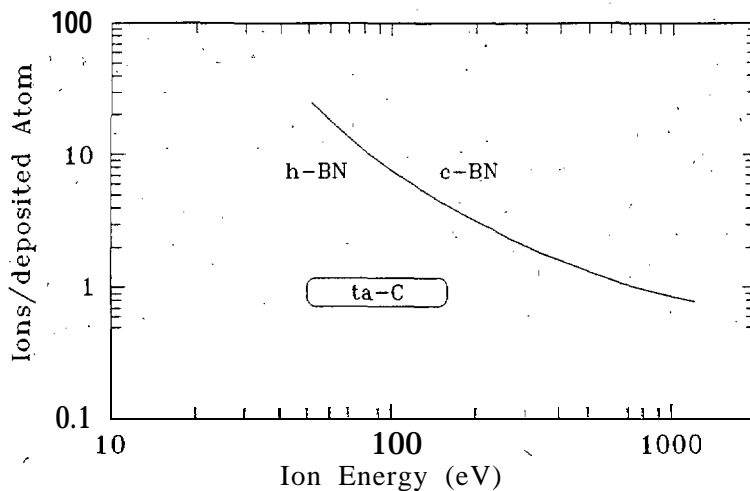


Figure 7: Schematic comparison of ta-C and c-BN deposition conditions. Note that in contrast to Fig. 3, the number of ions per deposited atom (boron and nitrogen in case of EN) is shown.

Indeed, amorphous boron rich BN films with densities up to 2.7 g/cm³ have been reported [58] (for comparison the densities of h-BN and boron are 2.29 g/cm³ and 2.47 g/cm³, respectively). They were deposited by IBAD at room temperature with low energy pure nitrogen ion bombardment (250 eV N₂ corresp. 125 eV per N atom). With increasing ion energies the film densities decrease. The above findings are in agreement with the subplantation model. Nevertheless the existence of stoichiometric ta-BN has not been confirmed yet. One possible explanation may be that the relatively high ionic character of the BN bond favours the formation of crystalline structures.

In case of carbon only the energy dependency in ion beam deposition ($F \approx 1$) is well investigated. In our view also the flux ratio dependency is important and it should also be investigated if close to the resputter boundary and at elevated temperatures a carbon modification occurred which can be compared to nanocrystalline c-BN. The future aim must be to fill the unknown regions of Fig. 7 with reliable information.

7 Problems in ion assisted c-BN deposition

At the present state no deposition method leading to well crystallized (at least microcrystalline) c-BN films is known. Furthermore due to the high stress, adhesion of c-BN films is generally poor limiting the film thickness" to typically 100 nm. The growth rates are low and commonly only flat substrates can be coated. Some approaches exist to overcome these problems even in conventional ion assisted deposition:

Adhesion can be improved by interlayers of boron, i-BN (ion assisted boron rich h-BN) or graded SiBN [59, 60, 61]. Also, approaches with dynamic ion mixing in the first stage of deposition exist [62]. Furthermore, increasing the ion angle of incidence' [63], as well as post deposition annealing lead to a reduction of film stress [64, 65, 66]. The first is in accordance with the sputter model because at higher angles less ion bombardment is needed. However, the microscopic mechanism for the stress reduction by annealing is not known yet. Coating" of complex geometries (e.g. tools) is principally difficult with ion assisted' methods. Some first investigations with waving substrates exist [35] but different ion angles strongly influence the growth rate. Furthermore the growth rate is principally low because of sputtering ($p_B < 0.4$, compare above). It is further limited by the ion currents obtainable; approx $1 \mu/\text{hour}$ is realized yet. Upscaling by a factor of 2-3 may be realistic.

The above improvements may in future be sufficient for applications as protective coatings. Nevertheless, in order to use the, enormous potential of c-BN e.g. in microelectronics, well crystallized material 'is needed. Conventional ion assisted growth will always result in nanocrystalline material because of the unavoidable radiation damage. Therefore, two directions have to be investigate ed which can be compared to the carbon modifications t a-C. and diamond, respectively, for which electronic, applications may be expected for the near future. The first is to clarify whether an amorphous sp^3 bonded BN modification exists and if so to investigate its electrical' properties. The second is' to enhance tryst al size either by supporting tryst allization in conventional ion assisted growth (here some approaches with UV illumination exist) or by developing new processes without ion' bombardment. Efforts in the second approach will be summarized in the following.

.8 C-BN without ion bombardment

"Few experiments leading to c-BN films have been reported which can not be classified in terms of ion assisted deposition (see Tab. 4). Plasma jet, DC plasma and micro wave CVD are typical techniques also used in diamond deposition [67].

Table 4:

author	method	gases	p (mbar)	T_s	(°C)
Ichinose [68]	ICP + Fil.	$\text{NH}_3\text{B H}_3$ in Hz.	0.2 - 5	800	
Saitoh [69]	Plasma Jet	$\text{B}_2\text{H}_6 + \text{NH}_3$ in Hz	67.-133	600	
Wang [70]	DC Plasma	$\text{B}_2\text{H}_6 + \text{NH}_3$ in Hz	20-200	600	
Saitoh [71]	MWCVD	$\text{NaBH}_4 + \text{NH}_3$ in Hz	5 - 100	800	

CVD experiments which can not be classified in terms of ion assisted deposition.

The hot filament method has not yet been shown to be succesful in the case of c-BN, but filament assisted plasma deposition processes exist [68]. The general features of the methods are quite similar to diamond deposition: Few percent of a boron containing source gas in hydrogen are used at high pressures and high exitation energies per volume [68]. This results in high amounts of atomic hydrogen and high gas ternperat ures, conditions which are expected to play a mayor role in diamond deposition [67]. Also the substrate temperatures used were comparable to diamond. Therefore the possibility whether a chemical way to c-BN films exist can not be

ruled out. But so far none of the above methods led to microcrystalline material which is easily achieved in the case of diamond. Also the mechanisms under the above conditions are not understood at all. For the "future it will be important to establish the differences in chemistry between carbon and BN. Perhaps then the questions whether selective etching of h-BN by atomic hydrogen occurs or if the surface reconstructions under the influence of hydrogen is comparable to the diamond case can be answered.

9 Summary and Conclusions

For ion induced c-BN deposition universal parameter ranges were found which are independent "of the deposition method (CVD or PVD). By comparing the experimental data to existing models, it is found that the c-BN growth process can be well described in terms of the sputter model: The growth occurs at the surface of a film by preferential bonding. The surface purity is governed by selective sputtering of h-BN. This influences the growth velocities in favour of c-BN. The above concept is supported by sputter yield measurements and the energy and angle of incidence dependencies of c-BN growth. The c-BN nucleation process is less well understood but the build-up of a textured h-BN layer due to compressive stress may support nucleation by lattice matching. Despite the progress in ion assisted c-BN deposition serious problems which nowadays hinder applications, even as protective coatings, exist. These may be overcome in the next future but the principle unsuitability of ion assisted c-BN for electronic applications (crystal size, phase purity, epitaxy) is obvious. Therefore to use the full advantages of the challenging material c-BN alternative deposition methods have to be developed.

10 Acknowledgements

The authors gratefully acknowledge financial support of the present work by the Deutsche Forschungsgemeinschaft (DFG) carried out "under the auspices of the trinational 'D-A-CH' German, Austrian and Swiss cooperation on the 'Synthesis of Superhard Materials'.

This work was also supported financially by the European Community (BRITE/EURAM Proj # BE 4484-89) which is gratefully acknowledged.

References

- [1] S. Reinke, M. Kuhr, and W. Kulisch. *Diamond Relat. Mater.*, 3:341, 1994.
- [2] R. H. Wentorf. *J. Chem. Phys.*, 26:956, 1957.
- [3] L. Vel, G. Demazeau, and J. Etourneau. *Mat. Sci. Eng.*, B10:149, 1991.
- [4] C. Weissmantel, K. Bewilogua, D. Dietrich, H.J. Erler, H.J. Hinneberg, S. Klose, W. Nowick, and G. Reisse. *Thin Solid Films*, 72:19, 1980.
- [5] R. Messier, A.R. Badzian, T. Badzian, K.E. Spear, P. Bachmann, and R. Roy. *Thin Solid Films*, 153:1, 1987.
- [6] T. Ichiki, T. Momose, and T. Yoshida. *J. Appl. Phys.*, 75(3), 1994.
- [7] JCPDS cards No. 35-1365, 34-421..
- [8] A. Weber, U. Bringmann, R. Nikulski, and C.P. Klages. *Diamond Relat. Mater.*, 2:201, 1993.
- [9] G.P. Lamaze, R.G. Downing, L.B. Hackenberger, L.J. Pilione, and R. Messier. *Diamond Relat. Mater.*, 3:728, 1994.
- [10] M. Kuhr, S. Reinke, and W. Kulisch. to be presented at the Plasma Surface Engineering '94, Garmisch Partenkirchen, Germany.
- [11] W. Dworschak, K. Jung, and H. Erhardt. accepted for publication in *Thin Solid Films*, 1994.

- [12] A. Weber, U. Bringmann, R. Nikulski, and C.P. Klages. In *11th International Symposium on Plasma Chemistry - ISPC 93*, Loughborough, UK, 1993.
- [13] H. Yokoyama, M. Okamoto, and Y. Osaka. *Jpn. J. Appl. Phys.*, 30:344, 1991.
- [14] W. Dworschak, K. Jung, and H. Erhardt. *Diamond Relat. Mater.*, 3:337, 1994.
- [15] Y. Osaka, A. Chayahara, H. Yokoyama, T. Hamada, T. Imura, and M. Fujisawa. *Mat. Sci. For.*, 54/55:277, 1990.
- [16] K. Bewilogua, J. Buth, H. Hubsch, and M. Grischke. *Diamond Relat. Mater.*, 2:1206, 1993.
- [17] M. Mieno and T. Yoshida. *Surf. Coat. Tech.*, 52:87, 1992.
- [18] S. Ulrich, I. Barzen, J. Scherer, and H. Ehrhardt. to be presented at Diamond'94, Castelveccio, Italy.
- [19] T. Ikeda, T. Satou, and H. Satoh. *Surf. Coat. Tech.*, 50:33, 1991.
- [20] M. Murakawa and S. Watanabe. *Surf. Coat. Tech.*, 43/44:128, 1990.
- [21] K. Inagawa, K. Watanabe, H. Ohsone, K. Saitoh, and A. Itoh. *J. Vat. Sci. Technol.*, A 5(4):2693, 1987.
- [22] D.R. McKenzie, W.D. McFall, W.G. Sainty, C.A. Davis, and R. E. Collins. *Diamond Relat. Mater.*, 2:970, 1993.
- [23] D.J. Kester and R. Messier. *J. Appl. Phys.*, 72:504, 1992.
- [24] D. Bouchier, M. A. Sené, Djouadi, and P. Müller. to be published in *Nucl. Instr. Meth. B*, 1994.
- [25] T. Wada and N. Yamashita. *J. Vat. Sci. Technol.*, A10:515, 1992.
- [26] N. Tanabe, T. Hayashi, and M. Iwaki. *Diamond Relat. Mater.*, 1:883, 1992.
- [27] R. Ganzetti and W. Gissler. presented at SMT 7, Nov. 1-3 (1993), Niigota, Japan; to be published in *Material and Manufacturing Processes*.
- [28] D.L. Medlin, T.A. Friedmann, P. B. Mirkarimi, P. Rez, M.J. Mills, and K.F. McCarty. *J. Appl. Phys.*, 76(1):295, 1994.
- [29] S. Reinke, M. Kuhr, R. Beckmann, W. Kulisch, and R. Kassing. In *Proc. of the 3rd International Symposium on Diamond Materials*, Honolulu, Hawaii, May 1993. The Electrochemical Society.
- [30] P.B. Mirkarimi, K.F. McCarty, D.L. Medlin, T.A. Wolfer, T.A. Friedmann, E.J. Klaus, G.F. Cardinale, and D. G. Hewitt. accepted for publication in *Jour. Mat. Res.*, 1994.
- [31] B. N. Chapman. *Glow discharge processes*. Wiley, 1982.
- [32] S. Reinke, M. Kuhr, and W. Kulisch. to be presented at Plasma Surface Engineering '94, Garmisch Partenkirchen, Germany.
- [33] N. Matsunami, Y. Yamamura, Y. Itikawa, N. Itoh, Y. Kazumata, S. Miyagawa, K. Morita, R. Mizu, and H. Tawara. *Atomic Data and Nuclear Data Tables*, 31:1, 1984.
- [34] H. Windischmann. *J. Appl. Phys.*, 62(5):1800, 1987.
- [35] M. Sueda, T. Kobayashi, H. Tsukamoto, T. Rokkaku, S. Morimoto, Y. Fukaya, N. Yamashita, and T. Wada. *Thin Solid Films*; 228:97, 1993.
- [36] W. Dworschak. PhD thesis, University of Kaiserslautern, Germany, 1994.
- [37] S. Ulrich. Private communication, 1994.
- [38] D.J. Kester, K.S. Ailey, and R.F. Davis. *Diamond Relat. Mater.*, 3:332, 1994.
- [39] T.A. Friedmann, P.B. Mirkarimi, D.L. Medlin, K.F. McCarty, E.J. Klaus, D.R. Boehme, H.A. Johnsen, M.J. Mills, and D.K. Ottesen. *J. Appl. Phys.*, 76(5):3088, 1994.
- [40] H.H. Anderson and H.L. Bay. In R. Behrisch, editor, *Sputtering by particle bombardment*, volume 1, chapter 4, page 200. Springer Verlag, Berlin, 1981.
- [41] H.H. Anderson and H. L. Bay. In R. Behrisch, editor, *Sputtering by particle bombardment*, volume 1, chapter 4, page 166. Springer Verlag, Berlin, 1981.

- [42] M. Kuhr, S. Reinke, and W. Kulisch. to be presented at the Diamond'94, Castelveccio, Italy.
- [43] M. Kuhr. Thesis in preparation, University of Kassel, Germany.
- [44] D.L. Medlin, T.A. Friedmann, P.B. Mirkarimi, M.J. Mills, and K.F. McCarty. *Phys. Rev. B*, 1994.
- [45] W.A.L. Lambrecht, Lee. C. H., B. Segall, J.C. Angus, Z. Li, and M. Sunkara. *Nature*, 364:607, 1993.
- [46] Y. Lifshitz, S.R. Kasi, J.W. Rabalais, and W. Eckstein. *Phys. Rev. B*, 41:10468, 1990.
- [47] J. Robertson. *Diamond Relat. Mater.*, 3:361, 1994.
- [48] C.A. Davis. *Thin Solid Films*, 226:30, 1993.
- [49] D.R. McKenzie, D. Muller, B.A. Pailthorpe, Z.H. Wang, E. Kravtchinskaia, D. Segal, P.B. Lukins, P.D. Swift, P.J. Martin, G. Amaratunga, P.H. Gaskell, and A. Saeed. *Diamond Relat. Mater.*, 1:51, 1991.
- [50] G. Demazeau. *Diamond Relat. Mater.*, 2:197, 1993.
- [51] J. Cuomo, D.L. Pappas, R. Lossy, J.P. Doyle, and J. Bruley. *J. Vat. Sci. Technol.*, A 10(6):3414, 1992.
- [52] B. Rother, J. Siegel, I. M^uhling, H. Fritsch, and K. Breuer. *Mat. Sci. Eng.*, A 140:780, 1991.
- [53] M.A. Djouadi, D. Bouchier, P. M^oller, and G. Sene. In *9th International Colloquium on Plasma Processes (CIP93)*, Antibes, France, June 1993. Societe Francaise du Vide.
- [54] D.R. McKenzie, Y. Yin, N.A. Marks, C.A. Davis, G.A.J. Pailthorpe, B.A. Amaratunga, and V.S. Veerasamy. *Diamond Relat. Mater.*, 3:353, 1994.
- [55] K. W.R. Gilkes, P.H. Gaskell, and J. Yuan. *Diamond Relat. Mater.*, 3:369, 1994.
- [56] R.F. Davis. Private communication, 1994.
- [57] J.E. Butler and R.L. Woodin. *Phil. Trans. R. Soc. Lond.*, A 342:209, 1993.
- [58] D. Bouchier and W. M^oller. *Surf. Coat. Tech.*, 51:190, 1992.
- [59] M. Okamoto, H. Yokoyama, and Y. Osaka. *Jpn. J. Appl. Phys.*, 29:930, 1990.
- [60] T. Ikeda, Y. Kawate, and Y. Hirai. *J. Vat. Sci. Technol.*, A8:3168, 1990.
- [61] K. Inagawa, K. Watanabe, K. Saitoh, Y. Yuchi, and A. Itoh. *Surf. Coat. Tech.*, 39/40:253, 1989.
- [62] N. Yamashita, T. Wada, M. Ogawa, T. Kobayashi, H. Tsukamoto, and T. Rokkaku. *Surf. Coat. Tech.*, 54/55:418, 1992.
- [63] D. Bouchier. Private communication, 1994.
- [64] M.A. Djouadi. PhD thesis, Universtite Paris-Sud, France, 1994.
- [65] M. Murakawa, S. Watanabe, and S. Miyake. *Diam. Films Tech.*, 1 No.1:55, 1991.
- [66] I. Muraguchi and Y. Osaka. In *Proceedings of the 6th Symposium on Plasma Science for Materials*, Tokyo, 1993.
- [67] P.K. Bachmann and W. van Enckevort. *Diamond Relat. Mater.*, 1:1021, 1992.
- [68] Y. Ichinose, H. Saitoh, and H. Yoshihiko. *Surf. Coat. Tech.*, 43/44:116, 1990.
- [69] H. Saitoh, H. Merino, and Y. Ichinose. *Jpn. J. Appl. Phys.*, 32:L1684, 1993.
- [70] W.L. Wang, K.J. Liao, and J.Y. Gao. *phys. stat. sol. (a)*, 139:K25, 1993.
- [71] H. Saitoh and W.A. Yarbrough. *Appl. Phys. Lett.*, 58 (22):2482, 1991.
- [72] N. Tanabe, T. Hayashi, and M. Iwaki. *Diamond Relat. Mater.*, 1:151, 1992.
- [73] W. Dworschak. Private communication, 1994.
- [74] N. Tanabe and M. Iwaki. *Nucl. Instr. and Meth.*, B 80/81:1349, 1993.

Deposition of Cubic Boron Nitride with a Inductively Coupled Plasma (ICP)

M. Kuhr, S. Reinke, W. Kulisch
Institute of Technical Physics
University of Kassel

Heinrich-Plett-Strasse 40

D - 3 4 1 0 9 Kassel, F R G

Tel: 49 561/8044519; FAX: 49 561/804-4136

Abstract

Cubic boron nitride (c-BN) films have been deposited by inductively coupled plasma (ICP) CVD. With this technique films with a c-BN content of nearly 75 % can be achieved. Investigations on the influence of the process parameter which are most important to deposit c-BN (ion flux, ion energy and, substrate temperature) have been carried out. The results show good agreement with our theoretical sputter model [1]. Furthermore, from these experiments it is possible to draw the conclusion that the deposition of c-BN films with PVD methods and with ion induced CVD techniques relies on the same deposition mechanisms among which physical sputtering is most important.

Int reduction"

Owing to the outstanding material properties of c-BN [f?], the deposition of thin c-BN films has attracted considerable interest during the last years. The great majority of successful deposition methods described up to now in literature belongs to either of two groups (see [1]): ion assisted PVD (e.g. ion beam assisted deposition (IBAD), ion "plating) or ion induced CVD (e.g. ECR and ICP plasmas plus additional substrate bias). It is therefore evident that ion bombardment plays a decisive role in c-BN formation. In recent publications [3, 4] we have summarized all available IBAD data thereby showing that a well defined c-BN domain exists, dependent on the main parameters ion energy, ion to atom flux ratio and substrate temperature. Furthermore, a model was developed which assumes selective sputtering of h-BN with respect to c-BN to be the major function of the ion bombardment. Experimental evidence for this model was provided very recently [1, 5].

Nowadays, IBAD of c-BN is well established and characterized. There are, however, several reasons to investigate (ion induced) CVD of cubic boron nitride: CVD experiments could extend the range of reliable data on c-BN formation down to, lower energies which can not be reached with IBAD due to the high ion currents required according to our model. Second, the ion bombardment during c-BN formation causes some serious problems among which the nanocrystallinity and the high compressive stress of the films are most important [1]. Therefore it is worthwhile to investigate

whether the ion bombardment can at least in part be replaced by chemical effects. Finally, CVD has advantages with respect to IBAD in terms of costs, throughput and large area and 3-dimensional coating. On the other hand, it is evident from our model that a CVD technique for c-BN formation must be able to provide high plasma densities at low pressures. The inductively coupled plasma (ICP) technique has been shown to fulfill these requirements [6, 7].

"In this paper, we will first describe a self designed ICP set-up. It will be shown that high density plasmas at low pressures are possible with ICP and, most important, that ion energy and ion flux can "be varied independently and within wide ranges. We will then discuss the influence of major process parameters such as substrate bias voltage (i.e. ion energy), plasma density (i.e. ion flux), and substrate temperature on the phase composition of boron nitride films. Finally we will compare our results to those from PVD and other CVD techniques in terms of microscopic deposition parameters thereby demonstrating that ion assisted PVD and ion induced CVD of cubic boron nitride rely on the same mechanisms, and that sputtering plays a dominant role among these mechanisms.

Experimental

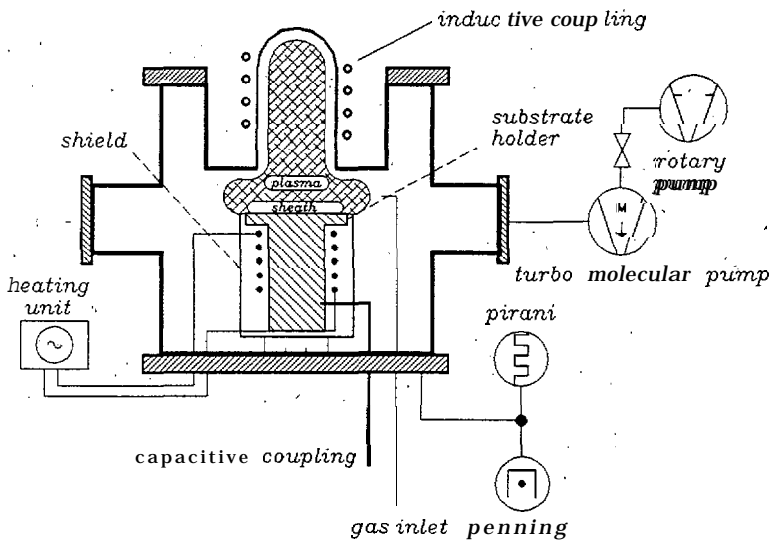


Figure 1: Schematic drawing of the ICP set-up.

Inductively Coupled Plasma (ICP) set-up The experiments have been carried out, in a stainless steel vacuum chamber schematically shown in Fig. 1. On its top plate there is a quartz tube of 10 cm height and 4 cm diameter. A 13.56 MHz RF-signal (Advanced Energy RFX-600) is coupled inductively into this tube by means of a copper coil. In this way, a very intense plasma is created within the quartz tube which reaches almost down to the substrate holder. The signal of a second 13.56 MHz generator (Hüttinger PFG 300) is coupled capacitively to the substrate holder in order to provide a substrate bias. A low working pressure ($2 \cdot 10^{-2}$ mbar) is accomplished by means of a turbo pump (Balzers TPH 330) backed by a two stage rotary pump (Leybold Trivac D8B) which leads to a base pressure of $2 \cdot 10^{-5}$ mbar. With high

substrate bias and low working pressure, ion energies up to several hundred electron volts are reachable. The substrate holder is heatable up to 800 °C

process Parameters		
base pressure	[mbar]	2 · 10 ⁻⁵
working pressure	[mbar]	2 · 10 ⁻²
rf power (ind.)	[W]	80
rf substrate bias	[V]	50 - 200
ion density	[cm ⁻³]	5 · 10 ¹⁰
substrate temperature	[°C]	500
argon flow	[seem]	50
nitrogen flow	[seem]	2.5
T B M flow	[seem]	≈ 1 - 2
film properties		
growth rates	[nm/min]	< 10
stoichiometry		0.9 ≤ B/N ≤ 1.1
carbon content	[%]	< 5
oxygen content	[%]	< 2
max. c-BN content	[%]	75

Table 1: Summary of the major process parameters of the ICP process used "in our investigation, and of some important properties of the resulting c - B N film.

The gas inlet is a stainless steel ring above the substrate holder. All experiments described in the following sections have been carried out with a mixture of trimethyl borazine (TMB, HBN(CH₃)₃), nitrogen and argon. Tab. 1 summarizes typical process parameters of a c-BN deposition.

Langmuir-probe measurements Prior to, the deposition experiments, the ICP set-up shown in Fig. 1 was characterized by Langmuir double probe measurements in order to determine the plasma densities respective the ion fluxes achievable. The space charge limited current from a plasma can be calculated from the plasma density n_e and the electron temperature T_e [8]:

$$J_{ion} = 0.6 * n_e e \sqrt{kT_e / m_{ion}} \quad (1)$$

with e : electron charge, k : Boltzmann constant, m_{ion} : ion mass.

From our recently published sputter model [4] and from other authors [9] it is evident that high ion fluxes are necessary for deposition of c-BN with ion induced methods like the ICP technique. Therefore high plasma densities at low pressures are required while on the other hand low pressures have to be used in order to achieve sufficient ion energies. An example of probe measurements is given in Fig. 2. "It can be seen that even at pressures as low as 2 · 10⁻² mbar plasma densities of about 3 · 10¹¹ cm⁻³ can be achieved. Besides this proof of high plasma densities "Langmuir probe measurements yield another important result: for a given pressure and gas flow, the plasma density is determined by the inductively coupled plasma. It is almost independent of the power coupled capacitively to the substrate holder. It follows that plasma density and therefore ion flux on the one hand, and substrate bias voltage and therefore ion energy on the other hand, can be chosen nearly independent ly.

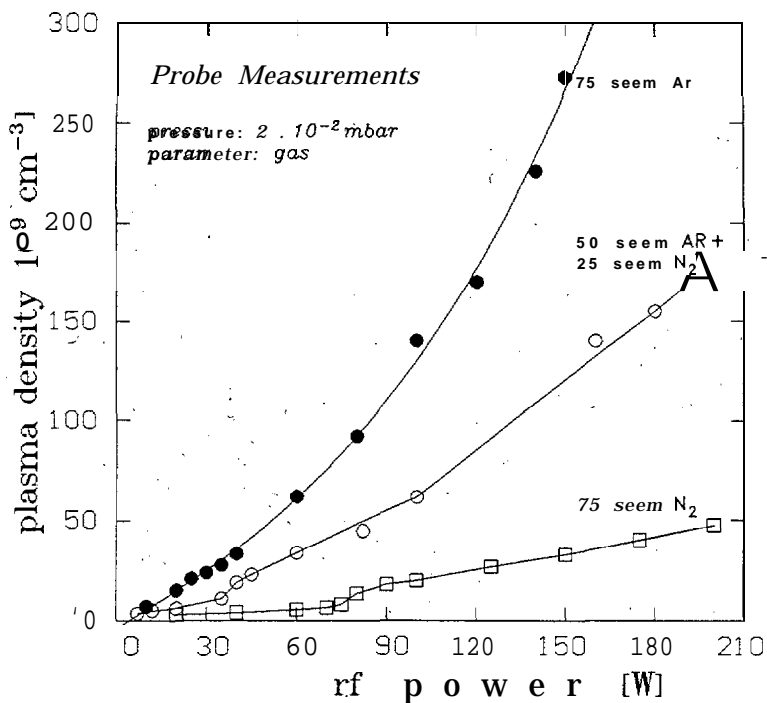


Figure 2: Dependence of the plasma density on the inductively coupled "RF-power for different process gas mixtures.

This is a great advantage of our set-up compared with some other techniques [10]. Furthermore, this is of importance in view of investigations of the ion energy and ion flux dependencies of c-BN deposition.

To summarize, an ICP set-up has been designed and realized that is able to provide the conditions to investigate the formation of c-BN: high plasma densities, low working pressure, an independent control of ion flux and ion energy, and a large range" of deposition temperature. Moreover, it is relatively cheap as compared to other set-ups with high plasma densities (e.g. ECR).

Characterization methods The thickness and the refractive index of the films was measured by ellipsometry (Plasmos SD 2100). The composition (stoichiometry, content of contaminations) was determined by Auger electron spectroscopy (AES). Calibration was performed by means of a standard boron nitride sample with known concentrations of oxygen and carbon, measured by EDAX. Fourier transform infrared spectroscopy (FTIR) (Biorad FTS 60a) was used to determine the c-BN content by a procedure described in [11]. The crystal modification and the crystal size were measured with transmission electron diffraction (TED), and, finally the morphology was investigated with scanning electron microscopy (SEM).

Results and discussion

General film properties With the ICP set-up shown in Fig. 1, and the parameters given in Tab. 1, it is possible to deposit boron nitride films with a considerable content of the cubic phase. TED measurements (cf Fig 3) confirm the existence of c-BN. They further reveal a crystal size of about 5 nm and a weak texture of the c-BN films. A maximum c-BN content of 75 % was obtained as measured with FTIR

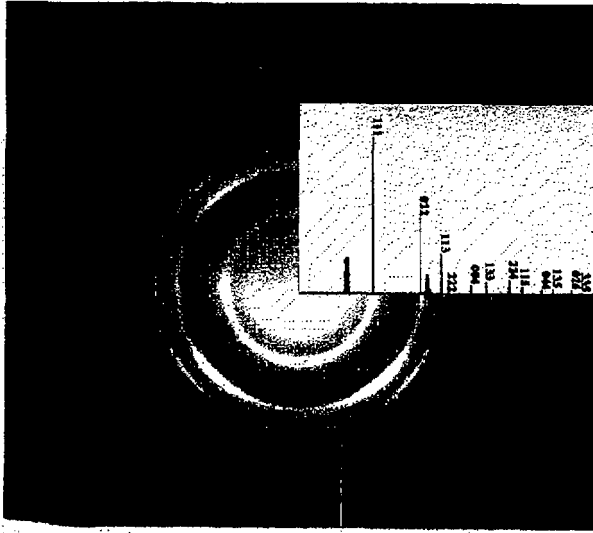


Figure 3: TED picture of a boron nitride film with a c-BN content of nearly 50%

(cf Fig. 4) which, seems to be typical for CVD techniques [10, 12, 9], in contrast to IBAAD deposition where c-BN contents >90 % are possible [13]. The reason for the limitation to 75 % c-BN could be the incorporation of hydrogen during the deposition which is inevitably present in CVD.

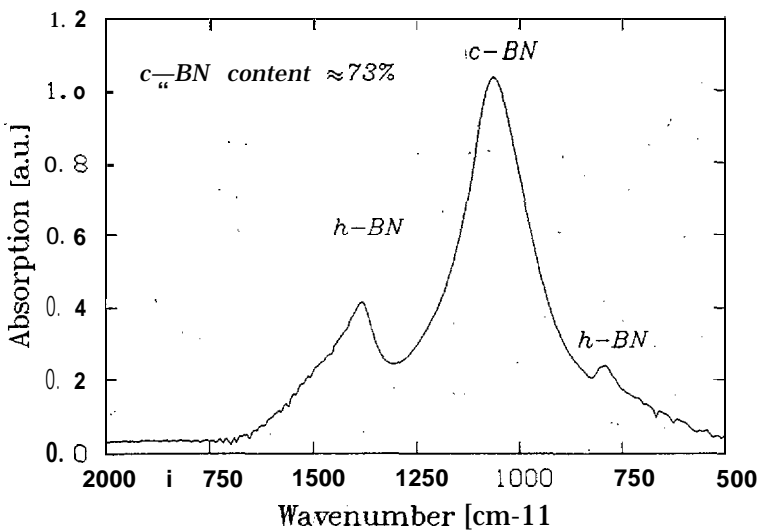


Figure 4: Infrared spectrum of a boron nitride film with a c-BN content of 73%.

The deposition of c-BN critically depends on the process parameters. With wrong sets of process parameters only h-BN layers are obtained. As already mentioned, ion energy and ion flux play a decisive role in the process of c-BN deposition. Their influence will be discussed below. The stoichiometry of the films is also important. With AES measurements we observed a range of $0.9 < B/N < 1.1$ for the formation of c-BN. The stoichiometry in turn depends on the ion bombardment (sputtering effects) [11] and the flow of the process gases. Furthermore the content of contaminations must be kept below a certain level, which can be estimated to 10% carbon and 5% oxygen. Typically, our c-BN films possess an oxygen content <2% and a carbon content <5%.

The main problem with the ICP deposition of c-BN is the stress of the films as is the case with all ion induced techniques of c-BN deposition. Films with c-BN contents of 30 – 75 % show microcracks or even peel off. No ellipsometric and stress measurements could be performed with such films. From literature it is known that boron rich or silicon boron nitride interlayers could avoid such microcracks [14]; will investigate the deposition process with such interlayers in the future.

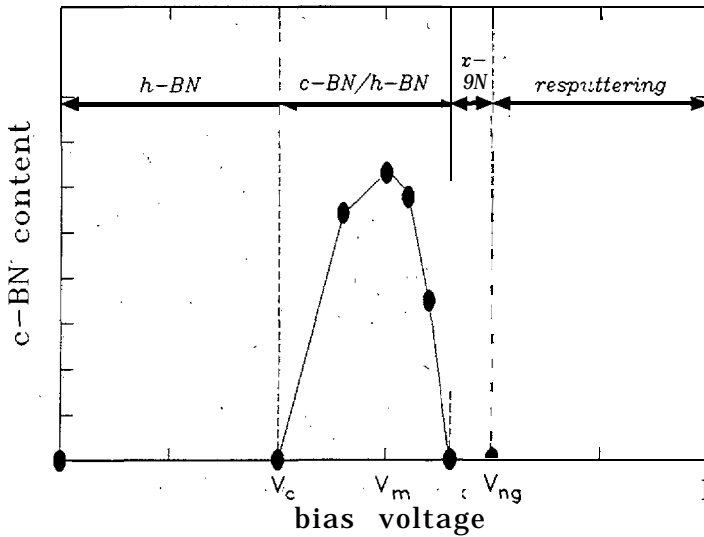


Figure 5: Schematic diagram of the bias voltage sequence.

The bias voltage sequence In all our experiments, the following sequence has been found inevitably as a function of the bias voltage (Fig. 5):



This means that for any given set of parameters; at low voltages hexagonal boron nitride (h-BN) is obtained. If V_B is increased over a certain threshold V_c , c-BN/h-BN mixtures are deposited. For $V_B > V_c$, the c-BN content of the films first increases. However, 'under any conditions a maximum c-BN content is obtained at V_m , while for $V_B > V_m$ the c-BN content decreases again. At very high V_B ($V_B \geq V_x$) films are obtained which show no IR peak due to c-BN but are quite different from the low ion bombardment h-BN,

In order to indicate that this material is not the standard h-BN we refer to it as x-BN. It should be mentioned that a sp^2 BN phase close to the no growth region was also found in other investigations (PVD as well as CVD) [15, 16, 12]. Fig. 6 shows the surface of a x-BN sample. h-BN films deposited at low bias are smooth and without any features. In contrast, Fig. 6 shows the x-BN surface to have a distinct morphology. Furthermore, whereas h-BN films are transparent in the visible, the x-BN films are opaque which renders ellipsometric determination of thickness and refractive index impossible. Finally, there are distinct differences in the FTIR spectra of h-BN and x-BN. This is evident from Fig. 7 where a spectrum of an x-BN sample is compared with those of a commercial h-BN powder (Alfa products, 325 mesh) and

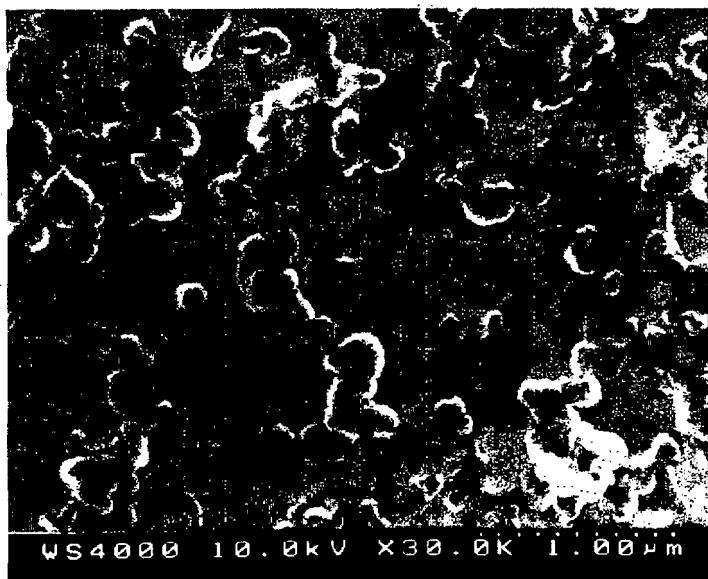


Figure 6: SEM picture of a x-BN film.

a h-BN film deposited in the low voltage region. All three spectra show the two peaks common for h-BN, and there is no hint at c-BN in the spectrum of the x-BN film. But on the other hand it can be seen in Fig 7 that the B-N stretching peak at 1380 cm^{-1} is extremely broad in the case of x-BN. Such a high FWHM of this peak is only found for x-BN films. At the present stage, neither the structure of this x-BN nor reason of its existence are clear. However, AES measurements of these films yield an interesting result: All x-BN films are boron rich ($B/N \approx 1.1 - 1.2$). Stoichiometry on the other hand, has been shown to be an important requirement for c-BN formation (see above). A closer examination of the AES data reveals that preferential sputt of nitrogen with respect to boron may be the reason for this overstoichiometry. These boron rich films are stable against ion bombardment at high ion energies and ion fluxes; therefore the existence of x-BN is not in contrast to the sputter model [5].

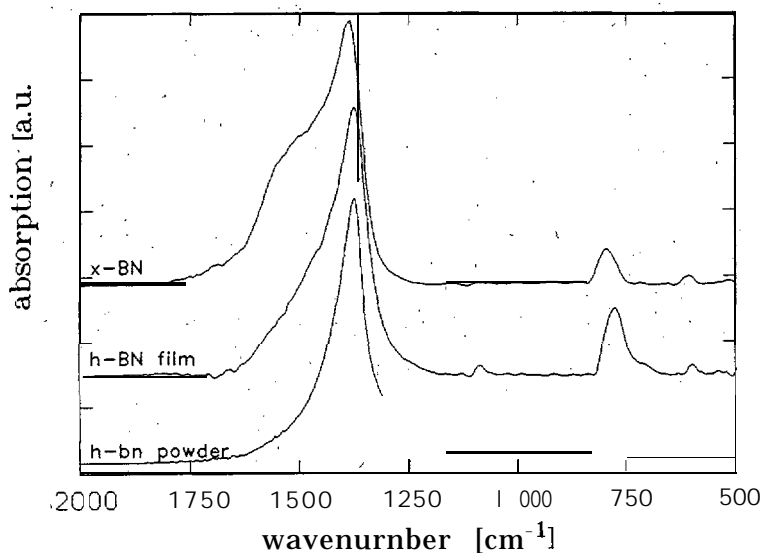


Figure 7: Infrared spectra of a x-BN and a h-BN film, and of commercial h-BN powder.

As has already been pointed out, the bias voltage sequence is observed irrespecti of the other process parameters. However these parameters, and among them namely

the substrate temperature T_S and the plasma density n_e , strongly influence the position of, the important points (i.e. V_B , V_t , V_m and V_x) on the voltage scale, and also the maximum c-BN content at V_m . The influence of T_S and n_e on the bias voltage sequence –which is a direct consequence of our sputter model– will be described in the following sections.

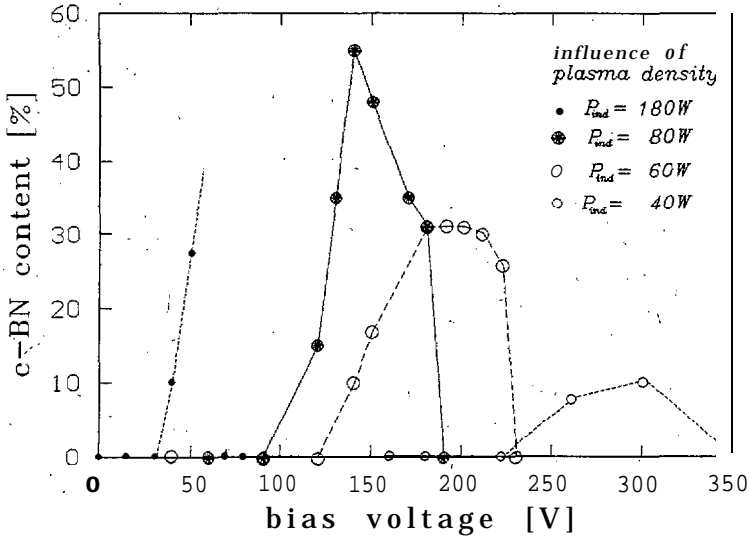


Figure 8: Dependence of the bias voltage sequence on the inductively coupled RF power

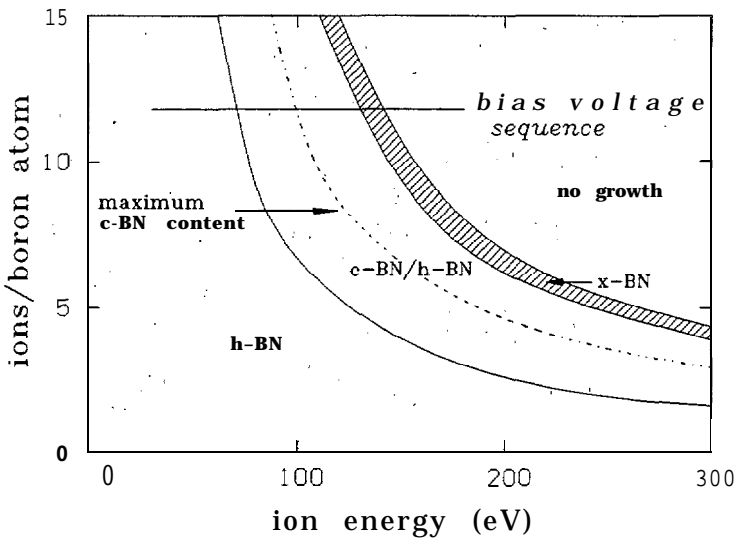


Figure 9: Schematical drawing of the c-BN domain in the F/E diagram. . .

Influence of the plasma density n_e The influence of the plasma density n_e on the bias voltage sequence is shown in Fig. 8. As predicted by our model, the sequence shifts to lower V_B if the inductively coupled RF power is increased, since this results in an increase of n_e and therefore of the ion flux (see Fig. 2). This result shows that low ion energies can be compensated by high ion fluxes and vice versa, and is in a good agreement with our sputter model. Fig. 9 shows a schematic F/E (F = ion per boron atom, E = ion energy) diagram according to [1] with a domain where films with c-BN content can be obtained. Below the boundary F_h only h-BN is deposited whereas

above F_x no film growth takes place. As discussed above, there is an h-BN domain close to the no growth boundary. With each bias voltage 'sequence a cut is performed through the different regions. In order to compare our data to other CVD as well as PVD data we introduced the parameter F^* ($F^* =$ ions per incorporated boron atom) [1] which can be calculated according to equation (1) and from the known composition of the deposited film. The results are shown in Fig. 10. Since with our ICP set-up ion flux and ion energy can be varied independently and in wide ranges, we are able to cover a large part of the F^*/E diagram.

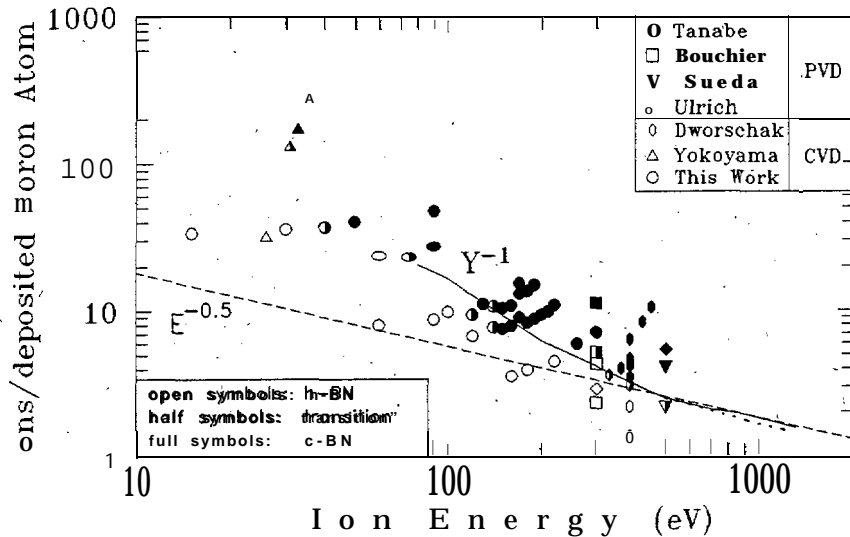


Figure 10: Dependency of the boundary between h-BN and c-BN on ion energy E_{ion} and the number of bombarding "ions per" incorporated B atoms for CVD as well as PVD deposition methods. CVD data from this work; Yokoyama et al. [17] and Dworschak et al. [10]. PVD data from Ulrich et al. [18], Bouchier et al. [19, 20], Tanabe et al. [21] and Sueda et al. [15]. The full line represents the dependency of the inverse sputter yield Y^{-1} of Si under argon bombardment [22], fitted to the data at 500 eV.

Fig. 10 shows a well defined boundary over a large energy range which separates the h-BN region from the c-BN region. An inverse sputter yield can be fitted as is discussed in [1] which indicates that the transition boundary indeed represents a sputter limit as expected from our model.

From Fig. 10, two major conclusions can be drawn: At first the energy range of c-BN growth reaches down to energies well below 100 eV. Lower energies can be compensated by high ion fluxes and vice versa. Second PVD and ion induced CVD of c-BN rely on the same mechanisms. Therefore, chemical mechanisms can be excluded in ion induced CVD of c-BN.

Influence of the substrate temperature, T_s Fig. 11 shows the influence of the substrate temperature T_s on the bias voltage sequence. The following observations can be made: With increasing temperature, the sequence shifts to lower energies, the.

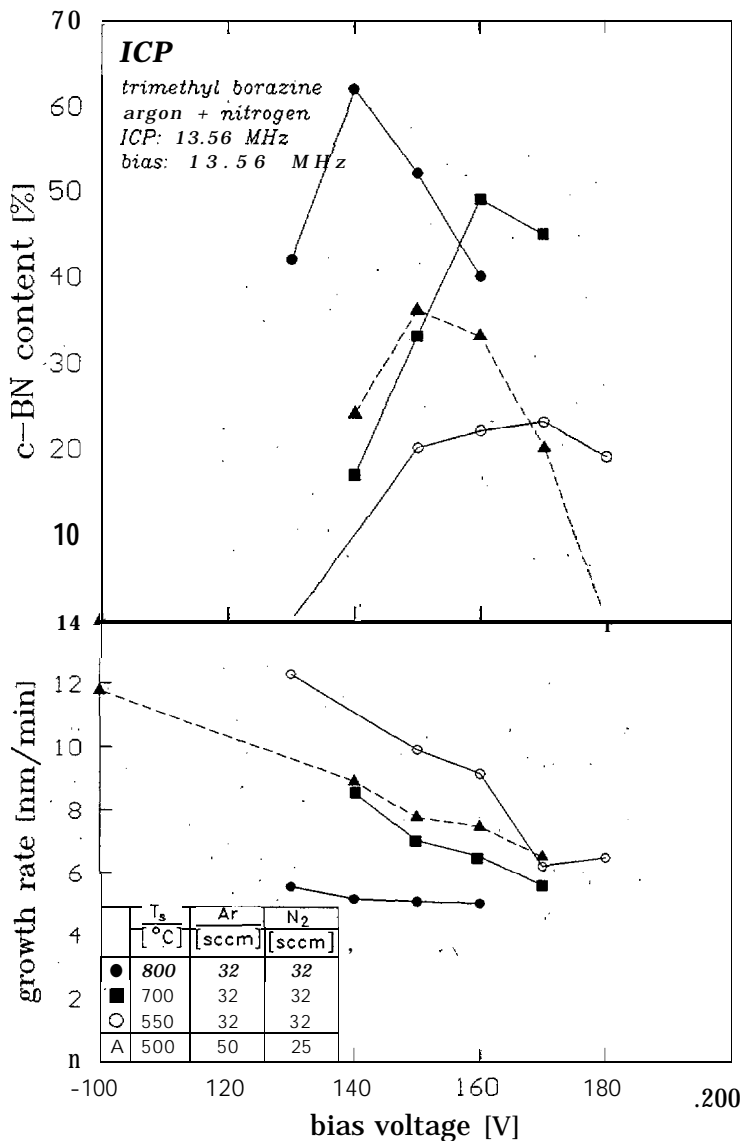


Figure 11: Bias voltages sequences and growth rates in dependence of the substrate temperature and the Ar/N₂ gas mixtures.

maximum c-BN content increases, and the growth rates decrease. Observation one and three are easily explained by our model [4]: At higher temperatures, desorption processes become more and more important which leads to a decrease of the deposition rates. As a consequence, the number of incorporated boron atoms per unit time decreases whereas the number of incoming ions remains constant; as a result, F^* increases and the sequence shifts to lower energies according to Fig. 8. The explanation of increase of the maximum, however, needs further investigations: Increase of the surface mobility, and decrease of hydrogen incorporation are two possible mechanisms.

Fig. 11 also shows one set of data for an increased Ar/N₂ ratio in the gas phase. Compared with the data with Ar/N₂=1 at the same temperature, the rates are lower, and the maximum of the c-BN content is shifted to lower energies. These effects can be explained by the Langmuir measurements in Fig. 2: The plasma density increases for higher Ar/N₂. Therefore the number of ions impinging the surface and alongside F^* increase leading to enhanced sputtering. We discussed in [1] that the sputter yields

of nitrogen and argon are similar and therefore the ion beam composition can not be the reason for this result.

Summary

An ICP set-up has been presented which allows the deposition of BN films with a maximum c-BN content "up to 75 %". Our experiments show a distinct bias voltage sequence. Higher ion "fluxes and higher substrate temperatures lead to a shift of the important points of the bias voltage sequence to lower ion energies which can be well explained by the sputter model [1]. Quantification of our results in terms of ions per incorporated boron atoms and comparison to other deposition techniques shows that the deposition mechanisms of PVD and ion induced PECVD are the same. Sputtering seems to be the most important mechanism, as proposed from our model [1].

Acknowledgements

We like to thank Dr. Pongratz and Dr. Wurtzinger, University Vienna, for TED measurements. The authors gratefully acknowledge financial support of the present work by the Deutsche Forschungsgemeinschaft (DFG) carried out under the auspices of the trinational 'D-A-CH' German, Austrian and Swiss cooperation on the 'Synthesis of Superhard Materials'.

This work was also supported financially by the European Community (BRIT EURAM Proj # BE 4484-89) which is gratefully acknowledged.

References

- [1] R. Reinke, M. Kuhr, W. Kulisch, and R. Kassing. Cubic boron nitride deposition - state of the art. Paper presented at the diamond 94 conference, Castelveccio, Italy. Submitted to *Diamond Relat. Mater.* (this volume), 1994.
- [2] G. Demazeau. Growth of cubic boron nitride by chemical vapor deposition and high-pressure high-temperature synthesis. *Diamond Relat. Mater.*, 2:197, 1993.
- [3] S. Reinke, M. Kuhr, R. Beckmann, W. Kulisch, and R. Kassing. A sputter model for ion induced c-BN growth. In *Proc. of the 3rd International Symposium on Diamond Materials*, Honolulu, Hawaii, May 1993. "The Electrochemical Society.
- [4] S. Reinke, M. Kuhr, and W. Kulisch. Mechanisms in, ion induced c-bn deposition. *Diamond Relat. Mater.*, 3:341, 1994.
- [5] S. Reinke, M. Kuhr, and W. Kulisch. Critical test of the c-bn sputter model. to be presented at Plasma Surface Engendering '94, Garmisch-Partenkirchen, Germany."
- [6] J. Ocampo. Alternative plasma etch sources. *European Semiconductor*, September 1991:15, 1991.
- [7] J. Amorim, H.S. Maciel, and J.P. Sudano. High density plasma mode of an inductively coupled radio frequency discharge. *J. Vac. Sci. Technol.*, B9:362, 1991.

- [8] B. N. Chapman. *Glow discharge processes*. Wiley, 1982.
- [9] A. Weber, U. Bringmann, R. Nikulski, and C. P. Klages. Influence of a substrate bias on the formation of cubic boron nitride in an ECR plasma CVD process. In *11th International Symposium on Plasma Chemistry — ISPC 93*, Loughborough, UK, 1993.
- [10] W. Dworschak, K. Jung, and H. Erhardt. Growth of cubic boron nitride coatings in a magnetic field enhanced rf-glow discharge. *Diamond-Relat. Mater.*, 3:337, 1994.
- [11] M. Kuhr, S. Reinke, and W. Kulisch. Nucleation of cubic boron nitride (c-bn) with ion induced pecvd. to be presented at the Diamond' 94, Castelveccio, Italy.
- [12] T. Ichiki, T. Momose, and T. Yoshida. Effects of the substrate bias on the formation of cubic boron nitride by inductively coupled plasma enhanced chemical vapor deposition. *J. Appl. Phys.*, 75(3), 1994.
- [13] D. J. Kester and R. Messier. Phase control of cubic boron nitride thin films, *J. Appl. Phys.*, 72:504, 1992.
- [14] M. Okamoto, H. Yokoyama, and Y. Osaka. Formation of cubic boron nitride film on Si with boron buffer layers. *Jpn. J. Appl. Phys.*, 29:930, 1990.
- [15] M. Sueda, T. Kobayashi, H. Tsukamoto, T. Rokkaku, S. Morimoto, Y. Fukaya, N. Yamashita, and T. Wada. Fundamental research on the deposition of cubic boron nitride films on curved substrates by ion-beam-assisted vapor deposition. *Thin Solid Films*, 228:97, 1993.
- [16] T. Ikeda, Y. Kawate, and Y. Hirai. Formation of cubic boron nitride films by arc-like plasma-enhanced ion plating method. *J. Vat. Sci. Technol.*, A8:3168, 1990.
- [17] H. Yokoyama, M. Okamoto, and Y. Osaka. Effects of a negative self-bias on the growth of cubic boron nitride prepared by plasma chemical vapor deposition. *Jpn. J. Appl. Phys.*, 30:344, 1991.
- [18] S. Ulrich, I. Barzen, J. Scherer, and H. Ehrhardt. Rf-ion plating induced phase transition from h-bn to nanocrystalline c-bn. to be presented at Diamond'94, Castelveccio, Italy.
- [19] D. Bouchier and W. Möller. Temperature dep. *Surf. Coat. Tech.*, 51:190, 1992.
- [20] D. Bouchier, M. A. Sené, Djouadi, and P. Möller. Effect of noble gas ions on the synthesis of c-bn by ion beam assisted deposition. to be published in *Nucl. Instr. Meth. B*, 1994.
- [21] N. Tanabe, T. Hayashi, and M. Iwaki. Deposition of cubic boron nitride thin films by ion-beam-enhanced deposition. *Diamond Relat. Mater.*, 1:883, 1992.
- [22] N. Matsumami, Y. Yamamura, Y. Itikawa, N. Itoh, Y. Kazumata, S. Miyagawa, K. Morita, R. Shimizu, and H. Tawara. Energy dependency of the ion-induced sputtering yields of monoatomic solids. *Atomic Data and Nuclear Data Tables*, 31: 1, 1984.

“Critical’ test of the. c-BN sputter model’

*S. Reinke, M. Kuhr, W. Kulisch
Institute of Technical Physics, University of Kassel
Heinrich Plett Str. 40, 34109 Kassel, FRG*

Abstract

C-BN films are commonly deposited with ion assisted methods (CVD as well as PVD). It will be shown that all ion assisted techniques work within the same range of deposition parameters which implies a common growth mechanism. Recently, we proposed a model for ion induced c-BN deposition in which material removal processes due to sputtering and resorption play the major roles. Measurements of the sputter yields of BN films confirm the basic assumptions of the model with respect to sputtering. Nevertheless, under special conditions additional influences of compressive stress and film stoichiometry have to be taken into account which are, however, not contradictory to the model.

1 Introduction

Boron nitride exists similar to carbon in two main crystalline modifications, hexagonal BN (h-BN) and cubic BN (c-BN) which are similar to graphite and diamond, “respectively. C-BN exhibits excellent material properties, and several applications are imaginable [1]. Therefore, the deposition of high quality c-BN thin films is a great challenge but understanding of the basic mechanisms is the key to improve film quality. Nowadays, c-BN films are commonly deposited by ion assisted deposition methods (CVD as well as PVD) which lead to nanocrystalline films. All these deposition methods have been shown to work within the same range of microscopic deposition parameters and, therefore, to rely on the same basic mechanisms [2]. A model was developed which assumes selective sputtering of h-BN with respect to c-BN to play the dominant role in the c-BN growth process [3]. The nucleation process for which additional mechanisms have to be taken into account will not be treated here. For a detailed discussion we refer to [2, 4]. In order to bring more insight into the sputter behaviour of BN films we performed ion beam sputtering experiments with h-BN and c-BN. The main results, high absolute sputter yields and a selectivity of approx. 1.5 between the yields of h-BN and c-BN are discussed in light of the sputter model.

2 The sputter model

Recently, we presented a data collection for ion beam assisted deposition (IBAD) of c-BN and developed a model which assumes selective sputtering of h-BN to be the basic mechanism for c-BN deposition [3]. Meanwhile the data collection could be extended; in Fig. 1 data from 5 independent experiments are included, covering a wide energy range from 200 to 1200 eV.

The figure shows the dependency of the deposited BN, phase on the ion energy E_{ion} and the ion to boron atom arrival ratio $F = F_{ion}/F_B$ (F_{ion} , ion flux; F_B , flux of boron atoms). The other deposition parameters were kept nearly constant: In every investigation mixtures of argon and nitrogen ions and substrate temperatures of about 400 °C were used [2]. H-BN is found for low F values but with increasing ion bombardment a quite sharp transition to c-BN occurs. If the ion flux is increased further, no net film growth can be detected. Two more findings are worth to be mentioned but will not be discussed in detail: First, the behaviour at high energies is somewhat unclear. Some data indicate a transition from c-BN to a mixture of h-BN and c-BN which may be attributed to radiation damage. In contrast, Mirkarimi et al. found 80%

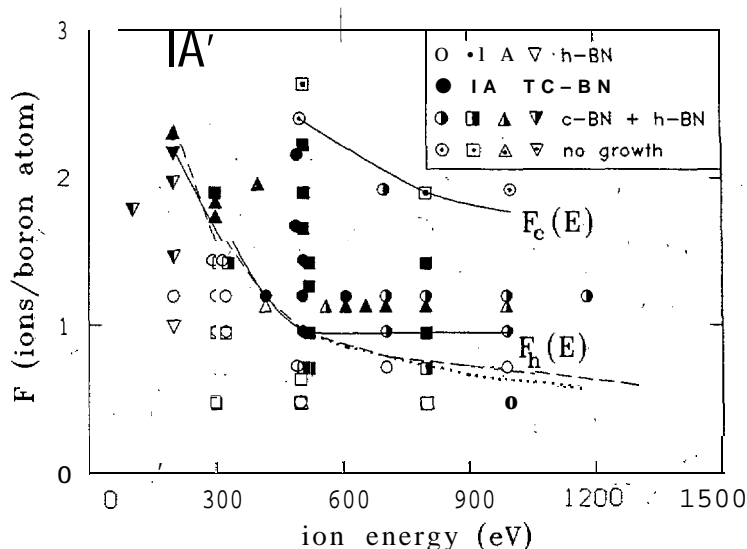


Figure 1: Dependence of the structure of IBAD BN films on ion energy E_{ion} and the ion to B atom arrival ratio F . Circles, data from Tanabe et al. [25]; squares, data from Kester et al. [6]; triangles data from Bouchier et al. [26]; up side “down triangles: data from Ganzetti et al. [27]. The dotted represents the transition evaluated by Mirkarimi et al. with laser ablation IBAD [5] and the dashed the dependency of the inverse sputter yield Y^{-1} of Si under argon bombardment [8]. Both were fitted to F_h at 500 e V.

c-BN even at an ion energy of 1200 eV [5]. Second, -above 500 eV, the flat dependency of the boundary between h-BN and c-BN F_h is determined by the fact that a B/N ratio of nearly 1 is required for c-BN growth [3]. In conventional IBAD, the nitrogen is sustained only by the ion beam (mostly as N_2^+) and therefore with a 1:1 mixture of nitrogen and argon ions stoichiometry can only be achieved above approx. $F \approx 1$. In contrast, with ion beam assisted laser ablation (where nitrogen is also offered from the BN target), the transition from h-BN to c-BN is not determined by stoichiometry, even at high ion energies (dotted line).

In Fig. 1 only IBAD is considered but it is known that c-BN can also be deposited with ion assisted plasma deposition (CVD as well as PVD). With these methods the determination of the flux ratio F is nearly impossible. Therefore we focused on the number of incorporated boron atoms per incident ion F^* [2]. The resulting data are shown in Fig. 2. With this parametrization, the energy range for which some knowledge exists could be extended down to about 30 eV.

From Fig. 2 it is evident that the parameter ranges and therefore the basic mechanisms in PVD as well as CVD ion assisted c-BN deposition are the same and that low ion energies can be compensated by high ion currents. F and F^* are only specified in terms of total ions per incoming respective incorporated boron atom although in the relevant experiments different ion compositions (mainly with the plasma “methods different argon to nitrogen ratios) were used [2]. This simplification is justified because the sputter yields of h-BN under argon and nitrogen bombardment are similar (see below). Therefore, the well known fact that the c-BN growth region becomes extremely narrow with pure nitrogen bombardment [6] must be attributed to differences in the nucleation process. It has been shown that c-BN films, in contrast to h-BN, possess a markable amount of incorporated argon [7] which may support the build-up of compressive stress required for nucleation [2].

According to the sputter model, the boundaries in Fig. 1 between h-BN and c-BN (below 500 eV plus dotted line above 500 eV) respective c-BN and the ‘no growth’ region are interpreted to be due to material removal processes. Two processes are taken into account. First, resorption of incoming material which is governed by the temperature dependent sticking probability of boron $s_B(T)$, and second sputtering of incorporated atoms by the ion bombardment. Because surplus

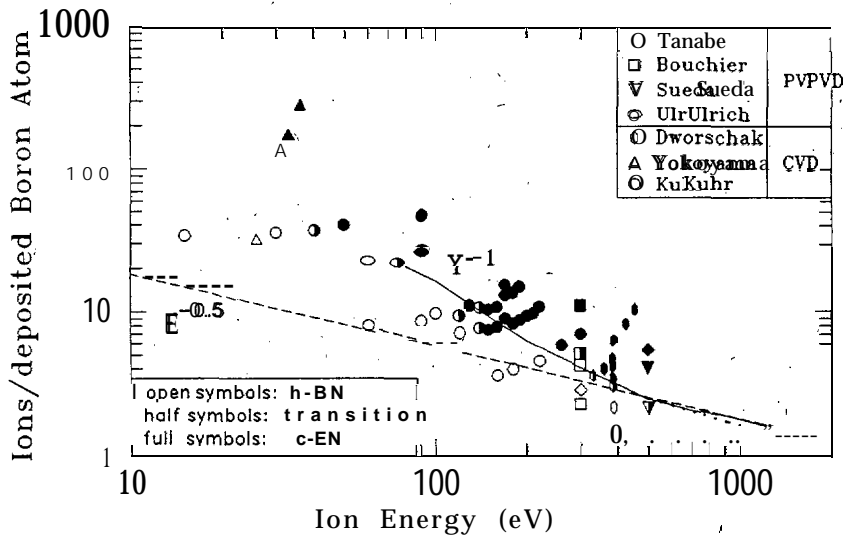


Figure 2: Dependency of the boundary between h-BN and c-BN on ion energy E_{ion} and the number of bombarding ions per incorporated B atom for CVD as well as PVD deposition methods. CVD, data Yokoyama et al. [17], Kuhr et al. [21] and Dworschak et al. [28, 29]. PVD data from Ulrich et al. [30, 31], Bouchier et al. [26, 32], Tanabe et al. [25, 33] and Sueda et al. [23]. The dotted line represents the data of Mirkarimi et al. [5]. The full line represents the dependency of the inverse sputter yield Y^{-1} of Si under argon bombardment [8], fitted to the data at 500 eV.

nitrogen diffuses out [3], only the boron is considered, and the boundaries are characterized by the equality of the incoming boron flux F_B and the flux of removed boron F_B^{rem} :

$$F_B = F_B^{rem} = (1 - s_B(T))F_B + 0.5Y_{h,c}(E_{ion}, \Theta)F_{ion} \quad (1)$$

$Y_{h,c}(E_{ion}, \Theta)$ represents the sputter yields (B- plus N-atom: per ion) of h-BN resp. c-BN under the relevant bombardment conditions [2]. From equ. (1), it follows for the boundaries

$$F_{h,c} = \frac{2s_B(T)}{Y_{h,c}(E_{ion}, \Theta)} \quad (2)$$

from which several conclusions for the transition from h-BN to c-BN can be drawn. First, the absolute sputter yields should be sufficiently high to explain the boundaries, and a selectivity between the sputter yields of h-BN and c-BN should exist. These points are investigated by the sputter experiments presented below. Second, according to Equ. (2) the energy and angle of incidence dependencies should vary like the inverse sputter yield of h-BN under argon and nitrogen bombardment. Unfortunately these dependencies are not known; nevertheless, parallels to well investigated materials can be drawn. In case of the angle of incidence it has been shown that with increasing angle the boundary between h-BN and c-BN shifts to lower F values [2, 26] which is in agreement with collision cascade theory. Evaluation of reliable energy dependencies down to low energies is somewhat critical. Monte carlo simulation methods significantly underestimate experimental sputter yields below 200 eV. The same holds for analytical calculations [8]. Therefore experimental data have to be taken for comparison. Some energy dependencies for light elements may be taken from [8]. Between 200 and 500 eV the yield is nearly proportional to the ion energy, the dependency becoming stronger below 200 eV down to the sputter threshold, and weaker than $Y \propto E$ above 500 eV [8]. Data for $Ar \rightarrow Si$ are included in Figs. 1 and 2 which fit the transition from h-BN to c-BN well.

3 Experiment

Sputter yield measurements were performed at the ISA 150 sputter facility at the Institut für Oberflächenmodifizierung, Leipzig. The ion beam was extracted from a Kaufmann ion source. During the measurements, the beam was neutralized by thermal electrons from a heated filament. The homogeneity of the beam is better than $\pm 5\%$ for a beam diameter of 150 mm. The ion beam current densities were between 0.1 mA/cm^2 at 200 eV and 0.38 mA/cm^2 at 800 eV. They were measured without charge neutralization by means of a Faraday cup before and after the etching step. The ion energy was determined from the accelerating voltage. The samples were mounted on a water cooled substrate holder and were irradiated under normal incidence. The distance between ion source and sample was 38 cm. A base pressure of 10^{-4} Pa was achieved by means of a 1500 1/s turbo pump. The working pressure was 10^{-2} Pa due to the gas flow into the ion source. Parts of the samples were coated by photoresist (type AZ 1350). After the measurement, the resist was released, and the resultant step heights were measured by profilometry. For determination of the sputter yields a density of 2.29 g/cm^3 for h-BN was assumed. For c-BN containing films a linear approximation between the densities of h-BN and c-BN (3.48 g/cm^3) according to the c-BN content was used. The sputter yields are always given in 'total sputtered atoms per ion' disregard the detailed ion beam composition (in case of nitrogen).

For comparison; we calculated the sputter yields of h-BN with the well known binary collision code TRIMSP using Kr-C potentials [9]. The surface binding energy (SBE) is the only fit parameter. In case of nitrogen bombardment a beam composition of 80% N^+ and 20% N_2^+ was assumed which is a typical value for Kaufmann ion sources [10, 11]. One N_2^+ with the energy E was treated as two nitrogen atoms, each with energy $E/2$.

4 Results

In a first step, the dependence of the sputter yield of h-BN on the ion energy between 200 and 800 eV for argon and nitrogen bombardment was investigated.

In order to exclude influences of different samples, all measurements were performed

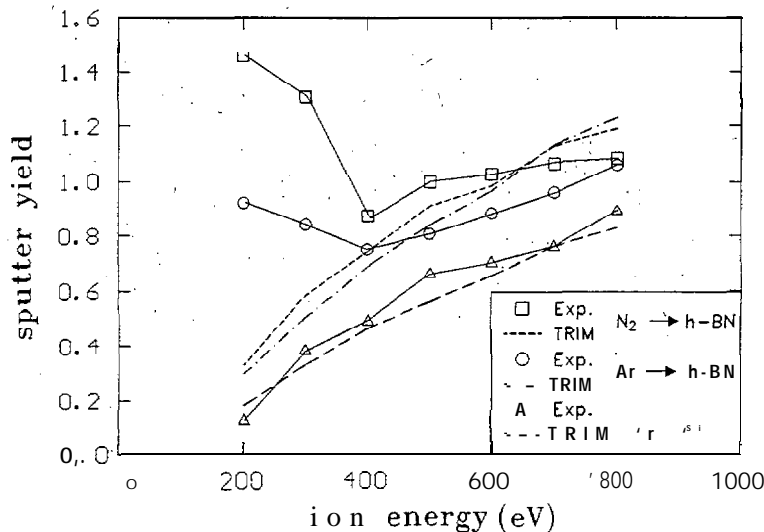


Figure 3: Energy dependence of the sputter yields of h-BN and silicon from experiment and TRIMSP calculations. For the calculations, the SBE's were set to 4.46 eV [8] and 3 eV for silicon and h-BN, respectively. In case of nitrogen bombardment an ion beam composition of 20% N and 80% N_2^+ was assumed.

small parts of one and the same h-BN film. For comparison, in every measurement a silicon sample was irradiated simultaneously. The h-BN film was prepared by RF plasma CVD from borane amine ($\text{BH}_3:\text{NH}_3$) and had a thickness of approx. 1 μm . With AES we proved that the h-BN sample was stoichiometric and the amount of contaminations was low (1 % C, 1 % O.). The infrared spectrum of the film showed two peaks characteristic for the BN “stretching and the BNB bending vibrations of h-BN. The refractive index was determined by ellipsometry (Plasmos SD 2100) to be $n = 1.72$ at a wavelength of 632 nm which is very close to the value of 1.71 reported for amorphous and polycrystalline h-BN [12].

Fig. 3 shows the resulting ion energy dependency. Under argon as well as nitrogen bombardment unexpected high sputter yields at energies below 400 eV were observed. A systematic error in the determination of the ion current or the step heights can be excluded since the simultaneously measured yields of $\text{Ar} \rightarrow \text{Si}$ fit well to other measurements [8] and TRIMSP calculations: Furthermore in test measurements with silicon sputtering a good reproducibility was found. “Possible reasons for the, above effect may be the smoothening of the surface with increasing ion dose (see below). Therefore, with low ion doses (at low ion energies) the yield of a rough surface is measured. Furthermore an influence of the residual gas which is most pronounced at low ion currents can not” be excluded, For sputtering of compounds also changes in surface topography, composition and morphology dependent on the ion dose have been observed which may influence sputter yields [13]. Such ‘dose effects do not occur in ion assisted deposition which represents in this view the steady state case.

In the following we will focus only on the high energy data which show a normal energy dependency. The yields under argon and nitrogen bombardment are similar that, of nitrogen being slightly higher (e.g. 0.9 and 1.0 at 600 eV). This is also found with TRIMSP calculations indicated in Fig. 3. The SBE was set to 3 eV for boron as well as nitrogen atoms which is distinctly lower than the value determined from the heat of formation (5.7 eV for boron and 6.32 eV for nitrogen [14]). However, such high SBE’s result in sputter yields of only 0.31 and 0.30 for 600 eV argon and nitrogen bombardment, respectively.

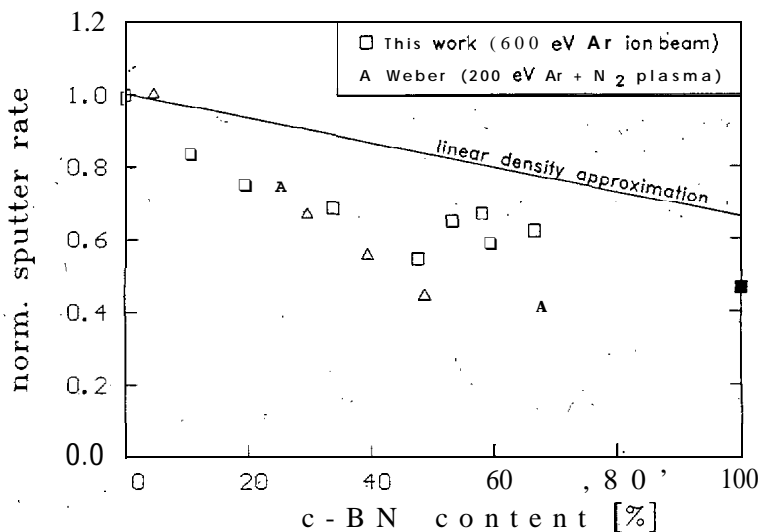


Figure 4: Dependency of the sputter rate of BN films on their c-BN content. Open, squares (BN films); full square (c-BN crystal) sputtered with 600 eV argon; circles, data of Weber et al. [16]. The full line indicates the pure density effect (rates which result in equal sputter yields). All data were normalized to 1.

On the other hand, high absolute sputter yields were also found experimentally by Sainy et al. with nitrogen bombardment, of IBA h-BN films [11]. From their data with a beam composition of 81% N_2^+ and 19% N^+ and an angle of ion incidence of 25° , a sputter yield (in

3. A selectivity γ between the sputter yields of h-BN and c-BN of approx. 1.5 exists.

Furthermore, some h-BN films were also investigated with atomic force microscopy (NanoScope III) before and after etching. It was found that nitrogen as well as argon etching of h-BN films results in smoothening of the surface. the effect being more pronounced with nitrogen. A dose of $6.7 \cdot 10^{18} \text{ cm}^{-2}$ under 600 eV nitrogen bombardment led to a reduction of the roughness from 28 nm to 6 nm rms.

5 Discussion

If material removal processes play a 'significant role, the probability-of an incoming boron atom to be incorporated in the BN film (p_B) should be significantly" below 1.

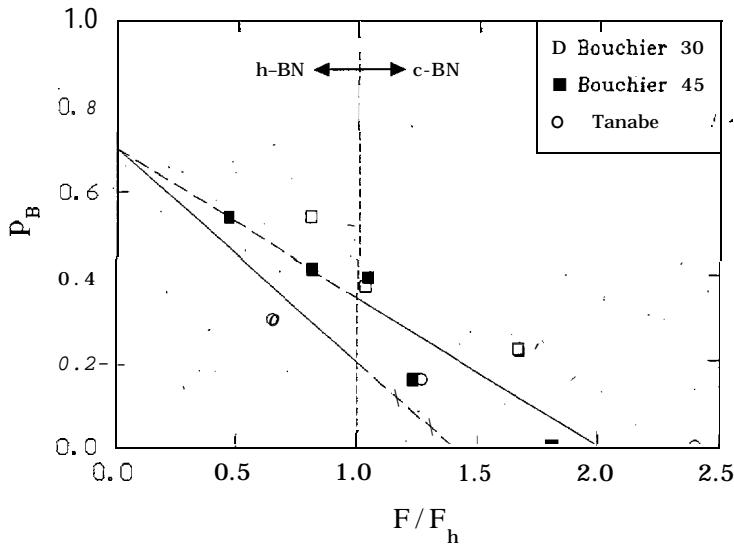


Figure 6: Boron incorporation probability p_B as a function of flux ratio F : squares, data from Bouchier et al. (300 e V and angles of incidence of 30 and 45°) [26; 32]; circles, data from Tanabe et al. (normal ion incidence and: 300 e V left point, 500 e V other points) [25, 33]. In order to compare different experiments, F values were normalized to F_h , representing the flux ratio of the transition from h-BN to c-BN under relevant experimental conditions. "The lines represent the dependency of p_B according to Equ. (3) with a sticking probability of $s_B = 0.7$ and sputter yields $Y_c = 0.7$ and $Y_h = 1$ for h-BN and c-BN, respectively.

In Fig. 6 experimental values for p_B -determined from IBAD experiments are shown as a function "of the ion to atom ratio F . Because of different experimental conditions the data were normalized to the value F_h denoting the transition from h-BN to c-BN. It can be seen that p_B decreases with F which is a direct-evidence for sputter processes. An upper limit of $p_B \approx 0.4$ for the occurrence of c-BN may be derived from the figure. According to the simple model sketched above, p_B can be calculated from Equ. (1) to be

$$p_B = \frac{F_B - F_B^{rem}}{F_B} = s_B - 0.5Y_{h,c}F \quad (3)$$

for pure, stoichiometric h-BN and c-BN films. Therefore p_B should vanish for h-BN at the transition F_h , and for c-BN at the resputter boundary F_c . With the values of the sputter yield derived above the predictions of the model can be tested. A yield for c-BN of $Y_c = 0.7$ and a reasonable value of the sticking coefficient of 0.7 (taking the substrate temperatures of about 400°C into account [2]) leads to a no growth boundary at $F = 2$. By comparison to Fig. 1 it is found that the absolute value of the c-BN sputter yield is well suited to-explain the position the no growth boundary.

In Fig. 6 in addition to the experimental data, the dependency of p_B according to equation (2), assuming $Y_c \approx 0.7$, $Y_h = 1$ and $s_T = 0.7$, is included for comparison (fitted to the experimental data at the no growth condition $F = 2F_h$). Experiment and model show qualitatively the same tendency, i.e. the highest values of p_B for h-BN at low F values and a decrease with increasing ion flux. It should be mentioned that there generally is some uncertainty in the determination of F (e.g. because of the possibility of charge exchange collisions) as well as in the determination of p_B . However, some quantitative differences between experiment and the simple model seem to exist:

First, the p_B values in case of h-BN are significantly underestimated by the model. The reason for this might be a boron enrichment of the surface, which would lead to a reduction of the sputter yield (see below). Although all data points of Fig. 6 were achieved with atomic flux ratios $N/B > 1$, this does not guarantee a stoichiometric surface composition. In a detailed study about the growth dynamics of h-BN remarkable discrepancies between the surface and the bulk B/N composition have been reported for low N/B fluxes [10].

Second, according to the measured sputter yields, h-BN growth should vanish at approx. $1.4F_h$ in contrast to the experimentally found value "of F_h ". Therefore it can be concluded that the transition boundary F_h is not determined by an absolute instability of h-BN with respect to the ion bombardment ("direct resputter boundary"). Nevertheless, even with a low sputter selectivity by the ion bombardment will influence the growth velocities in favour of c-BN. This in addition with the preferential bonding mechanism discussed below may shift the transition to F values somewhat lower as expected from the selectivity in sputter yields. Our model may not be misunderstood in the manner that the probability of incoming material bonded as h-BN or c-BN is independent of the material already deposited. In this case two possible conclusions can be drawn. Either, without ion bombardment a remarkable amount of c-BN should be present or the probability that an incoming atom will be bonded as c-BN must be very low because without ion bombardment the c-BN content is close to zero. But this requires that in case of c-BN, p_B is in the percent range. Both possibilities can be definitely excluded so that we conclude that a strong dependency of the bonding of an incoming atom on the surface bonding conditions must exist. In other words, an atom will be more likely sp^3 bonded on c-BN and sp^2 bonded on h-BN. This effect is not considered in the simple evaluation of p_B according to Equ. (3).

To summarize, despite some experimental as well as theoretical uncertainties, our model so far agrees well with the basic findings of c-BN deposition but the nucleation step can not be understood with our model, alone. In this case, additional effects have to be taken into account, which are discussed in more detail in Ref. [2]. Nevertheless, also in the c-BN growth step under special conditions secondary effects of ion bombardment have further to be taken into account:

Topography With ECR CVD it was shown that with a rough substrate surface lower ion energies are sufficient to reach the transition to c-BN and the no growth region [19]. In light of "the sputter model, this agrees well with the dependency of the sputter yield on the angle of ion incidence discussed above.

Morphology In the first step of growth even under c-BN growth conditions a textured h-BN layer (c-axis parallel to the substrate surface) is found [20, 4], the reason for the texture being the high compressive stress. Such a layer is expected to be stable with respect to the ion bombardment because of channeling effects [2]. Furthermore this layer was found to be boron rich [4] which also influences the sputter yields (see below).

Composition Just beneath the resputter boundary, some investigations (CVD as well as PVD) show a narrow region of films with h-BN like IR spectra [21, 22, 23, 24]. For such films the term x-BN was introduced [4] because they exhibit marked differences with respect to h-BN. IR spectra show a shoulder at higher wavenumbers of the 1380 cm^{-1} absorption peak of h-BN [21, 24] which is a hint for high B/N ratios. Indeed, measurements of the B/N atomic ratio by

AES, resulted always in values >1.2 for x-BN [21] but c-BN has been shown to tolerate only a narrow range of composition between 0.9 and 1.1 [2].

The surplus boron is also the reason for the stability of these films under deposition conditions. Boron films have been shown to have a much lower sputter yield than h-BN film [11]. Furthermore it should be kept in mind that the SBE is determined by the surface B/N ratio which may differ from the bulk ratio. The reason for the compositional changes might be preferential sputtering of nitrogen with respect to boron. This was assumed by Sainty et al. as explanation for the resulting boron enrichment with increasing ion energy in IBAD h-BN deposition (although a nitrogen to boron atom flux ratio of 1.5 was used) [11]. A detailed study with inductive coupled plasma (ICP) CVD of BN shows boron enrichment to accompany every phase transition [4]: An increase of the B/N ratio was found in the nucleation step (prior the transition from textured h-BN to c-BN) as well as during growth for films deposited with parameters close to the transitions from h-BN to c-BN respective from c-BN to x-BN in an ion energy sequence.

6 Summary and conclusions

In ion assisted deposition, well defined parameter ranges for the formation of c-BN exist. These have been shown to be independent of the deposition technique (CVD or PVD). The data interpreted in terms of a simple sputter model: The bonding state of an incoming atom is determined by the surface bonding conditions (sp^2 or sp^3) of the already grown film; the phase purity of the surface is governed by selective sputtering of h-BN with respect to c-BN. The predictions of the model concerning ion energy, ion angle of incidence and substrate temperature agree well with the experimental findings. Measurements of the absolute sputter yields of BN films result in values which are well suited to interpret the location of the c-BN domain in the parameter space. Furthermore, the measured dependency of the sputter yields of BN films on their content supports the model. The model is valid for appropriate conditions (stoichiometric and sp^3 terminated surface); deviations result from additional effects: During the nucleation the occurrence of textured h-BN is governed by compressive stress. Furthermore, under special conditions film stoichiometry influences the deposited phase.

7 Acknowledgements

We like to thank Dr. W. Dworschak, University of Kaiserslautern, for preparation of c-BN films and Prof. F. Bigl, Dr. H. Neumann, and Mrs. R. Fechner, IOM, Leipzig for performing of the sputter studies. The authors gratefully acknowledge financial support of the present work by the Deutsche Forschungsgemeinschaft (DFG) carried out under the auspices of the trinational 'D-A-CH' German, Austrian and Swiss cooperation on the 'Synthesis of Superhard Materials'. This work was also supported financially by the European Community (BRITE/EURAM Proj # BE 4484-89) which is gratefully acknowledged.

References

- [1] L. Vel, G. Demazeau, and J. Etourneau. *Mat. Sci. Eng.*, B10:149, 1991.
- [2] S., Reinke, M. Kuhr, W. Kulisch, and R. Kassing. to be presented at Diamond '94, Castelveccio, Italy.
- [3] S. Reinke, M. Kuhr, and W. Kulisch. *Diamond Relat. Mater.*, 3:341, 1994.
- [4] M. Kuhr, S. Reinke, and W. Kulisch. to be presented at the Diamond'94, Castelveccio, Italy.
- [5] P.B. Mirkarimi, K.F. McCarty, D.L. Medlin, T.A. Wolfer, T.A. Friedmann, E.J. Klaus, G.F. Canale, and D.G. Hewitt. accepted for publication in *Jour. Mat. Res.*, 1994.

- [6] D.J. Kester and R. Messier. *J. Appl. Phys.*, 72:504, 1992.
- [7] D.R. McKenzie, W.D. McFall, W.G. Sainty, C.A. Davis, and R.E. Collins. *Diamond Relat. Mater.*, 2:970, 1993.
- [8] N. Matsunami, Y. Yamamura, Y. Itikawa, N. Itoh, Y. Kazumata, S. Miyagawa, K. Morita, R. Shimizu, and H. Tawara. *Atomic Data and Nuclear Data Tables*, 31:1, 1984.
- [9] J.P. Biersack and W. Eckstein. *Appl Phys Lett*, A 34:73, 1984.
- [10] D. Bouchier and W. M^oller. *Surf. Coat. Tech.*, 51:190, 1992.
- [11] W.G. Sainty, P.J. Martin, R.P. Netterfield, D.J.H. McKenzie Cockayne, and D.M. Dwarde. *J. Appl. Phys.*, 64 (8):3980, 1988.
- [12] H. List. In *Gmelin Handbuch der anorganischen Chemie*, volume 13, Borverbindungen, part 1, chapter 1.1. Springer Verlag, Berlin, 1974.
- [13] G. Betz and G.K. Wehner. In R. Behrisch, editor, *Sputtering by particle bombardment 2*, volume 2, chapter 2, page 11. Springer Verlag, Berlin, 1983.
- [14] W. M^oller, D. Bouchier, O. Burst, and V. Stambouli. *Surf. Coat. Tech.*, 45:73, 1991.
- [15] W. Dworschak, K. Jung, and H. Erhardt. *Diamond Relat. Mater.*, 3:337, 1994.
- [16] A. Weber, U. Bringmann, R. Nikulski, and C.P. Klages. In *11th International Symposium on Plasma Chemistry — ISPC 93*, Loughborough, UK, 1993.
- [17] H. Yokoyama, M. Okamoto, and Y. Osaka. *Jpn. J. Appl. Phys.*, 30:344, 1991.
- [18] Y. Osaka, A. Chayahara, H. Yokoyama, T. Hamada, T. Imura, and M. Fujisawa. *Mat. Sci. For.*, 54/55:277, 1990.
- [19] M. Okamoto, Y. Utsumi, and Y. Osaka. *Jpn. J. Appl. Phys.*, 31:3455, 1992.
- [20] D. J. Kester, K.S. Ailey, and R.F. Davis. *Diamond Relat. Mater.*, 3:332, 1994.
- [21] M. Kuhr, S. Reinke, and W. Kulisch. to be presented at the Plasma Surface Engineering '94, Garmisch Partenkirchen, Germany.
- [22] T. Ichiki, T. Momose, and T. Yoshida. *J. Appl. Phys.*, 75(3), 1994.
- [23] M. Sueda, T. Kobayashi, H. Tsukamoto, T. Rokkaku, S. Morimoto, Y. Fukaya, N. Yamashita, and T. Wada. *Thin Solid Films*, 228:97, 1993.
- [24] T. Ikeda. *Appl. Phys. Lett.*, 61 (7):786, 1992.
- [25] N. Tanabe, T. Hayashi, and M. Iwaki. *Diamond Relat. Mater.*, 1:883, 1992.
- [26] D. Bouchier, M.A. Sené, Djouadi, and P. M^oller. to be published in *Nucl. Instr. Meth. B*, 1994.
- [27] R. Ganzetti and W. Gissler. presented at SMT 7, Nov. 1 - 3 (1993), Niigota, Japan; to be republished in *Material and Manufacturing Processes*.
- [28] W. Dworschak, K. Jung, and H. Erhardt. accepted for publication in *Thin Solid Films*, 1994.
- [29] W. Dworschak. Private communication, 1994.
- [30] S. Ulrich, I. Barzen, J. Scherer, and H. Ehrhardt. to be presented at Diamond'94, Castelveccio, Italy.
- [31] S. Ulrich. Private communication, 1994.
- [32] D. Bouchier. Private communication, 1994.
- [33] N. Tanabe and M. Iwaki. *Nucl. Instr. and Meth.*, B 80/81:1349, 1993.

(paper presented at the Diamond'94 Conference in Il Ciocco (Italy) to be published in *Diamond Relat. Mater.*),

Nucleation of Cubic Boron Nitride (c-BN) with ion induced PECVD

M. Kuhr, S. Reinke, W. Kulisch

Institute of Technical Physics

University of Kassel, FRG

Heinrich-Plett-Strasse 40

D-34 109 Kassel

Tel: 49 561/8044519; FAX: 49 561/804-4136

A b s t r a c t

Nucleation and growth of c-BN films by means of the ICP technique was investigated. Two different set of experiments, were performed: deposition in dependence of the bias voltage V_b and experiments with varying deposition times. The films were characterized by FTIR, AES and ellipsometry. Without substrate bias, crystalline oriented h-BN was obtained with the c-axis normal to the surface. With "Sufficient bias voltage, a layer of vertically oriented h-BN is observed" prior to the formation of c-BN, in agreement with TEM measurements recently published in the literature. We observed further a significant increase of the boron to nitrogen ratio prior to the c-BN formation. Preferential sputtering of nitrogen with respect to boron with increasing ion bombardment seems to be the reason for this behaviour.

Introduction

Films with a distinct content of c-BN can be deposited with two different types of deposition techniques, up to now: the ion beam techniques (e.g. IBAD) on the one hand and the ion induced PECVD methods on the other hand [1]. Recently [1, 2], we demonstrated that both depend on the same mechanisms among which ion induced sputtering plays a most important role [3, 4]. The ion bombardment and therefore the sputter mechanism, is detrimental to applications of the c-BN since it results in films with very small crystal sizes (5 - 50 nm) [5] and a large mechanical stress, causing the films to peel off.

In order to overcome these problems it is important to search for mild CVD processes, e.g. HFCVD and MWCVD similar, to the deposition of diamond. "One approach may be to separate the c-BN nucleation step from the growth of the films as has been successfully realized in the case of diamond. To our knowledge, such a separation has not been investigated up to now. The first step in this direction is obviously to collect more data and information about nucleation and growth of c-BN.

Unfortunately, literature data on nucleation are scarce. However, transmission electron microscopy (TEM) pictures recently presented by Kester et al. [6] and other groups [7] gave first insight into the nucleation mechanism of c-BN. It was found that prior to c-BN formation first a layer of amorphous boron nitride (a-BN) is deposited followed by

a crystalline, textured hexagonal boron nitride (h-BN) with the c-axis parallel to the surface.

In order to contribute to the evaluation of the nucleation mechanisms we investigate the nucleation and growth of c-BN as a function of time and ion energy. Films were deposited with the inductively coupled plasma (ICP) technique [5] and characterized by Fourier transform infrared spectroscopy (FTIR), Auger electron spectroscopy (AES), and ellipsometry. Our results are in good agreement to the sequence shown by Kester et al. [6], and will be discussed in view of possible mechanisms leading to this nucleation sequence.

Experimental

ICP deposition set-up The ICP set-up used in our experiments has been described in detail in another publication [5]. An inductively coupled plasma (RF, 13.56 MHz) with a very high ion density is created within a quartz tube on top of a stainless steel reactor. The signal of a second 13.56 MHz generator is coupled capacitively to the substrate holder leading to a substrate bias V_B . All experiments discussed in the following sections have been carried out with a mixture of trimethyl borazine (TMB), nitrogen and argon: In Tab. 1 we summarized the typical process parameters for c-BN deposition, and also some important properties of the resulting films.

process parameters		
base pressure	[mbar]	$2 \cdot 10^{-5}$
working pressure	[mbar]	$2 \cdot 10^{-2}$
rf power (ind.)	[W]	80
rf substrate bias	[V]	0-200
ion density	[cm ⁻³]	$5 \cdot 10^{10}$
substrate temperature	[°C]	500
argon flow	[sccm]	50
nitrogen flow	[sccm]	25
TBM flow	[sccm]	≈ 1 - 2
film properties		
growth rates	[nm/min]	< 10
stoichiometry		$0.9 < B/N \leq 1.1$
carbon content	[%]	< 5
oxygen content	[%]	< 2
max. c-BN content	[%]	75

Table 1: Summary of the major process parameters of the ICP process used in our investigation, and of some important properties of the resulting c-BN films [5].

Characterization The analytical measurements were performed by Auger electron spectroscopy (AES) for determination of stoichiometry and contaminations, by ellipsometry to measure the refractive index and the film thickness, and by Fourier transform infrared spectroscopy to determine the c-BN content and to investigate the structure of the deposited films. The AES measurements were performed with a standard procedure (1 min sputtering [Ar⁺, 12 keV] and calibration with a standard probe) described in more detail in [5].

There are three main absorption peaks in FTIR spectra of h-BN respective mixed h-BN/c-BN films (cf Fig. 2): The 1380 cm⁻¹ peak stems from the in-plane B-N stretching mode (ν_{ip}) of h-BN, the 780 cm⁻¹ peak is due to the out-of-plane B-N-B deformation

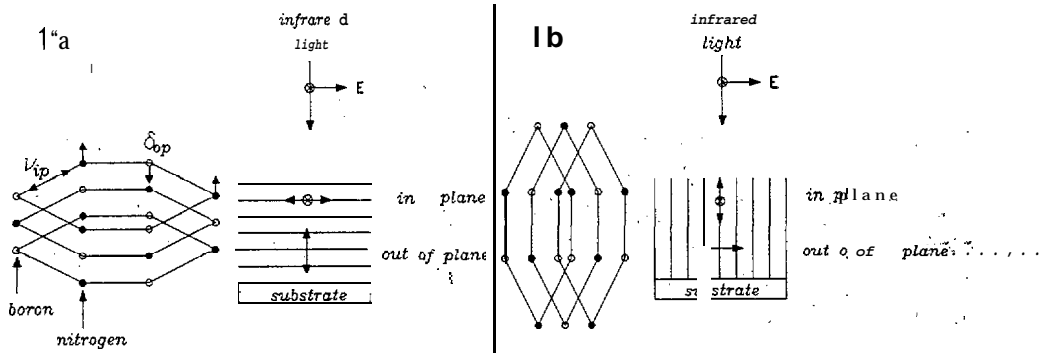


Figure 1: Schematic drawing of the infrared active modes in hexagonal boron nitride and the relationship of the vibration axis of these modes to the electric field vector of unpolarized light for horizontal respective vertical arrangement of the h-BN layers. Only those modes with the vibration axis parallel to the electric field vector are seen in our experiments.

mode (δ_{op}), of h-BN [8]. Both vibration modes are shown schematically in Fig. 1. At approximately 1080 cm^{-1} there is the reststrahlen band (TO_c) of c-BN [9]. The standard procedure to determine the c-BN content CC of a film is a comparison of the heights of the ν_{ip} respective TO_c peaks [1, 10]:

$$CC = \frac{A_{TO_c}}{A_{TO_c} + A_{\nu_{ip}}} \quad (1)$$

Usually, evaluation of the IR spectra of c-BN/h-BN mixed films is restricted to the determination of CC according to (1). However, these spectra contain a lot of further informations on the structure and properties of h-BN and h-BN/c-BN films, respectively, as becomes evident from a closer examination of the spectra in Fig. 2. For example, differences can be seen in the ratio of the heights of the h-BN ν_{ip} and δ_{op} peaks ($R_{\nu\delta} := A_{\nu_{ip}}/A_{\delta_{op}}$), the FWHM of the ν_{ip} band, and the position of the three peaks:

In the following, we will restrict our discussion to the ratio $R_{\nu\delta}$ of the two h-BN peaks, and the position σ_{op} of the B-N-B deformation mode: Crystalline hexagonal boron nitride consists of stacked layers of hexagonal rings (Fig. 1). Therefore, the optical properties of h-BN are anisotropic. If unpolarized light at normal incidence is used for the IR measurements, $R_{\nu\delta}$ will depend on the orientation of the h-BN layers with respect to the substrate surface (cf Fig., 1): If the c-axis is normal to the surface (horizontal arrangement of the layers) (Fig. 1a), only the ν_{ip} mode will be observed. In the case of a vertical arrangement (c-axis parallel to the surface) (Fig. 1b), both peaks will be seen but $R_{\nu\delta}$ will become minimal.

The dependence of σ_{op} of the structure of h-BN films has been investigated by Rozenberg et al. [11]. They show that σ_{op} is at about 8.16 cm^{-1} for crystalline films and shifts to lower wavenumbers if the crystalline order is disturbed. For amorphous h-BN, σ_{op} is in the range between 760 and 780 cm^{-1} .

The anisotropy of h-BN also reflects in the refractive index which has been reported to be $n_0 = 2.05$ parallel to the c-axis whereas perpendicular to it $n_1 = 1.65$ was found

[12]. For polycrystalline and amorphous h-BN a value of $n_h = 1.71$ was established [12]. Finally, the refractive index of c-BN n_c is 2.10 [14].

Results and discussion

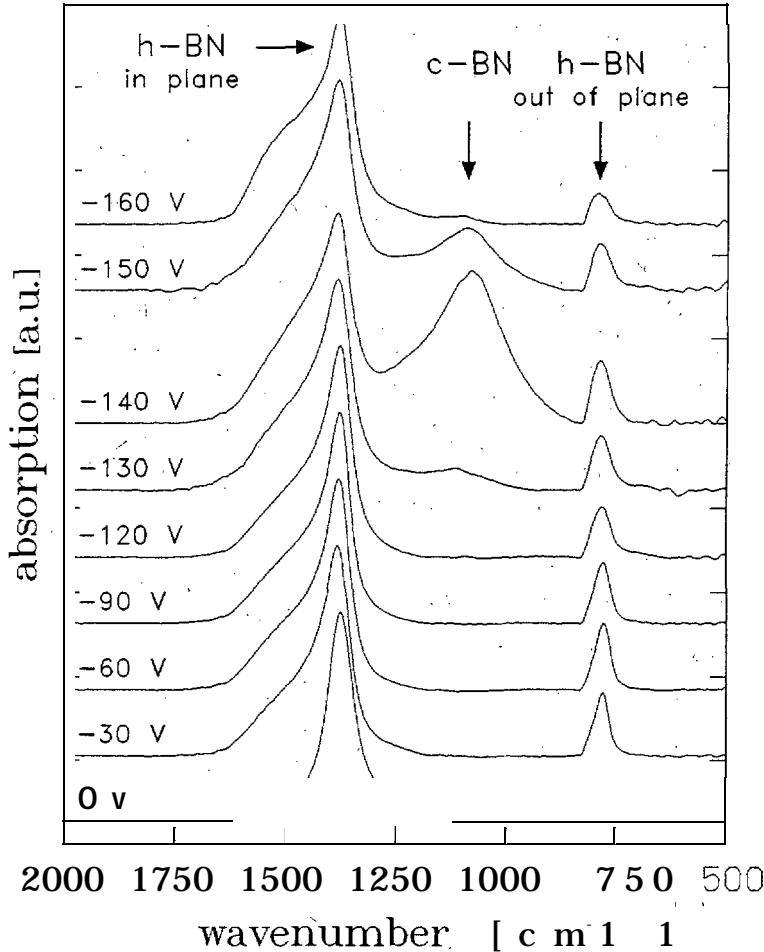


Figure 2: FTIR spectra of a series of h-BN respective h-BN/c-BN films deposited at constant parameters under variation of the substrate bias voltage V_B .

To investigate the nucleation of the c-BN films we performed two sets of experiments: First we varied the bias voltage V_B and deposited films of approx. 100 nm thickness. Subsequently we fixed V_B at 130 V and investigated the nucleation and growth as a function of time. Fig. 2 shows the FTIR spectra, Fig. 3 the ratio $R_{\nu\delta}$, the refractive index and the boron to nitrogen ratio (B/N) for the bias voltage series. Fig. 5 depicts the c-BN content, $R_{\nu\delta}$ and B/N as a function of time for the second experiment, It was impossible to measure the refractive index of those films with short deposition times owing to the very small film thicknesses of these samples.

With the ICP set-up and the parameters given in Tab. 1, it is possible to deposit boron nitride films with considerable contents of the cubic phase (up to 75 %) [5]. In all experiments, on variation of the bias voltage while keeping all other process parameters constant, the following sequence has been found:



This means that for a given set of parameters, on increasing the bias voltage first hexagonal boron nitride and then c-BN/h-BN mixtures are obtained. Increasing V_B further to the so called x-BN and then finally to the no growth region. Let us first comment shortly on the x-BN which is discussed in more detail elsewhere [5]: According to its FTIR spectrum (Fig. 2, 160 V) it consists obviously of a sp^2 BN modification. However, the peak shapes are very different to spectra from h-BN. There are also differences between x-BN and h-BN with respect to film morphology and optical properties. Finally we have to mention that these x-BN films are boron rich [5]. However, at the moment the exact identification of this modification is still standing out.

The bias voltage sequence described by (2) was observed irrespective of the other process parameter which, however, determine its position on the V_B axis and also the maximum c-BN content obtainable [5]. Fig. 2 shows the FTIR spectra of such a sequence. For $0 \text{ V} \leq V_B \leq 120 \text{ V}$ only the h-BN peaks but no reststrahlen band of c-BN is observed. The TO_c peak appears at $V_B = 130 \text{ V}$ and increases then up to 40 %. Further increase the bias voltage then leads to a decrease of the TO_c band back to zero.

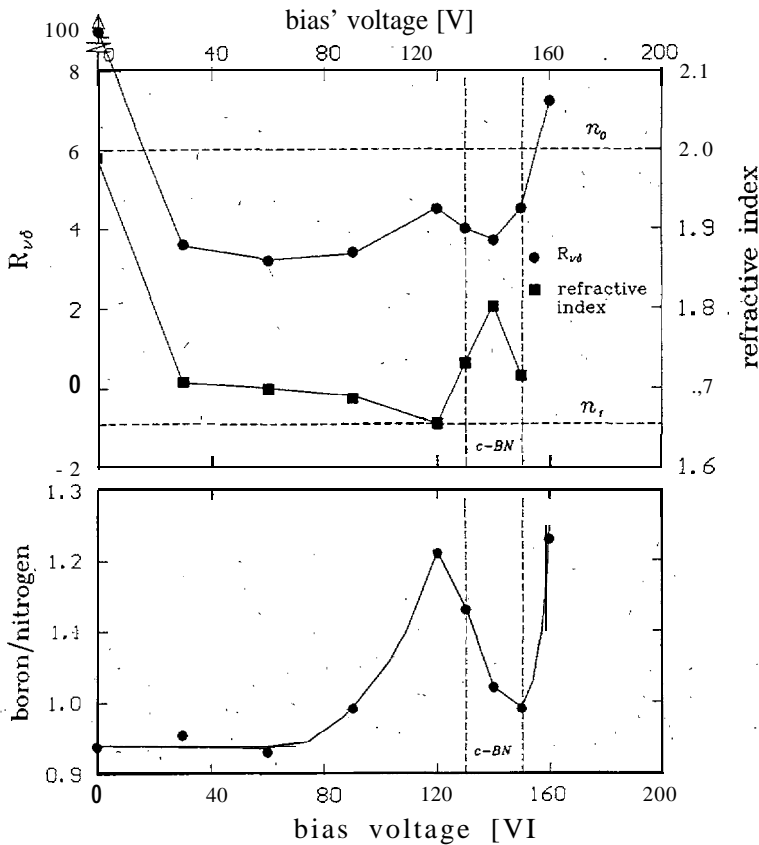


Figure 3: Refractive index n , the ratio $R_{\nu\delta}$ of the h-BN ν_{ip} and δ_{op} peaks (upper part), and the boron to nitrogen ratio (lower part) as a function of the bias voltage. The error of $R_{\nu\delta}$ was estimated to 10-70% for films with $R_{\nu\delta} < 10$ and to about 50% for those films with $R_{\nu\delta} \geq 50$ which is due to the small denominator. The boron to nitrogen ratio < 1 depends on the increased carbon incorporation (ca. 9%) of the films deposited with bias voltage $< 100 \text{ V}$.

Further information about the nucleation process can be obtained from the bias dependence of the ratio $R_{\nu\delta}$ and the refractive index shown in Fig. 3. All films deposited without bias or with $V_B < 10 \text{ V}$ possess a refractive index in the range of 2.0 and a ratio $R_{\nu\delta} > 50$ as shown in Fig. 3. These results from two independent characterization methods allow the conclusion that without substrate bias oriented h-BN films are obtained with the (0001) planes arranged parallel to the substrate surface. Further, evidence is provided,

by FTIR measurements performed under angles of 45° respective 60° . In these spectra a peak at 816 cm^{-1} appears in addition to the very small one at $\approx 770\text{ cm}^{-1}$ (cf Fig. 4a) confirming the crystallinity as well as the orientation of this h-BN. The reason for this oriented growth "which was found for Si(100) as well as Si(111) substrate, is still not understood up to now.

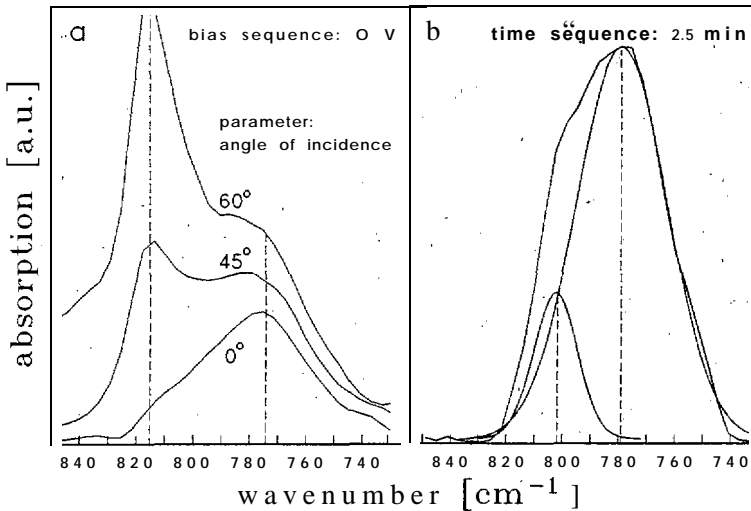


Figure 4: B-N-B deformation mode δ_{op} of films deposited without bias voltage in the bias voltage sequence in dependence of the measuring angle (a) and after 2.5 min deposition time in the time sequence (b).

If the bias voltage is increased above 10 V, the refractive index and $R_{\nu\delta}$ decrease rapidly with V_B . The decline of $R_{\nu\delta}$ shows that the layered, oriented arrangement is destroyed as a consequence of the increasing ion bombardment during the deposition. The refractive index $n = 1.7$ hints at polycrystalline or amorphous h-BN. The position of the B-N-B deformation mode $\sigma_{op} = 770\text{ cm}^{-1}$ finally shows these films to be amorphous.

On further increasing the bias voltage V_B to 120 V the refractive index decreases to 1.65. This value is identical with the literature value of n , as discussed above, and therefore a strong hint at a textured h-BN layer, this time with the c-axis parallel to the surface. If this interpretation is correct, one would expect a minimum of $R_{\nu\delta}$ at $V_B = 120\text{ V}$ in Fig. 3. First hints of this behaviour were obtained by Friedmann et al. [15]. In contrast, the figure shows a slight increase of $R_{\nu\delta}$. The reason for this increase is the missing stoichiometry since the boron to nitrogen ratio increases rapidly at this point as is also evident from Fig. 3. In other experiments with boron rich films always an increase of $R_{\nu\delta}$ with B/N was observed.

Two more regions have to be addressed to complete the discussion of Fig. 3. For $130\text{ V} \leq V_B \leq 150\text{ V}$, the films contain c-BN. The refractive index reflects the c-BN content since n will be a superposition of the n_h and n_c . Further, the films become stoichiometric again at the onset of c-BN formation which in turn causes $R_{\nu\delta}$ to decrease again. Finally, for $V_B \geq 160\text{ V}$ x-BN is deposited. As has been mentioned earlier, this results in boron rich films; as a consequence, $R_{\nu\delta}$ increases again.

Let us now turn to the time sequence shown in Fig. 5. One most important result is that c-BN is observed only after an incubation time of approx. 7 min after which the c-BN content increases reaching finally a saturation level of 52%. This means that initially a h-BN layer is deposited. These results are in agreement with similar FTIR measurements of Kester et al. [6] and Friedmann et al. [16]. As has been mentioned above neither its

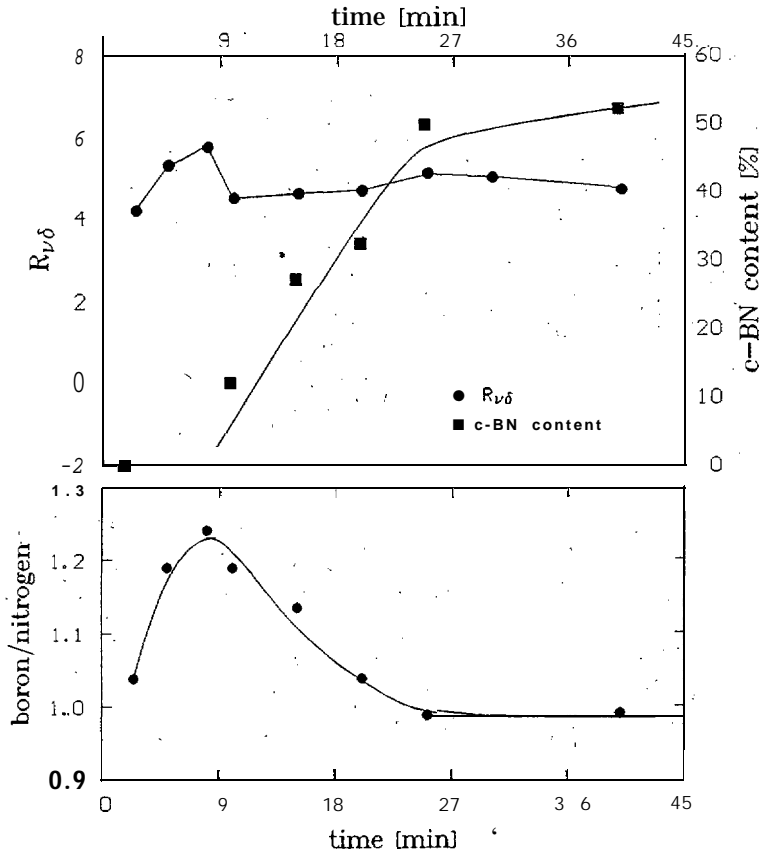


Figure 5: C-BN content C_c , the ratio $R_{\nu\delta}$ of the h-BN ν_{ip} and δ_{op} peaks (upper part); and the boron to nitrogen ratio (lower part) as a function of the deposition time for $V_B = 130$ v.

refractive index nor its thickness could be determined by ellipsometry but an upper limit of 40 nm. could be estimated for the latter.

Fig. 5 further shows an increase of the B/N. ratio just before the onset of c-BN formation, similar to the bias voltage sequence (Fig. 3). Once c-BN has formed, the stoichiometry is restored, again in analogy "to the bias sequence. (As already mentioned the AES measurements were performed after a short Ar sputter cleaning, i.e. 'near the surface [5].) This analogy between the bias and the time sequence also holds for $R_{\nu\delta}$ the increase of which after about 5 mins is again due to overstoichiometry. At this point we like to note that the δ_{op} peaks in the spectra of the films with $t \leq 7$ min are a superposition of two peaks, one of them below 780 cm^{-1} and the other above 790 cm^{-1} (cf Fig. 4b); however, up to now these peaks could not be resolved entirely due to the small, film thickness. Nevertheless, this is a further indication of two phases in these films, one amorphous and one with a much higher degree of order. In combination with the analogy to the bias sequence, this allows therefore the conclusion here also textured layers with the c-axis parallel to the surface are obtained.

Several aspects of the results presented above are worth to discuss. The proof of the deposition of textured crystalline h-BN with the c-axis normal to the surface in the case of deposition without bias emphasizes the suitability of FTIR as a tool to investigate the structure of h-BN and also c-BN films. It would even be enhanced if measurements with polarized light under oblique incidence" would be performed.

Further, our results are in good agreement with the sequence a-BN, textured h-BN,

c-BN proposed by Kester et al. [6]. The exact reasons of its formation are not known yet but we like to emphasize the following considerations. The 'initial a-BN layer may act as a transition zone. As suggested by McKenzie et al. [17], the increasing biaxial stress as a result of the ion bombardment will then play an important role in the transformation from a-BN to textured h-BN since the c-axis is the axis of highest compressibility. In our experiment we always found evidence for this high stress but were not able to quantify it owing to microcracking of the films or even peeling off.

The formation of the metastable c-BN instead of the equilibrium phase h-BN on top of this textured layer has to be explained finally. McKenzie et al. [17] argue again with the stress; the internal pressure in the film will be sufficiently high to reach the regime in the BN phase diagram where c-BN is stable. However, one can also speculate that formation of c-BN on top of the vertically arranged h-BN layers may be facilitated by lattice 'mat thing, 'similar to the case of diamond where enhanced nucleation at the edges of the (0001) basal planes of highly oriented pyrolytical graphite has been demonstrated recently [18]. In this case the stress would be needed for the creation of the textured h-BN layer only, whereas in the other case it would directly cause the c-BN creation.

Finally, we like to address the occurrence of overstoichiometric films immediately before c-BN formation in the time sequence as well as in the bias sequence, and also the return to stoichiometry once c-BN nucleation has occurred. This has been observed in all of our experiments. (It should be noted that the maximum value of B/N within either sequence depends on the deposition parameters, and that formation of c-BN does not take place if this maximum value is too high.) It is possible that with increasing ion bombardment nitrogen will be sputtered more easily than boron and that this preferential sputtering causes the non-stoichiometry at the point discussed above. This would imply that preferential sputtering of nitrogen is more pronounced in h-BN than in c-BN.

Summary

The nucleation and growth of cubic boron nitride by means of ICP CVD has been investigated as a function of substrate bias and deposition time. With low bias, only h-BN is obtained the structure of which strongly depends on the ion bombardment: A transition from crystalline h-BN oriented with the c-axis normal to the surface over a-BN to h-BN oriented with the c-axis parallel to the surface was established. Formation of c-BN is observed only for the last case. Likewise, in the time experiments the formation of c-BN is preceded by deposition of a vertically oriented h-BN layer. These results are in agreement with recently published TEM photographs of the substrate/c-BN interface. We also observed an increase of the B/N ratio immediately before the creation of c-BN, and assigned it to preferential sputtering.

Acknowledgements

The authors gratefully acknowledge financial support of the present work by the Deutsche Forschungsgemeinschaft (DFG) carried out under the auspices of the trinational 'D-A-CH' German, Austrian and Swiss cooperation on the 'Synthesis of Superhard Materials'.

This work was also supported financially by the 'European Community (BRITE/EURAM Proj. # BE 4484-89) which is gratefully acknowledged.

References

- [1] R. Reinke, M. Kuhr, W. Kulisch, and R. Kassing. Paper presented at the diamond 94 conference, Castelveccio, Italy. Submitted to *Diamond Relat. Mater.* (this volume), 1994.
- [2] S. Reinke, M. Kuhr, and W. Kulisch. to be presented at Plasma Surface Engineering '94, Garmisch Partenkirchen, Germany. Submitted to *Surf. Coat. Tee.*, 1994.
- [3] S. Reinke, M. Kuhr, R. Beckmann, W. Kulisch, and R. Kassing. In *Proc. of the 3rd., International Symposium on Diamond Materials*, Honolulu, Hawaii, May 1993. The Electrochemical Society.
- [4] S. Reinke, M. Kuhr, and W. Kulisch. *Diamond Relat. Mater.*, 3:341, 1994.
- [5] M. Kuhr, S. Reinke, and W. Kulisch. to be presented at the Plasma Surface Engineering '94, Garmisch Partenkirchen, Germany. Submitted to *Surf. Coat. Tee.*, 1994.
- [6] D.J. Kester, K.S. Ailey, and R.F. Davis. *Diamond Relat. Mater.*, 3:332, 1994.
- [7] D.L. Medlin, T.A. Friedmann, P.B. Mirkarimi, P. Rez, M.J. Mills, and K.F. McCarty. *J. Appl. Phys.*, 76(1):295, 1994.
- [8] R. Geick, C.H. Perry, and G. Rupprecht. *Phys. Rev.*, 146:543, 1966.
- [9] P.J. Gielisse, S.S. Mitra, J.N. Plendl, R.D. Griffis, L.C. Mansur, R. Marshall, and E.A. Pascoe. *Phys. Rev.*, 155:1039, 1967.
- [10] T. Ichiki, T. Momose, and T. Yoshida. *J. Appl. Phys.*, 75(3), 1994.
- [11] A.S. Rozenberg, Yu.A. Sinenko, and N.V. Chukanov. *J. Mater. Sci.*, 28:5675, 1993.
- [12] T. Ishii and T. Sate. *J. Cryst. Growth*, 61:689, 1983.
- [13] H. List. Bornitrid BN. In *Gmelin Handbuch der anorganischen Chemie*, volume 13, Borverbindungen, Teil 1, chapter 1.1. Springer Verlag, Berlin, 1974.
- [14] L. Vel, G. Demazeau, and J. Etourneau. *Mat. Sci. Eng.*, B10:149, 1991.
- [15] T.A. Friedmann, K.F. McCarty, E.J. Klaus, J.C. Barbour, W.M. Clift, Johnsen H. A.; K.F. Medlin, M.J. Mills, and D.K. Ottesen. *Thin Solid Films*, 237:48, 1994.
- [16] T.A. Friedmann. **In Materials Synthesis using Ion Beams.** Research Society, 198
- [17] D.R. McKenzie, W.D. McFall, W.G. Sainty, C.A. Davis, and R.E. Collins. *Diamond Relat. Mater.*, 2:970, 1993.
- [18] W.A.L. Lambrecht, Lee. C. H., B. Segall, J.C. Angus, Z. Li, and M. Sunkara. *Nature*, 364:607, 1993.